THE ROLE OF HEME OXYGENASE-1 AND THE CD163 PATHWAY IN TYPE 1 DIABETES PATHOGENESIS

Mahmoud Husseini (B.Sc. Honours)

Thesis submitted to the Faculty of Graduate and Postdoctoral Studies
In partial fulfillment of the requirements
For the M.Sc. degree in Biochemistry

Department of Biochemistry, Microbiology, and Immunology
Faculty of Medicine
University of Ottawa

© Mahmoud Husseini, Ottawa, Canada, 2013

ABSTRACT

Type 1 diabetes (T1D) is an autoimmune disease whereby the insulin-producing β-cells of the pancreas are destroyed by the immune system, possibly related to an inappropriate immune reaction to dietary antigens and/or microbes in the gut. We previously observed a deficit in gut-resident $CD163^+$ M2 anti-inflammatory macrophages in BioBreeding diabetes-prone (BBdp) rats. Heme oxygenase-1 (HO-1) is the rate-limiting enzyme of the CD163 pathway and through the breakdown of toxic heme releases potent antioxidants. We hypothesized that the treatment of animals with cobalt protoporphyrin (CoPP), an inducer of HO-1 expression, would inhibit development of T1D through modulation of the CD163/HO-1 pathway and increase M2 macrophages. HO-1 expression was significantly increased in the pancreas and gut. T1D incidence was inhibited in CoPP-treated rats and these animals showed an unexpected increase in cells expressing CD68 (an M1 pro-inflammatory macrophage marker) in the pancreas and gut. CoPP induced the expression of cathelicidin anti-microbial peptide (CAMP) in the jejunum, which co-localized with $CD163^+$ (M2) macrophages. KLF4, an M2 macrophage-specific transcription factor, was significantly upregulated in the pancreas and jejunum of CoPP-treated animals and co-localized with CD68 and HO-1 in the pancreas. We conclude that HO-1 induction prevented T1D through modulation of the gut immune system and potential recruitment of a unique population of anti-inflammatory M2 macrophages in the gut and pancreas.

ACKNOWLEDGEMENTS

I would like to first extend my deepest gratitude to my supervisor Dr. Fraser Scott for his tremendous mentorship, support, and inspiration through his passion and dedication to research. I am grateful to Dr. Scott for giving me this opportunity in his lab to challenge myself. I am indebted to my co-supervisor Dr. Amanda MacFarlane for her enthusiastic guidance and ongoing support throughout my project. I am most appreciative of the invaluable guidance and encouragement of my thesis advisory committee, Dr. Mary-Ellen Harper and Dr. Majambu Mbikay. I also want to thank the staff at the graduate studies office, especially Victoria Stewart, Fay Draper, and Nicole Trudel, for all of their help with administrative duties and keeping me on track. This work was supported by grants to Dr. Scott by CIHR, Canadian Diabetes Association and Cure Diabetes (Ottawa). I am grateful to the University of Ottawa for granting me admission scholarships and travel grants.

I would also like to thank all my fellow Scott lab members, past and present, for their help, friendship and source of constant laughs. I am particularly grateful to Jennifer Crookshank, Dr. Gen-Sheng Wang, and Christopher Patrick for their patience, knowledge, and continuous support over the past two years. Through your guidance and insightful discussions I have learned so much and honed my skills as a scientist, for which I will be forever thankful. I would also like to acknowledge and extend a big thank you to my fellow labmate Ariana Noel for her support and friendship during our stressful courses and deadlines.

Last but certainly not least I am grateful to my family: Mama, Baba, Eman, and Mimi, for their encouragement and unconditional support during my graduate studies. A big special thank you also goes out to my extended family of grandparents, aunts, uncles and cousins for their love, support and hot meals after long days in the lab.

TABLE OF CONTENTS

LIST OF ABBREVIATIONS

ANOVA: analysis of variance
BBc: BioBreeding control rats
BBdp: BioBreeding diabetes-prone rats
BSA: bovine serum albumin
CAMP/LL-37: cathelicidin anti-microbial peptide
CD68: M1 pro-inflammatory *or* pan-macrophage marker
CD163: hemoglobin scavenger receptor, marker of M2 regulatory macrophages
CDK: cyclin-dependent kinase
CoPP: cobalt protoporphyrin
DAB: 3,3'-diaminobenzidine
Defensins: small, arginine-rich proteins with broad, antimicrobial activity
Fab: fragment antigen binding
FABP: fatty acid binding protein
FBS: fetal bovine serum
FoxP3: forkhead box P3
GAD65: glutamic acid decarboxylase 65
GALT: gut-associated lymphoid tissue
Glo-3A: candidate diabetes-related wheat globulin protein
Hb: hemoglobin
HBSS: hank's balanced salt solution
HC: hydrolyzed casein
HO-1: inducible isoform of heme oxygenase
HLA: human leukocyte antigen
Hp: haptoglobin
HRP: horseradish peroxidase
IA-2: insulinoma-associated protein 2
IFN-γ: interferon-γ, a Th1 cytokine
IHC: immunohistochemistry
IL: interleukin, class of interleukins (IL-6, IL-17A, IL-2, etc)
IRF4: transcription factor involved with M2 macrophages
IRF5: transcription factor involved with M1 macrophages
KLF4: transcription factor involved with M2 macrophages
LPMC: lamina propria mononuclear cells
LPS: lipopolysaccharide
M1: pro-inflammatory subset of activated macrophages
M2: anti-inflammatory subset of activated macrophages
MHC: major histocompatibility complex
MIN6: mouse insulinoma pancreatic β-cell line
MLN: mesenteric lymph nodes
NOD: non-obese diabetic mice
OVA: chicken egg white ovalbumin protein
PBMC: peripheral blood mononuclear cells
PLN: pancreatic lymph node
PPAR: peroxisome proliferator-activated receptors
qPCR: quantitative real-time PCR

Reg: also known as regenerating islet-derived proteins, a family of C-type lectins involved in differentiation and proliferation of pancreas, liver, and gastro-intestinal cell types
RIN: rat insulinoma pancreatic β-cell line
SPF: specific pathogen-free
STAT1: transcription factor involved with M1 macrophages
STAT6: transcription factor involved with M2 macrophages
T1D: type 1 autoimmune diabetes
TGF-β: transforming growth factor-β
Th1, Th2, Th17: T helper cell subsets
TLR: toll-like receptor
TNF: tumor necrosis factor
T_{reg}: Regulatory T lymphocytes
WP: wheat peptides

LIST OF FIGURES

LIST OF TABLES

INTRODUCTION

Autoimmunity

Autoimmune diseases such as rheumatoid arthritis, multiple sclerosis, psoriasis, systemic lupus and type 1 diabetes affect between 3-8% of Western populations (Goodnow, Sprent et al. 2005). Typically these diseases are classified as either systemic or organ-specific (Davidson and Diamond 2001). The immune system has evolved an ability to discern self-reactive from nonself-reactive lymphocytes in a phenomenon known as self-tolerance (Janeway, Travers et al. 2008). There are several checkpoints by which the immune system inactivates developing and mature self-reactive lymphocytes. In the early stages of lymphocyte development, B and T cells that react too strongly to endogenous self-antigens in the bone marrow and thymus are deleted or inactivated (Janeway, Travers et al. 2008). While self-reactive lymphocytes will not encounter every self-antigen in these central lymphoid organs, they may still be inactivated or killed in the periphery. Mature B and T cells that bind to self-antigens in the periphery without proper co-stimulation are inactivated in a process known as anergy (Janeway, Travers et al. 2008) and can be further suppressed by regulatory T cells.

Autoimmune disease is thought to occur when self-reactive B and T cells have evaded all checkpoints and attack self-antigens. The disease progresses through epitope spreading, whereby effector T cells and antibodies begin to mount immune attacks on additional self-antigens/epitopes causing widespread tissue injury (Davidson and Diamond 2001). Both B and T cells are involved in all autoimmune diseases, regardless of when one particular response preferentially causes the tissue damage (Janeway, Travers et al. 2008).

It is important to note that not all autoreactivity is detrimental and a certain low level is crucial to normal immune function (Janeway, Travers et al. 2008).

In addition to a breakdown in inherent tolerance mechanisms, environmental and genetic factors are thought to play a role in the etiology of autoimmune diseases. Genetic factors are crucial determinants of susceptibility to autoimmune disease (Davidson and Diamond 2001). Most autoimmune diseases are polygenic, with multiple risk genes (Davidson and Diamond 2001). Mutations in risk genes predispose an individual to autoimmunity (Goodnow, Sprent et al. 2005). Epidemiological studies of genetically similar populations living in different conditions strongly suggest the importance of environmental factors; however in most cases the trigger is unknown (Davidson and Diamond 2001). Some autoimmune diseases can be promoted by viral or bacterial infections due to their disruption of peripheral tolerance through nonspecific inflammation and tissue damage (Janeway, Travers et al. 2008). Furthermore, antigens of microorganisms or constituents of food may induce a cross reactive autoimmune response due to resemblance to a self antigen (Mackay 2000).

Type 1 Diabetes

More than three million Canadians are currently living with diabetes and nearly 10% of these individuals have Type 1 diabetes (T1D), affecting young children as well as adults and shortening life expectancy by as much as 15 years (JDRF 2012). T1D is an autoimmune disease that is characterized by a T cell mediated attack on the insulin-producing β-cells in the pancreas, rendering an individual dependent on exogenous insulin for life (van Belle, Coppieters et al. 2011). While daily insulin injections help to partially maintain blood glucose homeostasis, they are not a cure and do not prevent serious complications including blindness, amputations, and kidney failure (JDRF 2012). Genetic risk for T1D is polygenic with at least 40 risk loci in humans, including genes in the human leukocyte antigen (HLA) region as well as other non-HLA genes (Lefebvre, Powell et al. 2006; van Belle, Coppieters et al. 2011).

T1D Environmental Factors

Over the past 60 years there has been a rapid 2-4 fold increase in T1D incidence that cannot be explained by genetic risk alone, suggesting an important role for environmental factors in addition to genetic factors (Vaarala 2008). The most widely-studied factors are dietary antigens and enteroviruses, both of which first make contact with the frontline immune responders in the gastrointestinal tract (Solly, Honeyman et al. 2001). Previous studies by our group indicated that animals and humans with T1D display abnormal pro-inflammatory responses in the gut immune system, where the majority of immune cells in the body reside, suggesting immune dysregulation in the gut could be a central predisposing factor.

T1D Pathogenesis

Before the onset of clinical symptoms of T1D, autoantibodies are frequently present in the serum and serve as markers of disease progression. The main autoantibodies in T1D are reactive to four islet antigens: insulinoma-associated antigen-2 (I-A2), insulin, glutamic acid decarboxylase 65 (GAD65), and zinc transporter 8 (ZnT8) (van Belle, Coppieters et al. 2011). Mononuclear cells are the first to infiltrate the pancreas and migrate to the islets of Langerhans, which is termed insulitis (van Belle, Coppieters et al. 2011). Studies in both human and animal models of T1D have shed light on the immune cells that destroy β-cells including both adaptive and innate components. Islet-specific $CD8^+$ and $CD4^+$ T cells promote β-cell death through direct killing via MHC class I and class II-mediated cytotoxicity, respectively, and production of pro-inflammatory cytokines (Lehuen, Diana et al. 2010). Pro-inflammatory cytokines such as interleukin 1β (IL-1β), tumor necrosis factor α (TNF-α), interferon-γ (IFN- γ), and IL-6 produced by infiltrating $CD4^+$ and $CD8^+$ T cells promote disease development (Singh, Nikoopour et al. 2011). While the adaptive immune system predominates in the destruction of the β-cells, there is evidence that innate immune cells are also required. Dendritic cells can capture and process β-cell antigens released after β-cell death and travel to the draining lymph nodes to prime β-cell antigen-specific T cells (Lehuen, Diana et al. 2010). In addition, activated macrophages present in both the pancreas and the lymph nodes can promote the activation of dendritic cells and T cells through pro-inflammatory cytokine secretion (Lehuen, Diana et al. 2010). In this way, crosstalk between innate and adaptive immune cells exacerbates the immune-mediated stress on β-cells and contributes to their ultimate destruction (Lehuen, Diana et al. 2010).

Macrophages in Disease

The innate immune system is often overlooked in disease pathogenesis and regarded as primitive compared with its sophisticated adaptive immune counterpart. While there is already a myriad of studies devoted to exploring the role of B and T cells in disease pathogenesis, a new role for innate immune cells, namely macrophages, has been emerging. Macrophages are phagocytic innate cells that are present in virtually all tissues. They differentiate from circulating peripheral blood mononuclear cells, which migrate into tissue in a steady state or in response to inflammation (Mosser and Edwards 2008). These monocytes migrate from the circulation into tissue to replenish long-lived tissue-specific macrophages of the bone (osteoclasts), connective tissue (histiocytes), gastrointestinal tract, and spleen to name a few (Mosser and Edwards, 2008). Macrophages have well-characterized roles in the primary response to pathogens, tissue homeostasis, inflammation, resolution, and repair (Martinez 2011). These phagocytic cells are constantly monitoring ‘danger’ via their Toll-like receptors (TLRs) and other specialized receptors that recognize pathogen-associated molecular patterns (PAMPs) (Mosser and Edwards 2008). Typically, macrophages fall into two polarization states based on their function: M1, classically activated, or M2, alternatively-activated. M1 macrophages are primed by pro-inflammatory cytokines IFN-γ and TNF-α which activate them to kill intracellular pathogens and promote a pro-inflammatory microenvironment by producing IL-6, iNOS, and others (Martinez 2011). M2 macrophages are primed by IL-4 or IL-13 and promote an anti-inflammatory microenvironment by producing IL-10 and transforming growth factor-β (TGF-β) rendering them conducive to tissue repair and wound healing (Mosser and Edwards 2008). The remarkable feature of macrophages is their plasticity and ability to readily switch their phenotypes based on the microenvironment in which they are present. As such, it is becoming increasingly common to classify macrophages based on their functions involved in maintaining homeostasis, such as host defence, wound healing, and immune regulation (Mosser and Edwards 2008). This more accurately describes how macrophages can exhibit characteristics that are shared by more than one macrophage population (Mosser and Edwards 2008). To this end, alternatively-activated macrophages have been further classified into subsets: M2a, induced by IL-4 or IL-13; M2b, induced by exposure to immune complexes, IL-1R and TLR agonists; and M2c, induced by IL-10 and glutocorticoid hormones (Mantovani, Sica et al. 2004). M2a and M2b macrophages promote immunoregulatory functions and drive Th2 responses, whereas M2c macrophages are more related to immune suppression, tissue repair and matrix remodeling (Orme and Mohan 2012). Recent studies have also aimed to identify key transcription factors that may skew macrophages to a particular polarized phenotype. Signal transducer and activator of transcription 1 (STAT1) and interferon regulatory factor 5 (IRF5) have both been implicated in controlling M1 macrophage phenotype (Lawrence and Natoli 2011) whereas STAT6, IRF4 and Krüppel-like factor 4 (KLF4) have been found to regulate M2 macrophage polarization (Lawrence and Natoli 2011; Liao, Sharma et al. 2011).

Regulatory Immune Network in the Gut

The gastrointestinal tract is considered the largest lymphoid organ in the body, housing the majority of the immune cells. A single layer of epithelial cells forms a barrier between the lymphoid areas and the underlying intestinal lumen (Mowat 2003). It is therefore crucial that the gut barrier and the associated immune cells respond appropriately to pathogens while avoiding inflammatory responses to harmless dietary antigens and commensal bacteria (Fasano and Shea-Donohue 2005). In the gut, this homeostatic state is referred to as *oral tolerance* and is mediated primarily by key innate and adaptive immune cells, namely CD163$^+$ macrophages, CD103$^+$ dendritic cells, and FoxP3$^+$ T regulatory (T_{reg}) cells. When the gut barrier becomes leaky, there can be an influx of antigenic material that breaks oral tolerance and shifts the system to an inflamed state with a potential to activate autoimmune processes (Fasano and Shea-Donohue 2005). A leaky gut barrier has been described in human T1D patients (Damci, Nuhoglu et al. 2003; Secondulfo, Iafusco et al. 2004). There is evidence that in the BBdp rat, a spontaneous animal model of T1D, a leaky and inflamed gut barrier is present (Meddings, Jarand et al. 1999; Courtois, Nsimba et al.

2005), which further strengthens the idea of gut immune dysregulation in the context of T1D

Studies in our lab have shown that diet can modify diabetes development. BB rats are fed cereal diets containing primarily wheat. As early as one week post-weaning to this diet, BBdp rat intestines display celiac-like inflammation, inflammatory cytokines are increased in the draining mesenteric lymph node (MLN) and the gut becomes leaky (Meddings, Jarand et al. 1999; Chakir, Lefebvre et al. 2005). When BBdp rats are fed a low antigen, hydrolyzed casein (HC) diet from weaning, disease onset is delayed and more than half are protected from diabetes (MacFarlane, Burghardt et al. 2003). Both BBdp rats and a highly wheat-sensitive patient with T1D and celiac disease showed antibodies and T-cell reactivity towards a specific wheat protein now termed Glo-3A (MacFarlane, Burghardt et al. 2003; Mojibian, Chakir et al. 2006; Loit, Melnyk et al. 2009). Taken together, these data suggest a strong involvement of gut immune regulation in the pathogenesis of T1D and for this reason our goal is to gain a better understanding of the role of the key gut immune regulatory cells, specifically $CD163^+$ macrophages.

The CD163/HO-1 pathway

The largest reservoir of tissue resident regulatory macrophages in the body is found in the lamina propria of the small intestine (Schenk and Mueller 2007). These cells are implicated in the suppression and resolution of inflammation (Fabriek, Dijkstra et al. 2005). Mature tissue macrophages express several receptors including the scavenger receptor cysteine-rich (SRCR) superfamily members. CD163 is a class B member of the SRCR family and is expressed on a population of lamina propria macrophages (Fabriek, Dijkstra et al. 2005). CD163 is specifically a scavenger receptor for hemoglobins (Fabriek, Dijkstra et al. 2005; Polfliet, Fabriek et al. 2006). Hemoglobins (Hb) in circulation bind to haptoglobins (Hp) forming Hp-Hb complexes. These complexes are recognized and bound by the CD163 receptor and subsequently endocytosed by $CD163^+$ macrophages and degraded, generating free heme, CO, and Fe^{2+}. As heme is toxic and needs to be detoxified, it is metabolized to biliverdin and bilirubin by the enzyme heme oxygenase-1 (HO-1) which is cytoprotective (Abraham and Kappas 2008; Van Gorp, Delputte et al. 2010). CO, biliverdin and bilirubin are antioxidants that protect against free radicals (Abraham and Kappas 2008). Furthermore, CD163 is expressed on the surface of alternatively activated (M2) macrophages which are characterized by their secretion of anti-inflammatory cytokines such as IL-10 and TGF-β (Martinez 2011). $CD163^+$ macrophages have been found to stimulate the development of $FoxP3^+$ T_{reg} cells via production of IL-10 and retinoic acid (Denning, Wang et al. 2007). While $CD163^+$ macrophages were found mostly in the lamina propria, they were also found unexpectedly in the epithelial layer. These macrophages appeared to extend processes into the mucin layer that coats the epithelium, suggesting they could sample antigens directly from the gut lumen. Previous studies in our lab indicated that there was a striking deficit in $CD163^+$ macrophages in BBdp rats fed a diabetes-promoting cereal-based diet compared with BBc control rats. $CD163^+$ macrophages and T_{reg} cells were increased in BBdp rats fed a protective HC diet, most notably one week after weaning at 30 days. Our lab also showed that a patient with T1D and celiac disease displayed putative autoantibodies to $CD163^+$ cells (Sonier, Strom et al. 2011).

High concentrations of zonulin, a protein that regulates gut permeability through tight junctions in humans and rats, have been found to promote gut leakiness in BBdp rats (Watts, Berti et al. 2005; Visser, Rozing et al. 2009). Of particular note was the discovery of zonulin as pre-haptoglobin-2 (Tripathi, Lammers et al. 2009) which is a precursor of haptoglobin, a major component of the CD163 pathway.

Animal Models of Spontaneous T1D

Animal models of T1D have proven crucial to better understand the disease. T1D can be induced experimentally with chemicals such as streptozotocin or by genetic manipulation (Lehuen, Diana et al. 2010). There also exist two major spontaneous rodent models of T1D: the non-obese diabetic (NOD) mouse and the BioBreeding diabetes-prone (BBdp) rat, which have been crucial in our understanding of the pathophysiology of the disease.

Both sexes of BBdp rats typically develop pancreatic insulitis around 50 days of age followed by a selective destruction of β-cells and subsequent diabetes development between 50-100 days of age (Mordes, Bortell et al. 2004; Bortell and Yang 2012). Due to a frameshift mutation in the *Gimap5* gene, BBdp rats are lymphopenic, resulting in a severe reduction in the number of $CD4^+$ T cells and nearly complete absence of $CD8^+$ T cells and regulatory T cells (Mordes, Bortell et al. 2004; Bortell and Yang 2012). Macrophages and dendritic cells are the first observed immune cells to infiltrate the islets followed by natural killer (NK) cells, $CD4^+$ and $CD8^+$ T cells, and some B cells (Mordes, Bortell et al. 2004). Closely resembling human T1D, the β-cells are then selectively destroyed and the rat rapidly develops hyperglycemia. As with humans, BBdp rats also require several T1D risk genes including the MHC class II region (*Iddm1*), two susceptibility loci (*Iddm4* and *Iddm5*) and others (Mordes, Bortell et al. 2004; Bortell and Yang 2012).

HYPOTHESIS

We hypothesized that treating BBdp rats with cobalt protoporphyrin (CoPP), an inducer of HO-1 expression, will protect animals against diabetes development and increase M2 macrophages.

RESEARCH QUESTIONS

Research Question 1: Does HO-1 upregulation by CoPP alter diabetes development in cereal-fed BBdp rats?

Aim and Approach: The aim was to upregulate HO-1 in BBdp rats by weekly injections of CoPP and to monitor diabetes development.

Rationale: Previous microarray studies using RNA isolated from mesenteric lymph node (MLN) and rat insulinoma cells incubated with wheat peptides (WP) revealed an upregulation of HO-1 in response to WP suggesting a key role for the CD163 pathway and its rate-limiting enzyme (HO-1) in diabetogenesis. To date, there are no published reports of the effects of HO-1 induction in the BBdp animal model of T1D.

Research Question 2: How does HO-1 upregulation affect macrophage phenotype in the pancreas and gut?

Aim and Approach: The aim was to determine the influence of HO-1 induction on macrophage phenotype by staining for established markers of M1 and M2 macrophages in pancreas and gut sections of CoPP or saline-treated BBdp rats at 51 d as well as in asymptomatic 120 d rats.

Rationale: Macrophages are categorized into two major subpopulations (M1 and M2), based on their pro- and anti-inflammatory properties. We wanted to investigate the macrophage phenotype(s) in the pancreas and gut associated lymphoid cells upon HO-1 upregulation.

Research Question 3: What cellular mechanisms in the pancreas and gut are involved in the upregulation of HO-1 in BBdp rats?

Aim and Approach**:** The aim was to elucidate mechanisms associated with HO-1 upregulation in the pancreas and gut of BBdp rats using microarray and PCR array technologies. Candidate genes of interest would be validated by immunohistochemistry.

Rationale: As HO-1 upregulation has not been characterized in the BBdp rat, we wanted to gain a better understanding of what mechanisms, pathways and factors are involved in the pancreas and gut of BBdp rats after HO-1 induction. These experiments could identify novel gene products in both organs that could prove to be potential therapeutic targets.

Research Question 4: How is HO-1 expression in response to oral antigens different in BBc and BBdp lamina propria mononuclear cells (LPMC) and what is the microenvironment status associated with different stimulation?

Aim and Approach**:** The aim was to investigate the upregulation of HO-1 in LPMC from BBc and BBdp rats in response to pro-inflammatory stimuli, namely, LPS and WP. LPMC were isolated from BBc and BBdp rats and cultured for 4 days with these antigens and subsequently analyzed by flow cytometry for their expression of HO-1. Supernatants from these cultures were interrogated against a panel of cytokines and chemokines to characterize the microenvironment associated with different antigen stimulation.

Rationale: HO-1 is a cytoprotective enzyme that is generally known to be upregulated in response to oxidative stress resulting in production of antioxidants bilirubin, biliverdin and CO. MLN and rat insulinoma cells challenged with WP both showed upregulation of HO-1 but no such data are available for LPMC. Our lab demonstrated that WP-stimulated peripheral blood mononuclear cells (PBMCs) from T1D patients showed a mixed pro-inflammatory cytokine response with large amounts of IFN-γ, IL-17A, IL-6 and increased TNF (Mojibian, Chakir et al. 2009). In addition, a lamina propria-specific decrease in CD103 dendritic cells and increase in class II MHC^{+} cells has been shown, suggesting a pro-inflammatory status in the gut of BBdp rats compared with controls (Graham, Courtois et al. 2004). We sought to expand on these data and further characterize the lamina propria microenvironment in response to dietary antigens.

MATERIALS AND METHODS

Ethics Approval

All animal studies were approved by the University of Ottawa/OHRI Animal Care Committee.

Animal Husbandry and CoPP injections

A total of 64 BioBreeding diabetes-prone (BBdp) rats were housed at the OHRI Loeb Building animal care facility in static isolator cages under specific pathogen free conditions. The colony is antibody-free with respect to Sendai virus, Pneumonia virus of mice, Rat Caronavirus/Sialodacryoadentis virus, Kilham rat virus, Toolan's H-1 virus, Reovirus type 3, *Mycoplasma pulmonis*, Lymphocytic choriomeningitis virus, Mouse polio virus, *Encephalitozoon cuniculi*, Hanta virus, CAR bacillus, rat parvovirus, NS-1. BBdp rats were weaned at 23 d to a Teklad Global 18% protein rodent diet (Table 1, Harlan, Mississauga, ON). Cobalt protoporphyrin (CoPP, Frontier Scientific, Inc., Logan, UT) was dissolved in 10 mmol/l Tris base and the pH was adjusted to pH 7.8 with HCl. An equal number of male and female rats from five different litters were randomly assigned to CoPP or saline injections. Beginning at 30 days of age, BBdp rats received intraperitoneal (IP) injections of CoPP (6.5 mg/kg, n=33) or saline (n=31) twice per week (2-3 days apart) for three weeks (Figure 1A). At 51 d, animals (n=16 per group) were anaesthetized under 4% isoflurane in oxygen, weighed, and killed by exsanguination from the aorta. Jejunum, pancreas and spleen were dissected, weighed, and either snap frozen in liquid nitrogen or fixed in Bouin's fixative solution for 12 hours.

Table 1. Macronutrient composition of the Teklad Global 18% Protein Rodent Diet

Macronutrient Information	
Crude Protein	18.6%
Fat (ether extract)	6.2%
Crude Fiber	3.5%
Energy Density	3.1 kcal/g
Calories from Protein	24%
Calories from Fat	18%
Calories from Carbohydrate	58%

Diabetes Monitoring

Remaining rats (n=15-17 per group) were monitored for development of T1D until 120 d. Starting at 55 d, animals were tested twice a week for the presence of glucose in urine using Chemstrip uG/K glucose/ketone test strips (Roche Applied Science, Laval, QC). When urine glucose values were greater than 5 mmol/l (100 mg/dl), animals were fasted overnight, blood samples from the tail were obtained and glucose was measured using a glucometer. Animals were considered diabetic when fasting blood glucose levels were above 11.1 mmol/l (200 mg/dl). Animals were weighed on the same days as glucose readings which allowed for plotting of a growth curve during the course of the study. Diabetic and asymptomatic animals were euthanized as described, weighed, and organs were harvested for immunohistochemistry analyses. A survival curve analysis was performed for each group.

Immunohistochemistry

To obtain sections for immunohistochemistry (IHC), Bouin's fixed pancreas and jejunum sections from 51 d and end of study (EOS) CoPP or saline-treated BBdp rats were first rinsed thoroughly with 70% ethanol and then sent to the Pathology Department (University of Ottawa) for paraffin embedding and cutting into 5 μm sections. Hematoxylin and Eosin (H&E) staining was performed by Pathology Department staff to assess the morphology of tissues. For IHC, slides were de-waxed in CitriSolv (Thermo Fisher Scientific, Inc., Waltham, MA), rehydrated, and antigen retrieval was performed depending on the primary antibody used (Table 2). Slides were incubated with 5% BSA blocking buffer (5 g BSA in 100 mL 0.01M PBS, pH=7.6) for 30 minutes to reduce nonspecific binding after which primary antibodies were applied for 2 hours at room temperature or

Table 2. Antibodies, antigen retrieval and optimal conditions for DAB staining.

Primary Antibody	Dilution	Company	Secondary Antibody	Dilution	Antigen Retrieval
Rabbit anti-rat HO-1	1/1200	Abcam, Toronto, ON	Goat anti-rabbit (E0432)	1:300	Citric Acid – 10 Mins
Mouse anti-rat CD68 (ED1)	1/50	AbD Serotec, Raleigh, NC	Rabbit anti-mouse (E0354)	1:300	Citric Acid– 10 Mins
Mouse anti- rat CD163 (ED2)	1/100	Santa Cruz Biotechnology, Santa Cruz, CA	Rabbit anti-mouse (E0354)	1:300	0.05% Trypsin – 10 Mins
Guinea Pig anti-swine Insulin	1/200	Dako, Burlington, ON	Donkey anti-guinea pig	1:300	Citric Acid – 4 Mins
Anti-rat Foxp3 (FJK-16s)	1/100	eBioscience, San Diego, CA	Rabbit anti-rat (E0468)	1:300	Microwave – 20 Mins
Rabbit anti- mouse Reg3β (RB21532)	1/1500	Abgent, San Diego, CA	Goat anti-rabbit (E0432)	1:300	Citric Acid – 10 Mins
Rabbit anti-mouse Reg3γ (RB27078)	1/750	Abgent, San Diego, CA	Goat anti-rabbit (E0432)	1:300	Citric Acid – 20 Mins
Rabbit anti-mouse iNOS	1/12,800	Pierce Antibodies, Rockford, IL	Goat anti-rabbit (E0432)	1:300	No Retrieval
Goat anti-mouse KLF4	1/800	R&D Systems, Minneapolis, MN	Rabbit anti-goat (E0466)	1:600	Citric Acid – 10 Mins
Rabbit anti-mouse CAMP	1/3000	Abcam, Toronto, ON	Goat anti-rabbit (E0432)	1:300	Citric Acid – 10 Mins

overnight at 4°C. Sections were then incubated with the appropriate secondary antibody, a solution of avidin-biotin complex and eventually with a 0.06% 3,3'-diaminobenzidine (DAB; Sigma-Aldrich Canada, Oakville, ON) and 0.03% H_2O_2 (Ricca Chemical Company, Arlington, TX) solution to develop brown positive staining. It is important to note that all antibodies were initially subjected to a panel of antigen retrieval methods and appropriate positive and negative controls were included for each experiment. Both of these measures were performed to ensure that the given antigen was localized to the correct tissue, cell type, or subcellular localization and to eliminate false positive staining. Nuclear counterstaining was done with hematoxylin. Slides were viewed and scanned on an Axioplan 2 light microscope (Zeiss, Mississauga, ON) at 200X (gut) or 400X (islets) magnification and Northern Eclipse software was used for morphometric analyses. In some cases the ScanScope CS eSlide capture device (Aperio, Vista, CA) was utilized along with the ImageScope™ software (Aperio, Vista, CA).

Immunofluorescence

Immunofluorescence staining and confocal microscopy of pancreas and jejunum sections were performed to investigate the co-localization of markers of interest. Various antigen retrieval methods were utilized based on the primary antibodies of interest (Table 3). Sections were incubated with appropriate secondary antibodies conjugated to the following fluorophores: Cy3 – red, Alexa 488 – green, Cy5 – far red. Slides were then incubated with BSA blocking buffer before the addition of any other primary antibody. Nuclear counterstaining with Hoechst was performed. To avoid cross-reactivity with primary antibodies from the same host species (for example, CD68 & CD163 – both of mouse origin) it was crucial to include an additional step to mask one marker as a different

Table 3. Antibodies, antigen retrieval and fluorophores used for immunofluorescence.

Primary Antibodies (Dilution)	Secondary Antibodies (or Fluorophore-conjugated Secondary Antibodies)	Dilution	Fab	Fluorophore	Antigen Retrieval
CD68 (1/10) HO1 (1/50)	CD68: Donkey anti-mouse *Alexa 488* HO1: Goat anti-rabbit (E0432)	1/100 1/300	--	HO1: *Streptavidin-Cy3(1/400)*	Citric Acid – 10 Mins
CD163 (1/10) HO1 (1/50)	CD163: Donkey anti-mouse *Alexa 488* HO1: Goat anti-rabbit (E0432)	1/200 1/300	--	HO1: *Streptavidin-Cy3(1/400)*	0.05% Trypsin – 10 Mins
CD68 (1/10) CD163 (1/10) HO1 (1/50)	CD68: *Rabbit anti-mouse Cy5* HO1: Goat anti-rabbit (E0432)	1/100 1/300	CD163: Goat anti-mouse Fab (1/100)	CD163: Donkey anti-goat *Alexa 488 (1/200)* HO1: *Streptavidin-Cy3(1/400)*	0.05% Trypsin – 10 Mins
CD68 (1/10) KLF4 (1/50) HO1 (1/50)	CD68: *Rabbit anti-mouse Cy5* KLF4: *Donkey anti-goat Alexa 488* HO1: Goat anti-rabbit (E0432)	1/100 1/200 1/300	--	HO1: *Streptavidin-Cy3(1/400)*	Citric Acid – 10 Mins
CD204 (1/100) CAMP (1/200) CD163 (1/10)	CAMP: *Donkey anti-rabbit Cy3* CD163: *Rabbit anti-mouse Cy5*	1/300 1/100	CD204: Goat anti-rabbit Fab (1/100)	CD204: Donkey anti-goat *Alexa 488 (1/200)*	0.05% Trypsin – 10 Mins

species. In brief, an excess (1/100) of an unconjugated Fab fragment (in this case goat anti-mouse Fab, Jackson ImmunoResearch, Inc., West Grove, PA) was added to slides after the first primary antibody incubation, masking the mouse-derived primary antibody and presenting it as a goat species. Only after this point could the next mouse-derived primary antibody be safely added to the same slide. All slides were viewed on a Zeiss 510 Meta confocal microscope and image processing and editing was performed using ZEN LE 2009 (Zeiss, Mississauga, ON) and Northern Eclipse (Empix Imaging, Inc., Mississauga, ON) software.

Pancreatic Microarray Analysis

Approximately 30 mg of pancreatic tissue from the body of the organ was harvested from 51 d saline and CoPP-treated BBdp rats (n=8/group). Due to the rapid degradative properties of enzymes released from the pancreas, it was crucial to minimize the time between excising the tissue and homogenizing it in tubes containing pre-cooled β-mercaptoethanol and kit-provided buffer and quickly snap freezing tubes in liquid nitrogen. Total pancreatic RNA was isolated using the Nucleospin RNA “L” RNA Isolation Kit (Machery-Nagel, Bethlehem, PA) according to the manufacturer’s protocol. RNA quantity and integrity was evaluated on a 6000 Nano LabChip using an Agilent 2100 Bioanalyzer (OHRI Stemcore Laboratories). Samples from each group of eight were pooled in 5 μL aliquots with a final concentration of 100 ng/μL and sent to StemCore Laboratories for analysis. Global gene expression in 51 d saline and CoPP-treated BBdp pancreata was compared using Affymetrix Rat Gene 1.0 ST microarrays. CEL files were processed using the AltAnalyze software (UCSF, CA) and a list of genes that were increased or decreased was generated.

Bioinformatics

In order to obtain functional interpretation of the generated genes, we utilized DAVID (Database for Annotation, Visualization and Integrated Discovery, NIH) to analyze the data. DAVID is an online bioinformatics resource that provides a set of tools to aid in extracting biological meaning from large gene lists by providing information about the biological processes and functions of genes (Jiao, Sherman et al. 2012). ENSEMBL gene IDs from genes upregulated more than 1.5 fold were uploaded into the DAVID online database tool in order to rank the overall importance (enrichment) of gene groups. The enrichment score is the geometric mean of all the enrichment *p*-values for each annotation term associated with the gene members in the group. A higher score for a group indicates that the gene members in the group are involved in more important (enriched) terms in a given study (Huang da, Sherman et al. 2009). Groups with the highest enrichment scores and with the lowest *p*-values were considered to be candidate genes of interest and were validated by IHC.

Jejunal PCR Array Analysis

Approximately 2 cm of frozen small intestine (jejunum) from 51 d saline or CoPP treated BBdp rats (n=8/group) were obtained and total RNA was isolated using the Nucleospin RNA II RNA Isolation Kit (Machery-Nagel, Bethlehem, PA) according to the manufacturer’s protocol. RNA quantity and integrity was evaluated as described above, after which cDNA was synthesized using the RT^2 First Strand Kit (SABiosciences/Qiagen, Mississauga, ON). Samples were analyzed using RT^2 profiler PCR quantitative arrays for “Innate and Adaptive Immune Responses” (PARN-052A, SABiosciences/Qiagen, Mississauga, ON) which profiles the expression of 84 genes involved in the host response to bacterial infection and sepsis. A total of 6 PCR Arrays was used (1 sample/array) to evaluate gene expression in jejunum tissue from three biological replicates per BBdp treatment group: 3 saline treated samples and 3 CoPP treated samples. A cutoff of 2 fold with *p* values less than 0.05 was used to identify genes up or down-regulated by CoPP treatment.

Isolation and culturing of LPMC

LPMC were purified from the small intestine of approximately 53 d cereal-fed BBc and BBdp rats (n=5/group) using an established protocol (Lefrancois and Lycke 2001) and modified in our lab. It is important to note that these were not from the cohort of animals receiving the CoPP or saline injections. Rats were anaesthetized under 4% isoflurane in oxygen, killed by exsanguination from the aorta, and the small intestine was harvested. The gut lumen was flushed with cold HBSS (Hank's Balanced Salt Solution, Gibco, Burlington, ON) containing an antibiotic-antimycotic solution (Gibco, Burlington, ON) to remove any residual fecal material. Peyer's patches were excised and the gut was opened longitudinally and cut into 0.5-1 cm wide pieces. Gut pieces were washed twice more with cold HBSS and then incubated in a chelation buffer made of HBSS containing 2 mM EDTA for 15 min in a rotating hybridization incubator (Robbins Scientific Corporation, Sunnyvale, CA) at 37°C and then washed vigorously with cold HBSS. This process was repeated twice to remove the epithelial cell layer. The remaining intestinal fragments were then digested twice (digestion 1 = 30 min, digestion 2 = 15 min) with RPMI containing 0.8 mg/ml collagenase Type VIII (Sigma-Aldrich, Oakville, ON) and 10 U/ml of DNase I (Roche Applied Science, Laval, QC) in the rotating hybridization incubator at 37°C. After the digestions, the intestinal fragments were shaken vigorously to disrupt the lamina propria matrix and the supernatant was collected. RP-10 (RPMI-1640 (Gibco, Burlington, ON) supplemented with 10% heat-inactivated Fetal Bovine Serum (Thermo Fisher Scientific, Inc., Waltham, MA), antibiotic-antimycotic solution (Gibco, Burlington, ON), and 50 μM mercaptoethanol) was added to the supernatant which was then strained through a 100 μm cell strainer. Cells were washed and pelleted 3 times with RP-10, resuspended in media and underlayed with warmed Histopaque-1077 gradient (Ficoll; Sigma-Aldrich, Oakville, ON). Cells were spun for 30 minutes on a Beckman-Coulter Allegra^{TM} 6KR centrifuge at 514 *x g* (without brake) to remove dead cells. After removing the buffy coat containing live cells and 3 washes with RP-10 to remove residual Ficoll, the total number of live cells was calculated using the Trypan blue exclusion assay. BBc and BBdp LPMC were seeded in 24 or 48-well plates at 1 x 10^6 cells/well or 0.5 x 10^6 cells/well, respectively, in RP-10. As negative controls, cells were incubated with medium alone or in the presence of chicken egg ovalbumin protein (OVA, 45 μg/mL). As a positive control, cells were incubated with lipopolysaccharide (LPS, 10 μg/mL). Cells were incubated with a solution of partially α-chymotrypsin-digested wheat peptides (WP, 12.5 μg/mL). Cells were incubated at 37°C in 5% CO_2 for 4 days.

Flow Cytometry

Supernatants were collected before cell harvesting and frozen for subsequent analysis of soluble cytokines and chemokines. Standard flow cytometry protocols were used to analyze intracellular HO-1 in cultured LPMC (Caraher, Parenteau et al. 2000; Mojibian, Chakir et al. 2009). In brief, approximately 0.5 x 10^6 cells were added to tubes, washed and pelleted with 1 mL of FACS buffer (1% BSA (w/v) in IsoFlow sheath fluid (Beckman Coulter, Inc., Fullerton, CA)) by centrifugation at 514 *x g* for 5 minutes. Permeabilizing the cells is necessary for intracellular staining and this was performed using the FOXP3 Fix/Perm Buffer Set (BioLegend, Inc., San Diego, CA). In brief, cells were fixed with a 1X FOXP3 Fix/Perm buffer (4X stock diluted 1:3 in PBS) for 20 minutes, washed, and permeabilized with a 1X FOXP3 Perm buffer (10X diluted stock 1:9 in PBS) for 15 minutes and washed once more. Cells were then resuspended in 100 μl of FACS buffer containing the primary antibody (Table 4) and left to incubate in the dark for 30 minutes and then washed once more. A final step of adding FACS buffer containing a

Table 4. Antibodies and fluorophores used for LPMC staining of HO-1 for flow cytometry

Primary Antibody	Volume	Company	Fluorophore-conjugated Secondary Antibody	Volume	Company
Mouse anti-rat HO-1	1 µL	Abcam, Toronto, ON	Goat Anti-Mouse (PE-TR) IgG2a (γ)	1 µL	Caltag Laboratories, Burlingame, CA

fluorochrome-conjugated secondary was performed, followed by washing with FACS buffer. Isotype controls and appropriate compensations were used for multi-color staining. Cells were resuspended in 350 μl of FACS buffer and analyzed using an FC500 flow cytometer (Beckman Coulter, Inc., Mississauga, ON). Cytomics™ CXP analysis software (Beckman Coulter, Inc., Mississauga, ON) was used for post-run analyses.

Cytokine/Chemokine Array

Culture supernatants from BBc and BBdp LPMC stimulated with 45 μg/mL OVA or 12.5 μg/mL of chymotrypsin-treated WP for 4 days were pooled (n=8/treatment). Pooled samples were analyzed using the Proteome Profiler Rat Cytokine Antibody Array (ARY008, R&D Systems, Minneapolis, MN) which simultaneously measures the expression of 29 cytokines and chemokines. In brief, pooled supernatant samples were mixed with a cocktail of biotinylated detection antibodies and incubated on nitrocellulose membranes spotted with capture antibodies which bind to specific target proteins. Cytokine + detection antibody complexes were bound by their cognate immobilized capture antibody on the membrane and Streptavidin-HRP and chemiluminescent detection reagents were added sequentially where light is produced at each spot in proportion to the amount of cytokine bound. Membranes were exposed to X-ray film and pixel densities were quantified by dividing the intensity of a spot over the total spot densities of a given membrane using Kodak image station 440CF (Eastman Kodak, Rochester, NY) (Hamelinck, Zhou et al. 2005). These pixel density values were used to generate bar graphs to graphically compare differential cytokine and chemokine expression between rat strains.

Insulitis Evaluation

Insulitis was evaluated on hematoxylin and eosin-stained sections of pancreata from 51 and 120 d BBdp rats treated with CoPP or saline at 400X magnification using the ScanScope CS eSlide capture device (Aperio, Vista, CA) and analyzed using the ImageScope™ software (Aperio, Vista, CA). A subjective overall rating of islet infiltration/damage (containing 5 or more mononuclear cells infiltrating) was determined using a previously established scoring system (Hoorfar, Scott et al. 1991). The extent of insulitis was determined by giving a score per islet and obtaining a mean score per animal. Data are presented as percentage of islet inflammation which encompasses values for both peri-insulitis and insulitis.

Statistical Analyses

Survival curve was generated on GraphPad Prism 3.0 software (GraphPad Software, La Jolla, CA) using the Kaplan–Meier method and survival analyses were performed using the log-rank test and Fisher's exact test (two-tailed) to compare final diabetes incidence between treatment groups. For morphometric analyses, means were calculated and differences among populations were compared using one-way analysis of variance (ANOVA) or Student's t-test. All statistics were performed using STATISTICA software, version 6.0 (StatSoft, Tulsa, OK). A p value less than 0.05 was considered significant. Data are presented as means ± standard deviation (SD).

RESULTS

HO-1 induction prevents T1D in BBdp rats

CoPP-treated animals were protected from diabetes compared with saline-treated animals (29% vs 73% incidence, p=0.01, log rank; p=0.03, Fisher's exact test, Figure 1B). Morphometric analyses of HO-1 expression in pancreas and jejunum sections of 51 d CoPP-treated BBdp rats revealed a significant increase in HO-1^+ cells associated with islets as well as in the lamina propria compared with saline-treated controls (Figure 1C). A growth curve was generated to assess effects of CoPP on growth and development; body mass was analyzed separately for each gender. There was no difference between CoPP or saline treated rats for both female and male BBdp rats at both 51 d and 120 d (Figure 2A, 2B). Pancreas mass was significantly higher in 51 d CoPP-treated BBdp rats compared with saline controls but no such difference was seen in asymptomatic rats at 120 d (Figure 2C). To assess β-cell status, insulin was stained in pancreas sections of saline and CoPP-treated BBdp rats at 51 d and 120 d (Figure 3A, 3B). There was no significant difference in β-cell area fraction (insulin area/pancreas section area) between treatment groups at either time point (Figure 3C). There was significantly less mononuclear cell infiltration (insulitis) in CoPP-treated BBdp rats compared with controls at both 51 d and ~120 d of age (Figure 4). H&E sections also allowed for analysis of tissue morphology and it was noted that pancreatic tissue from CoPP-treated rats had more fibrous connective tissue dispersed throughout and disconnected acinar lobes than in saline-treated pancreatic tissue.

Figure 1. Prevention of T1D by CoPP in diabetes-prone rats. (A) Experimental design for induction of HO-1 in cereal-fed BBdp rats injected with either saline or CoPP (6.5 mg/kg) twice a week for three weeks. Eight rats from each group were euthanized at 51 d for interim analyses; remaining rats from each group were monitored until approximately 120 d for development of diabetes. **(B)** Treatment with CoPP protected BBdp rats from developing diabetes (*p=0.01, log-rank test; final incidence, 29% vs. 73%, p=0.03, Fisher's exact*) **(C)** Morphometric analysis revealed a significant increase in $HO\text{-}1^{+}$ cells in pancreas and gut lamina propria of 51 d CoPP-treated animals compared with saline controls. Data are expressed as means ± SD. (Bars = 50 μm)

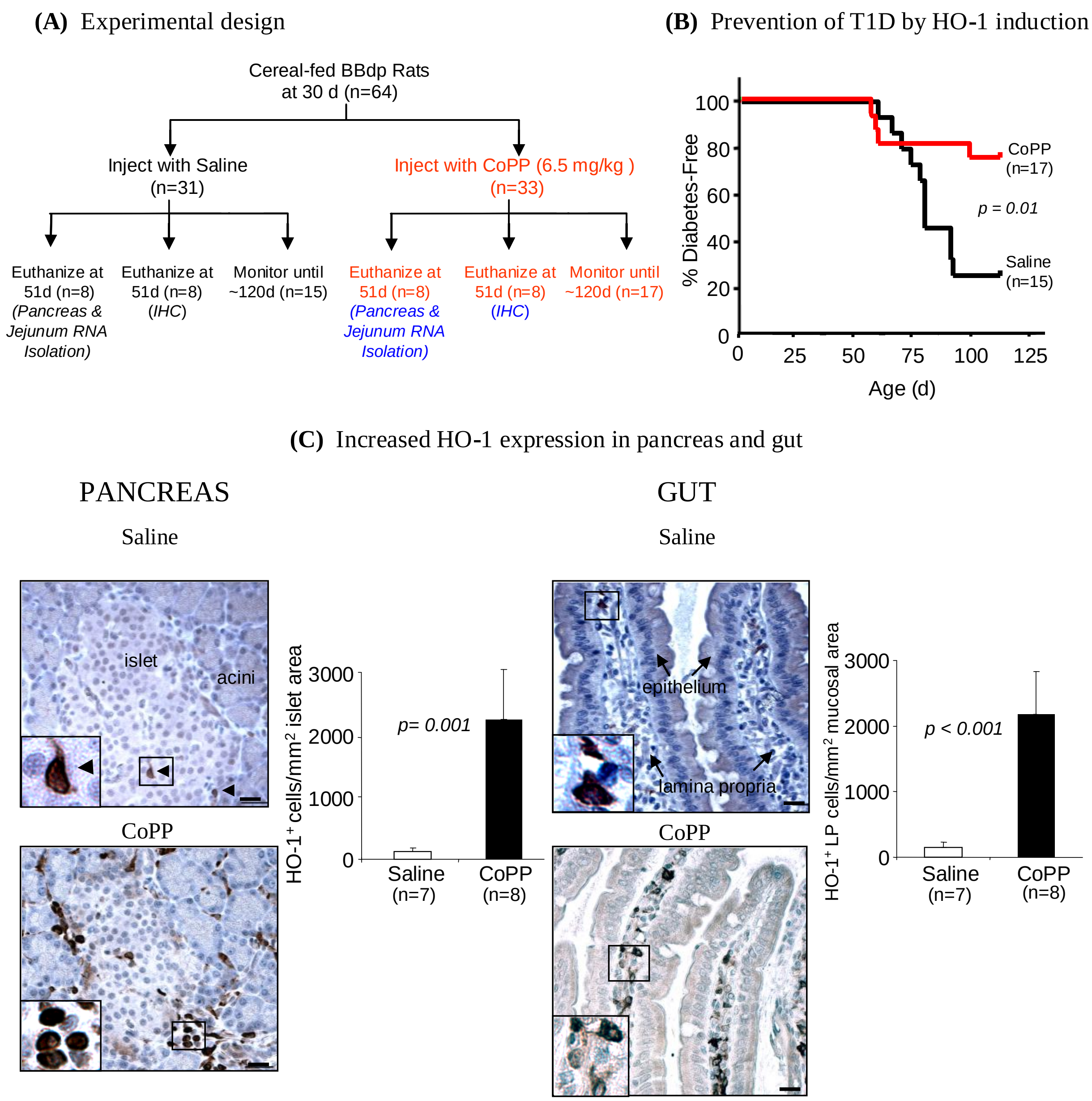
(A) Experimental design
Cereal-fed BBdp Rats at 30 d (n=64)
Inject with Saline (n=31)
Inject with CoPP (6.5 mg/kg) (n=33)
Euthanize at 51d (n=8) (Pancreas & Jejunum RNA Isolation)
Euthanize at 51d (n=8) (IHC)
Monitor until ~120d (n=15)
Euthanize at 51d (n=8) (Pancreas & Jejunum RNA Isolation)
Euthanize at 51d (n=8) (IHC)
Monitor until ~120d (n=17)
(B) Prevention of T1D by HO-1 induction
% Diabetes-Free
0
20
40
60
80
100
0
25
50
75
100
125
Age (d)
CoPP (n=17)
p = 0.01
Saline (n=15)
(C) Increased HO-1 expression in pancreas and gut
PANCREAS
Saline
islet
acini
CoPP
HO-1+ cells/mm2 islet area
0
1000
2000
3000
p= 0.001
Saline (n=7)
CoPP (n=8)
GUT
Saline
epithelium
lamina propria
CoPP
HO-1+ LP cells/mm2 mucosal area
0
1000
2000
3000
p < 0.001
Saline (n=7)
CoPP (n=8)

Figure 2. CoPP treatment increases total pancreas mass but does not affect animal growth. (A) Growth curve of BBdp rats throughout duration of experiment (treatment groups separated by gender). **(B)** No difference in body mass between treatment groups of **(i)** pre-diabetic (51 d) and **(ii)** asymptomatic (~120 d) BBdp rats for both genders receiving saline or CoPP injections. **(C)** Total pancreas mass is increased in **(i)** pre-diabetic but not in **(ii)** asymptomatic CoPP-treated BBdp rats compared with controls. Data are expressed as means ± SD.

(A) Growth Curve

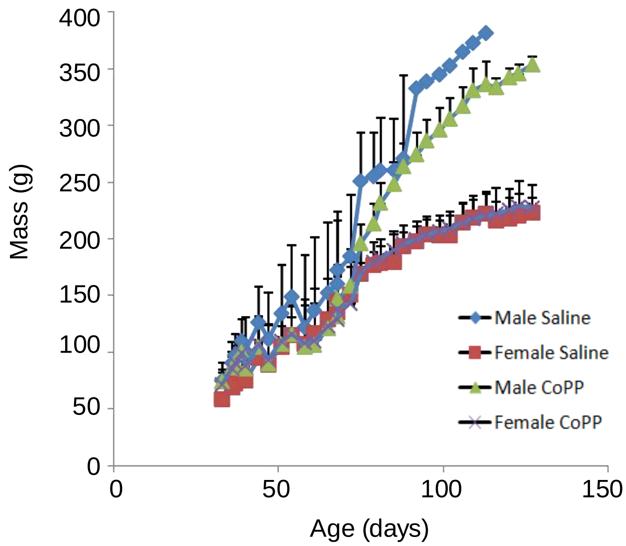

(B) Body Mass Differences by Gender

(i) Pre-diabetic period (51 d)

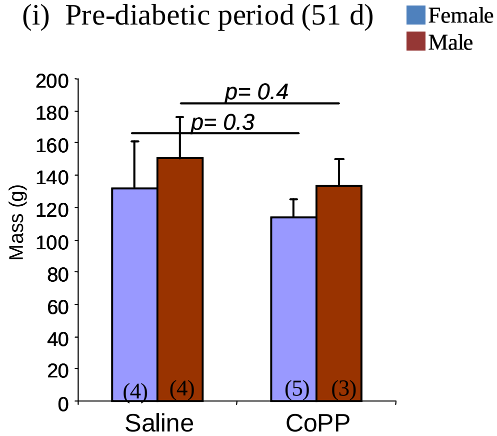

(ii) Asymptomatic – End of Study(~120 d)

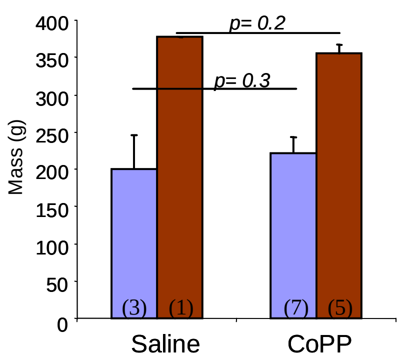

(C) Ratio of Whole Pancreas Mass/Body Mass

(i) Pre-diabetic period (51 d)

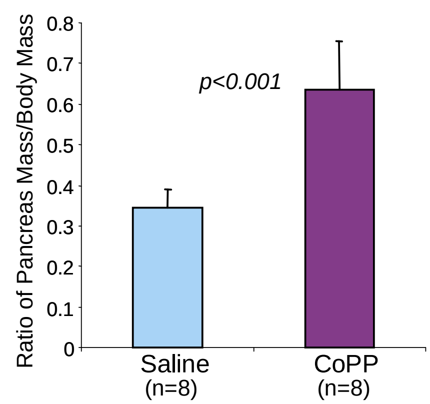

(ii) Asymptomatic – End of Study (~120 d)

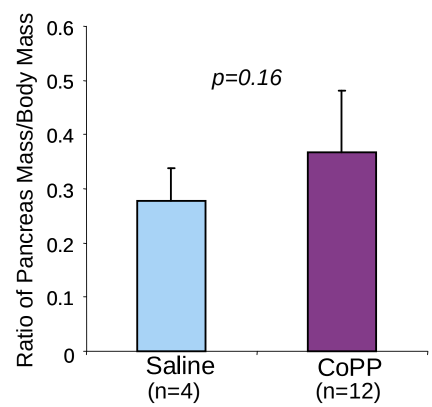

Figure 3. β-cell area unaffected by CoPP treatment. Representative superimages of pancreata from 51d **(A)** saline-treated and **(B)** CoPP-treated BBdp rats stained with anti-insulin polyclonal antibody. (Bars = 1000 μm) **(C) β-cell area fraction analysis** (insulin$^+$ area/pancreas section area) revealed no difference between the treatment groups in both **(i)** pre-diabetic (51 d) and in **(ii)** asymptomatic (~120 d) BBdp rats. Data are expressed as means ± SD.

(A) Saline

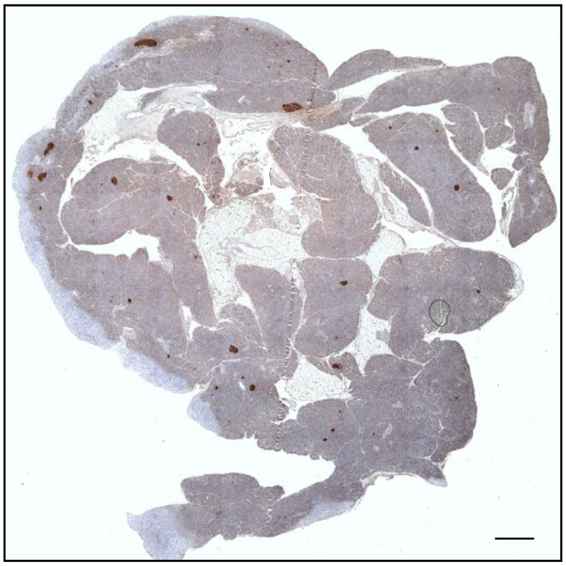

(B) CoPP

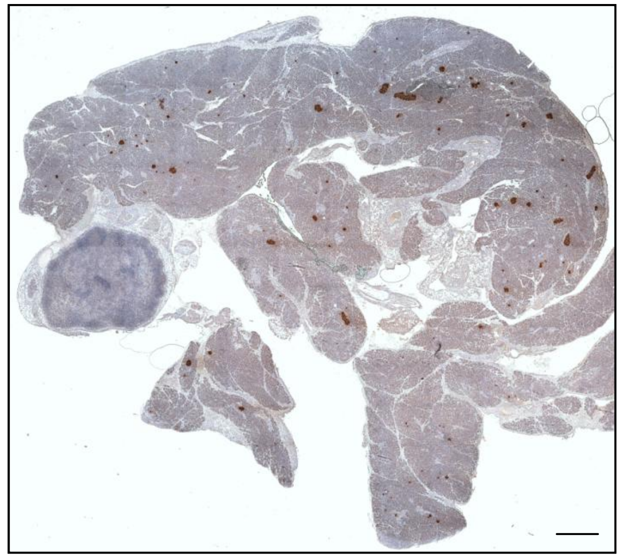

(C) β-cell Area Fraction

(i) Pre-diabetic period (51 d)

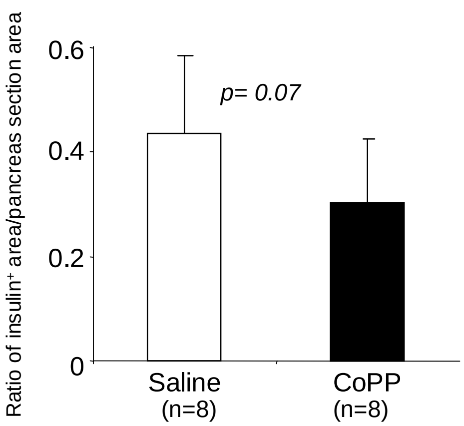

(ii) Asymptomatic – End of Study (~120 d)

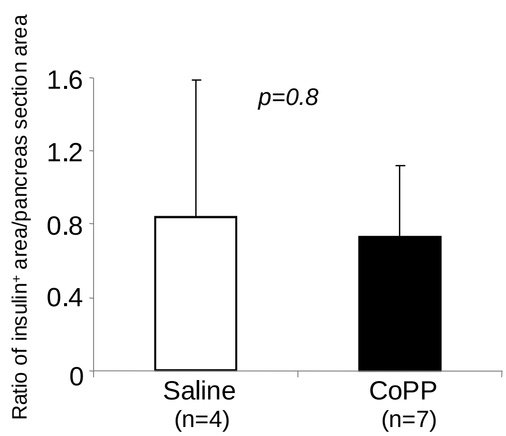

Figure 4. Less insulitis in CoPP-treated rats. Hematoxylin and eosin (H&E) stained pancreatic sections showing **(A)** a healthy islet from a CoPP-treated asymptomatic 120 d BBdp rat, **(B)** peri-insulitis with early mononuclear cells entering the islet, **(C)** mononuclear cell infiltration (insulitis) in the islet of a saline-treated 120 d BBdp rat, and **(D)** an end-stage infiltrated and damaged islet of a diabetic BBdp rat. Islet infiltration was less frequent in CoPP-treated rats compared with controls at both ages. Insulitis was evaluated based on a subjective overall rating of islet infiltration and damage using a previously established scoring system. Percentage of inflamed islets encompasses islets with peri-insulitis and frank insulitis. The number of animals analyzed is indicated and data are expressed as means ± SD. Asterisks denote statistical significance compared with saline-treated controls (**t*-test: $p < 0.05$). (Bars = 50 μm)

(A) Healthy Islet

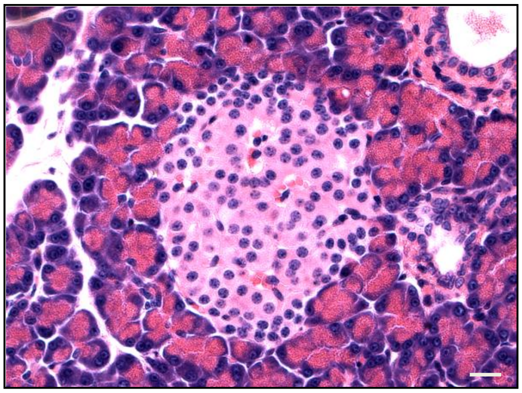

(B) Peri-insulitis

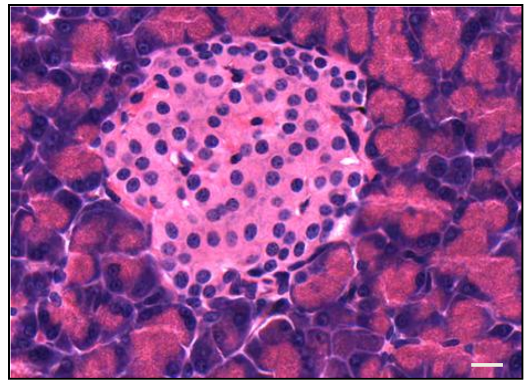

(C) Insulitis

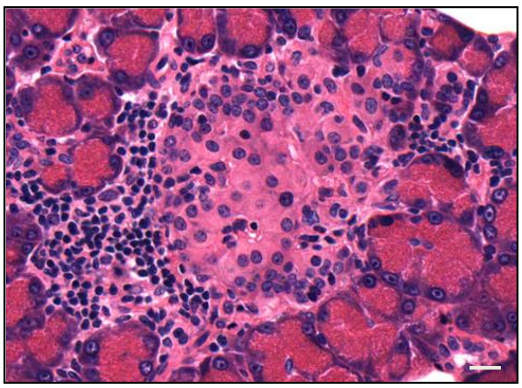

(D) Damaged Islet

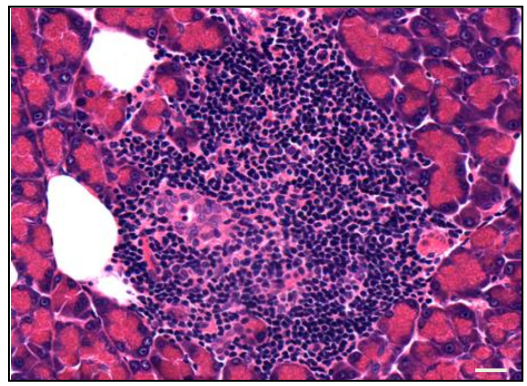

Age	*51 d*		*~120 d*	
Diabetes	Pre-diabetic		Asymptomatic	
Treatment	Saline	CoPP	Saline	CoPP
Number (*n*)	8	8	3	12
Inflamed Islets (%)	37.7 ± 9.0	23.2 ± 13.8*	73.4 ± 7.6	40.3 ± 10.5*
Healthy Islets (%)	62.3 ± 9.0	76.9 ± 13.8*	26.6 ± 7.6	59.7 ± 10.5*

HO-1 induction alters macrophage phenotypes

To investigate the potential protective mechanisms, pancreas and gut sections were stained for CD68 (a pan-macrophage marker, considered by some to be an M1 pro-inflammatory macrophage marker) and CD163 (a marker of M2 tolerogenic macrophages). CD68 and HO-1 expression was increased in the pancreatic lymph nodes (PLN) of 51 d CoPP-treated BBdp rats compared with controls (Figure 5A,5B). CoPP treatment was also associated with changes in staining pattern of $CD163^+$ cells and stronger intensity of $Foxp3^+$ cells in the pancreatic lymph nodes (PLN) of 51 d BBdp rats compared with controls (Figure 5C,5D). There was a significant increase in the number of $CD68^+$ cells localized inside islets or associated with islets in pancreata of 51 d CoPP-treated BBdp rats compared with controls (Figure 6). $CD163^+$ cells were localized in connective tissue and around islets, but were not as frequent as $CD68^+$ cells (Figure 7).

The expression of HO-1, CD68, and CD163 in 51 d and 120 d BBdp rats treated with CoPP or saline was analyzed. In saline-treated controls, there was no difference in HO-1 expression between the time points however CoPP-treated animals showed a significant ($p<0.001$) decrease in HO-1 expression at 120 d compared with 51 d (Figure 8A). Saline-treated controls showed a significant increase in CD68 expression in and around islets over time ($p=0.01$) while CoPP-treated animals did not ($p=0.3$) (Figure 8B). Both saline and CoPP-treated BBdp rats showed a significant increase in CD163 expression around islets in 120 d rats compared with 51 d rats (Figure 8C). As in the pancreas, CoPP-treated BBdp rats showed significantly less HO-1 expression in the lamina propria at 120 d compared with 51 d (Figure 8A). Both saline and CoPP-treated BBdp rats showed a significant decrease in CD68 expression in the lamina propria

Figure 5. HO-1 induction affects PLN composition. Representative images (n=4-5/group) show that CoPP caused an increase in **(A)** HO-1^+ and **(B)** $CD68^+$ cells in pancreatic lymph nodes of 51d BBdp rats compared with saline controls. CoPP also changed localization of **(C)** $CD163^+$ and **(D)** $FoxP3^+$ cells in PLNs of 51 d BBdp rats compared with saline controls. (Bars = 200 μm)

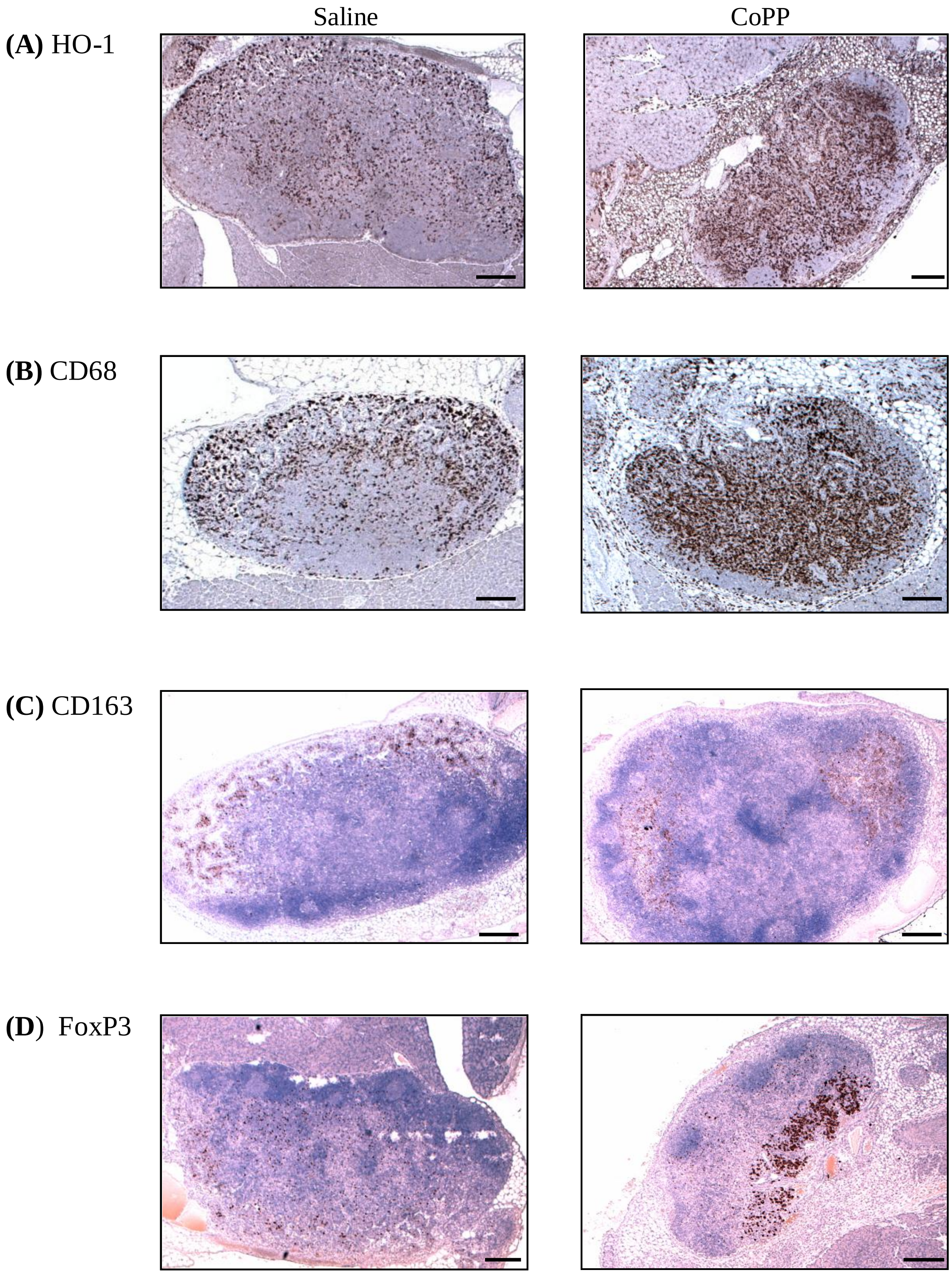
Saline
CoPP
(A) HO-1
(B) CD68
(C) CD163
(D) FoxP3

Figure 6. CoPP increases CD68^{+} cells in pancreas. HO-1 upregulation by CoPP is associated with an increase in CD68^{+} cells **(A)** in and around islets but not in the **(B)** lamina propria of 51 d CoPP-treated BBdp rats compared with saline controls. Data are expressed as means ± SD (Bars = 50 μm)

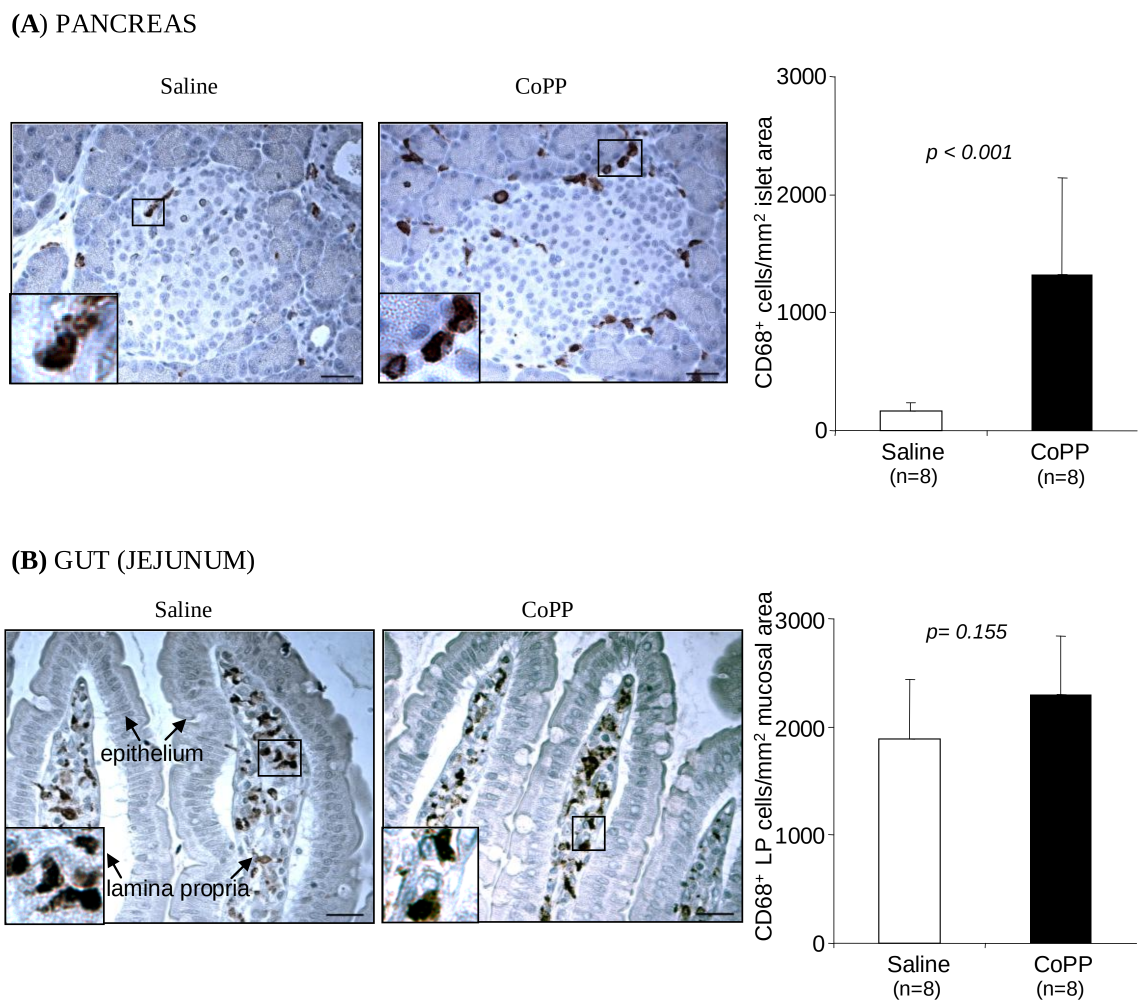
(A) PANCREAS
Saline
CoPP
3000
2000
1000
0
CD68+ cells/mm2 islet area
p < 0.001
Saline
(n=8)
CoPP
(n=8)
(B) GUT (JEJUNUM)
Saline
CoPP
epithelium
lamina propria
3000
2000
1000
0
CD68+ LP cells/mm2 mucosal area
p= 0.155
Saline
(n=8)
CoPP
(n=8)

Figure 7. No change in $CD163^+$ cells in pancreas and gut. HO-1 upregulation by CoPP has no effect on $CD163^+$ cells **(A)** in and around islets as well as **(B)** in the lamina propria of 51 d CoPP-treated BBdp rats compared with saline controls. Data are expressed as means ± SD (Bars = 50 μm)

(A) PANCREAS

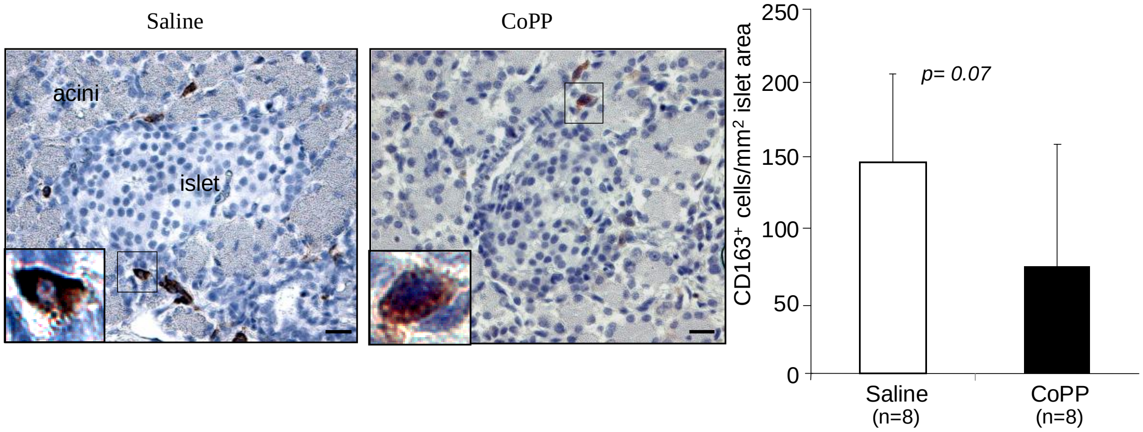

(B) GUT (JEJUNUM)

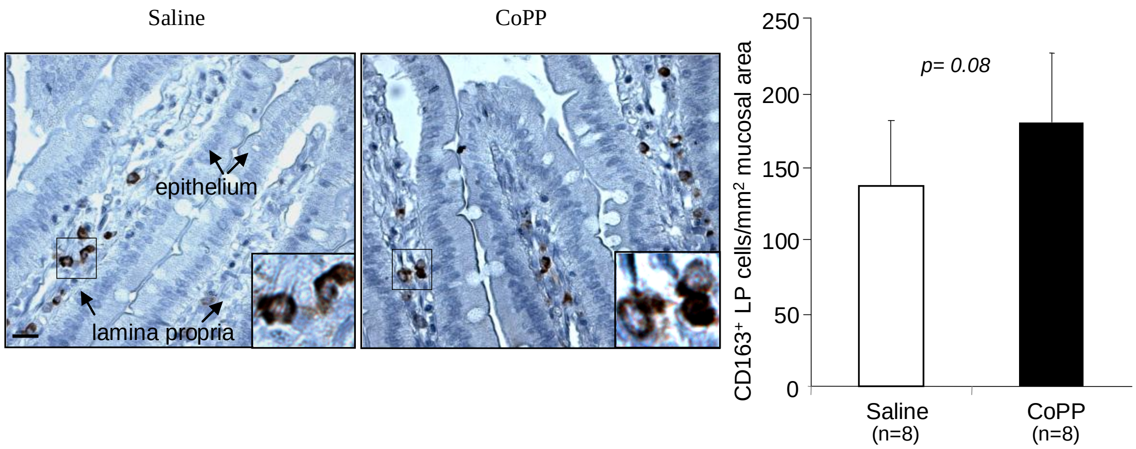

Figure 8. Comparison of HO-1, CD68, and CD163 expression in pancreas and gut in pre-diabetic (51 d) and asymptomatic (~120 d) animals. **(A)** HO-1 expression is significantly decreased in 120 d (EOS) BBdp rats compared to 51 d in both pancreas and gut. **(B)** CD68 expression is significantly elevated in the pancreas of 120 d saline-injected BBdp rats compared to 51 d saline controls. **(C)** CD163 expression was significantly increased at 120 d in both saline and CoPP-treated rats compared to 51 d in both the pancreas and lamina propria. Asterisks denote statistical significance compared with pre-diabetics (51 d). Data are expressed as means ± SD.

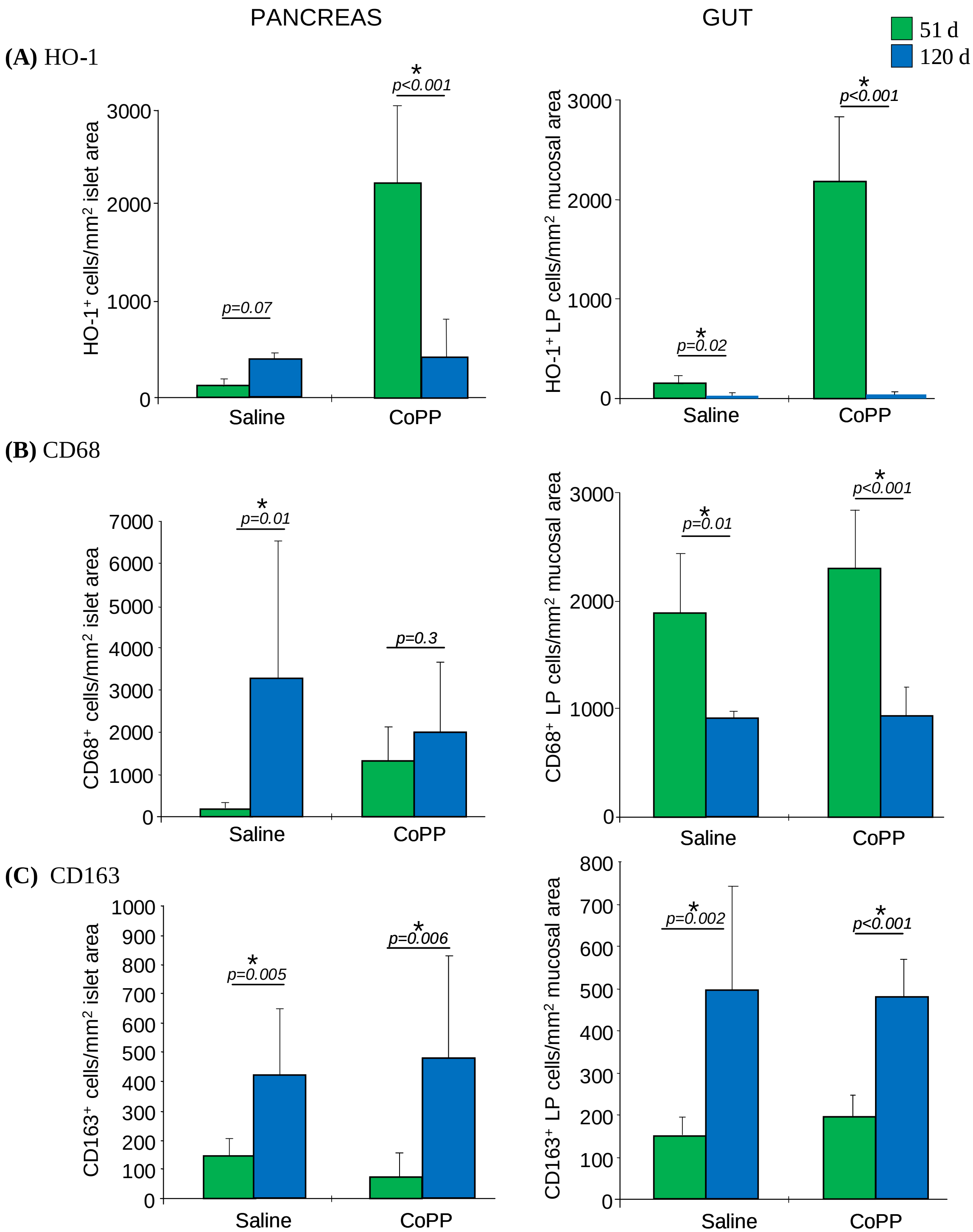
PANCREAS
GUT
51 d
120 d
(A) HO-1
HO-1+ cells/mm2 islet area
3000
2000
1000
0
p=0.07
*
p<0.001
Saline
CoPP
HO-1+ LP cells/mm2 mucosal area
*
p=0.02
*
p<0.001
(B) CD68
CD68+ cells/mm2 islet area
7000
6000
5000
4000
*
p=0.01
p=0.3
CD68+ LP cells/mm2 mucosal area
*
p=0.01
*
p<0.001
(C) CD163
CD163+ cells/mm2 islet area
1000
900
800
700
600
500
400
300
200
100
*
p=0.005
*
p=0.006
CD163+ LP cells/mm2 mucosal area
*
p=0.002
*
p<0.001

between time points (*$p=0.01$* and *$p<0.001$*, respectively). Both treatment groups also had a significant increase in lamina propria CD163 expression between time points (*$p=0.002$* and *$p<0.001$*, respectively) (Figure 8B,8C).

Co-localization of markers

Confocal analyses of pancreas and jejunum sections of CoPP-treated animals demonstrated that HO-1 expression was mainly in $CD68^+$ macrophages. We found $CD68^+HO\text{-}1^+$ macrophages associated with islets in pancreas sections of 51 d CoPP-treated BBdp rats as well as in the lamina propria (Figure 9). Distinct populations of $CD163^+HO\text{-}1^+$ macrophages were associated with islets (Figure 10A) and in the pancreatic lymph nodes in CoPP-treated BBdp rats. These double positive cells were also found in the connective tissue interspersed between acini (Figure 10B). An additional population of $CD68^+CD163^+HO\text{-}1^+$ cells was identified in both pancreas and jejunum of 51 d CoPP-treated BBdp rats. These triple positive cells were found in the lamina propria, associated with islets and dispersed throughout connective tissue as well as in the pancreatic lymph nodes (Figure 11).

Microarray gene expression analysis of pancreas

Gene expression analysis was performed in the pancreas after HO-1 induction using Affymetrix Rat Gene 1.0 ST chips and lists of up and down-regulated genes were generated. Top upregulated hits included lipid-related genes encoding intestinal fatty acid binding protein (*Fabp1* - upregulated ~300 fold) and gastrotropin (*Fabp6* – upregulated ~250 fold). Of particular interest was the increase in gene expression of the *Reg* and *α-defensin* family of genes in pancreata of CoPP-treated BBdp rats compared with controls (Figure 12A). Group enrichment analysis using DAVID online bioinformatics software

Figure 9. Co-localization of CD68 and HO-1 in pancreas and gut. Immunofluorescence labeling of **(A)** pancreas and **(B)** jejunum sections of 51d CoPP-treated BBdp rat with antibodies to CD68 (Alexa 488) and HO-1 (Cy3). Arrows indicate double positive $CD68^{+}HO\text{-}1^{+}$ cells. (Bars = 20 μm)

(A) Pancreas - Connective tissue between acini

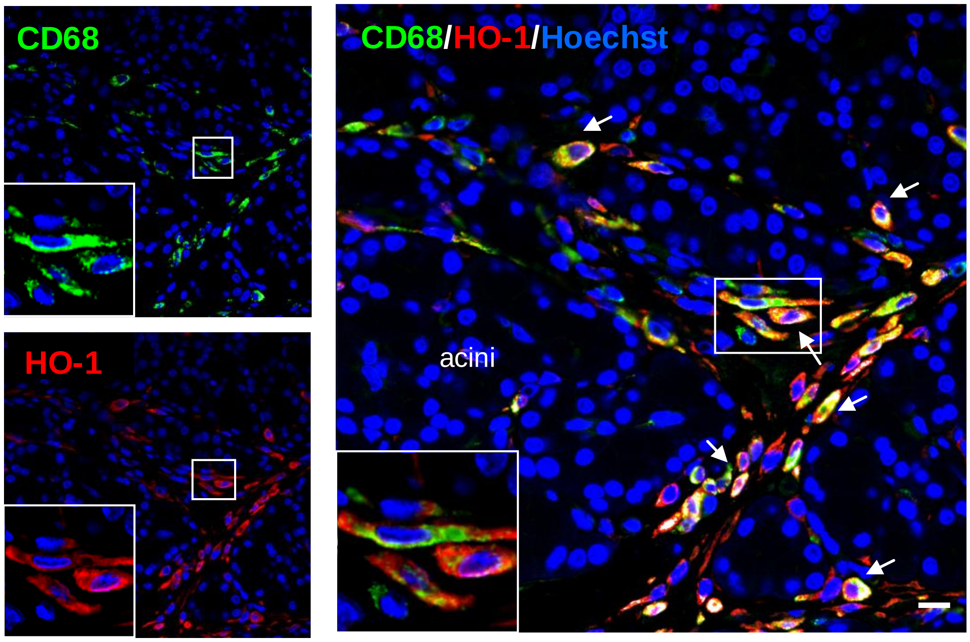

(B) Gut - Lamina propria

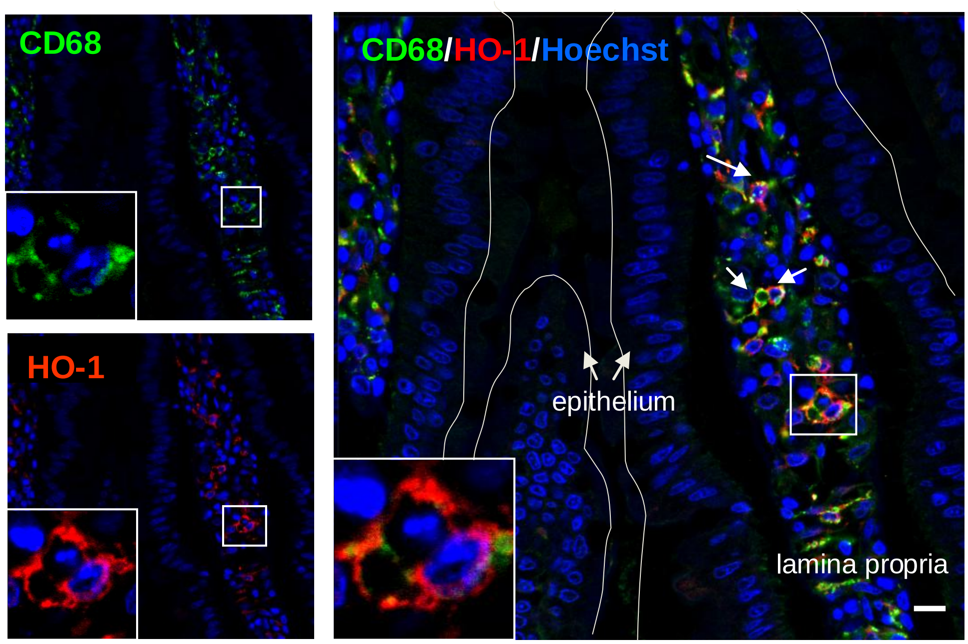

Figure 10. Co-localization of CD163 and HO-1 in pancreas. Immunofluorescence labeling of pancreas section of 51d CoPP-treated BBdp rat with antibodies to CD163 (Alexa 488) and HO-1 (Cy3). Arrows indicate double positive $CD163^{+}HO\text{-}1^{+}$ cells **(A)** associated with islet and **(B)** dispersed throughout connective tissue between acinar lobes. (Bars = 20 μm)

(A) Pancreas – Intra-islet and islet-associated

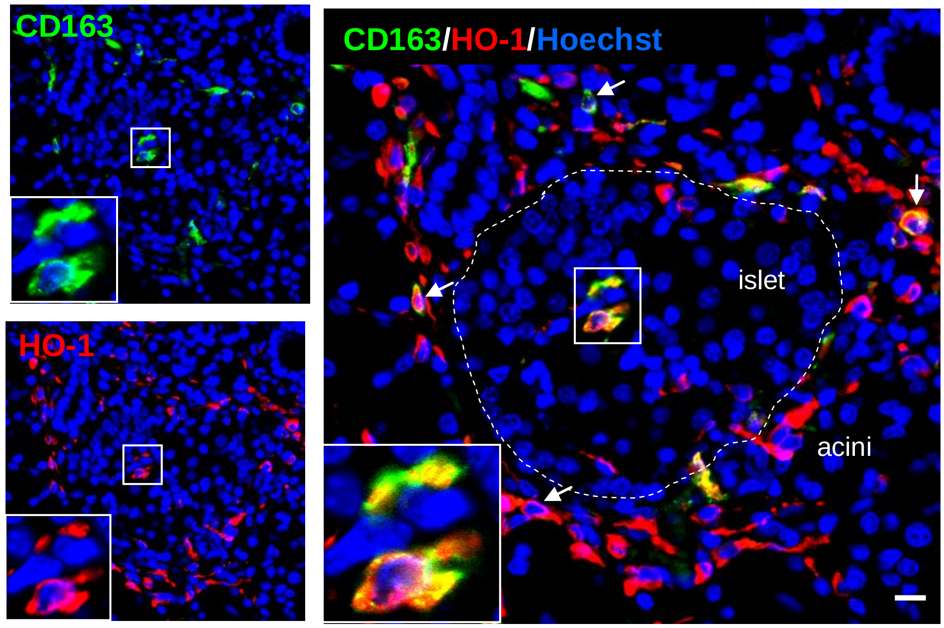

(B) Pancreas – Connective tissue between acini

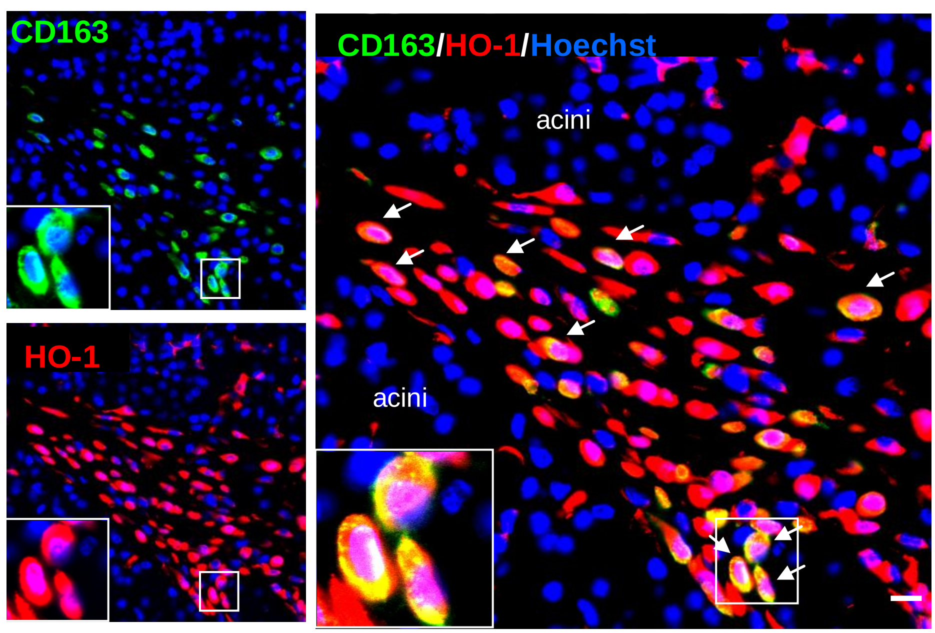

Figure 11. Co-localization of CD68, CD163 and HO-1 triple positive cells in pancreas and gut. Immunofluorescence labeling of **(A)** jejunum and pancreas (**(B)** islet, **(C)** PLN, **(D)** connective tissue between acini) sections of 51 d CoPP-treated BBdp rat with antibodies to CD68 (Cy5), CD163 (Alexa 488) and HO-1 (Cy3). CD163 primary antibody was first blocked with an excess of unconjugated goat anti-mouse Fab fragment to avoid same species cross-reactivity with CD68. Arrows indicate triple positive $CD68^{+}CD163^{+}HO\text{-}1^{+}$cells. (Bars = 20 μm)

(A) Gut

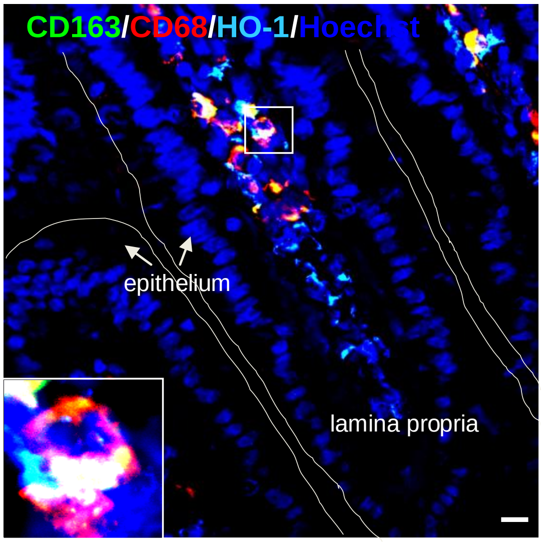

(B) Islet

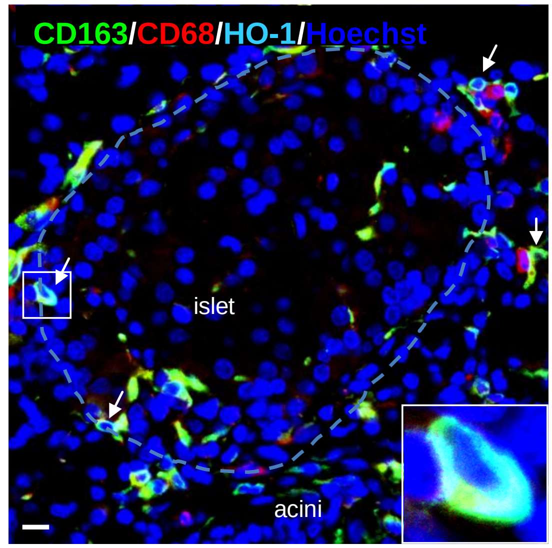

(C) PLN

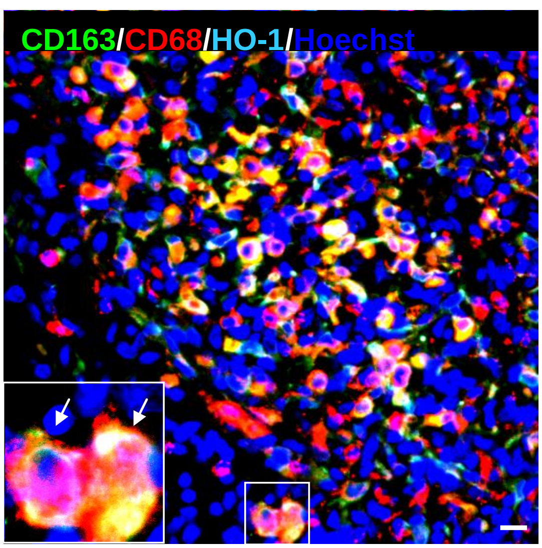

(D) Connective tissue between acini

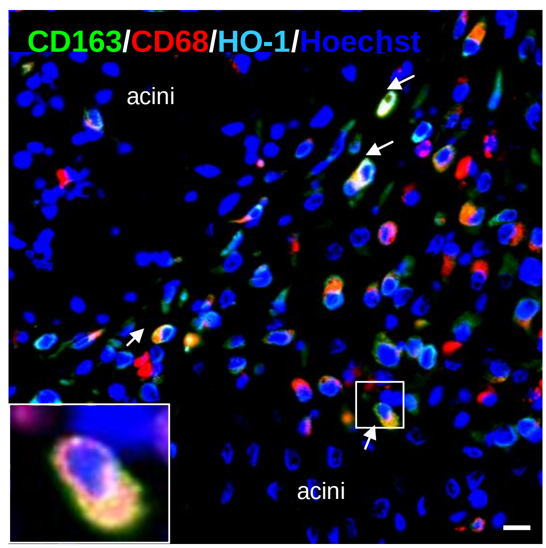

Figure 12. Microarray Analysis and Validation of Candidate Genes. Pancreas RNA was pooled from saline and CoPP-treated rats (n=7-8/ group); Affymetrix Rat Gene 1.0 ST chips were used for gene analysis. **(A)** Several *Regs* and *a-defensin* genes were upregulated in pancreas by CoPP treatment. (**B**) Group enrichment using DAVID online bioinformatics software highlighted the involvement of several antimicrobial *Regs* and *a-defensins* as well as chemokines. Morphometric analysis of **(C)** REG3γ^+ and **(D)** REG3β^+ cells in islets of 51d BBdp rats showed no difference between treatment groups while Reg3β intensity (Reg3β^+ area/islet area) was significantly higher in 51d CoPP-treated BBdp rats compared with saline controls. Data are expressed as means $\pm$ SD. (Bars = 50 μm)

(A) Genes upregulated in pancreas by CoPP

Gene Symbol	Name	Fold Change CoPP vs. Saline
Fabpi	Fatty acid-binding protein, intestinal	301
Fabp6	Gastrotropin (GT)	246
Si	Sucrase-isomaltase, intestinal	228
Muc13	Mucin 13, epithelial transmembrane	101
Ly6a	Lymphocyte antigen 6a	95
Np4	Neutrophil antibiotic peptide NP-4 prec.	71
Clca6	Chloride channel calcium activated 6	56
Reg3g	Reg III-gamma	56
Defa6	Alpha-defensin 6	52
Cdh17	Liver-intestine cadherin	46
Hmox1	Heme oxygenase 1	43
Defa9	Defensin alpha 9 (Defa9)	38
Defa8	Alpha-defensin 8	30
Mcpt2	Mast cell protease 2 precursor	29
Mucdhl	Mucin and cadherin-like protein precursor	27
Pap	RegIII-beta	27
Reg3a	Reg III-alpha	26
Lgals4	Galectin-4 (Lactose-binding lectin 4)	26
Clec2h	C-type lectin domain family 2H	25
Ccl25	chemokine (C-C motif) ligand 25	25
Akr1b8	Aldo-keto reductase family 1, B8	23
Clec2e	C-type lectin domain family 2E	22
Defcr4	Defensin 5 precursor (RD-5)	21

NOTE: Red = *Defensins*; Blue = *Regs*; Brown = *Hmox-1*

(B) Enrichment Groups by DAVID

Gene Symbol	Name	Fold Change CoPP vs. Saline
Enrichment	***α-Defensins***	
Np4	defensin RatNP-3 precursor; defensin NP-4 precursor	71
Defa-rs1	defensin alpha-related sequence 1	15
Defa8	defensin alpha 8	30
Defcr4	defensin, alpha, 24	21
Defa6	defensin alpha 6	52
Defa9	defensin alpha 9	38
Enrichment	***Regs***	
Pap	regenerating islet-derived 3 beta	27
Clec4d	C-type lectin domain family 4, member d	5
Reg3g	regenerating islet-derived 3 gamma	56
Reg3a	regenerating islet-derived 3 alpha	26
Dcir3	C-type lectin domain family 4, member a3	7
Enrichment	***Chemokines***	
Ccl6	chemokine (C-C motif) ligand 6	6
Ccl2	chemokine (C-C motif) ligand 2	6
Ccl25	chemokine (C-C motif) ligand 25	25
Ccl7	chemokine (C-C motif) ligand 7	5
Cxcl10	chemokine (C-X-C motif) ligand 10	7

(C) REG3γ **(D)** REG3β (PAP1)

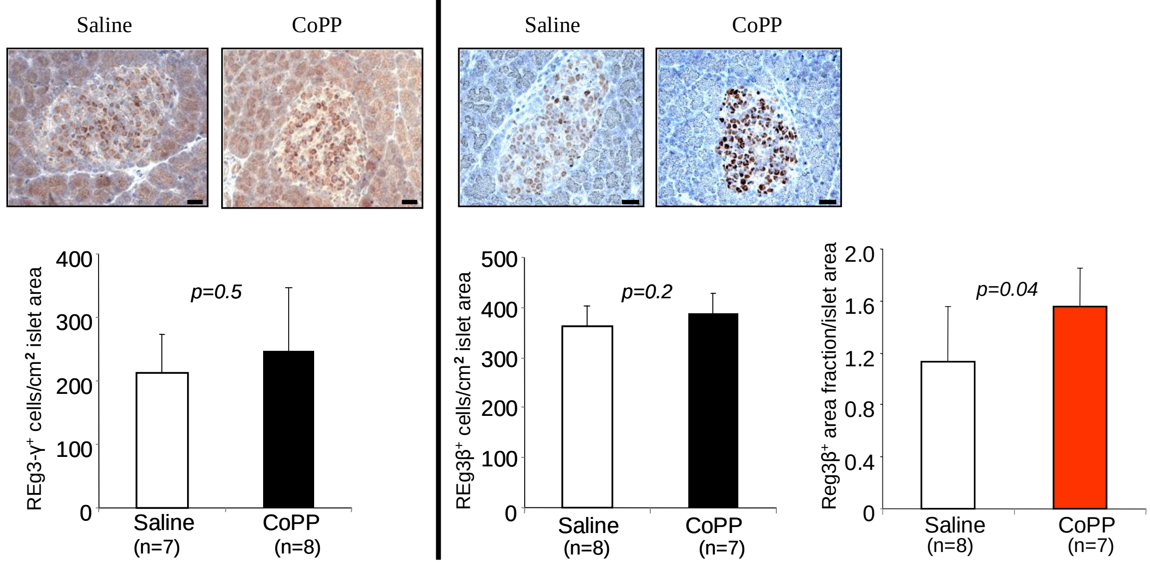

highlighted the involvement of several *Regs* and *α-defensin* genes as well as chemokines (Figure 12B). Morphometric analysis of REG3γ^+ and REG3β^+ cells in islets of 51 d CoPP and saline-treated BBdp rats revealed no difference between groups (Figure 12C,12D). Further analysis revealed an increase in REG3β intensity (REG3β^+ area/islet area) in CoPP-treated BBdp rats compared with controls (Figure 12D).

PCR array gene expression analysis of jejunum

Total RNA isolated from the jejunum of CoPP and saline-treated rats was analyzed by qPCR array and revealed a significant increase in *Camp* gene expression which encodes the cathelicidin anti-microbial peptide (CAMP) (Figure 13A,13B). Morphometric analysis of CAMP revealed a significant increase in CAMP$^+$ cells in the lamina propria in 51 d CoPP-treated BBdp rats compared with controls (Figure 13C) . There was also a significant increase ($p= 0.02$) in *Il1f9* gene expression in CoPP-treated BBdp rats compared with controls (Figure 13B).

Increase in M2 transcription factor

Krüppel-Like Factor 4 (KLF4) is a transcription factor known to polarize macrophages towards the M2 phenotype. Gene expression of *Klf4* was upregulated 2-fold in the pancreas of CoPP-treated BBdp rats compared with controls. Morphometric analysis on sections stained for KLF4 showed a significant increase in KLF4$^+$ cells surrounding islets as well as in the epithelial layer of the jejunum in 51 d CoPP-treated BBdp rats compared with controls (Figure 14A,14B). Triple immunofluorescence staining in pancreas sections revealed a distinct population of CD68$^+$HO-1$^+$KLF4$^+$ cells in 51 d CoPP-treated BBdp rats (Figure 14C).

Figure 13. HO-1 induction upregulates Camp in the jejunum. (**A**) PCR array analyses volcano plot revealed *Camp* as the most highly upregulated gene in BBdp rat jejunum. **(B)** Camp gene expression data from PCR array experiment showing upregulation of *Camp* and *Il1f9* in CoPP-treated BBdp rats compared to saline controls (n=3/group, p=0.006 and p=0.02, respectively). (**C)** Morphometric analysis of CAMP in BBdp gut showed a significant increase in CAMP^{+} cells in 51 d CoPP-treated BBdp rats compared with saline controls. (Bars = 50 μm)

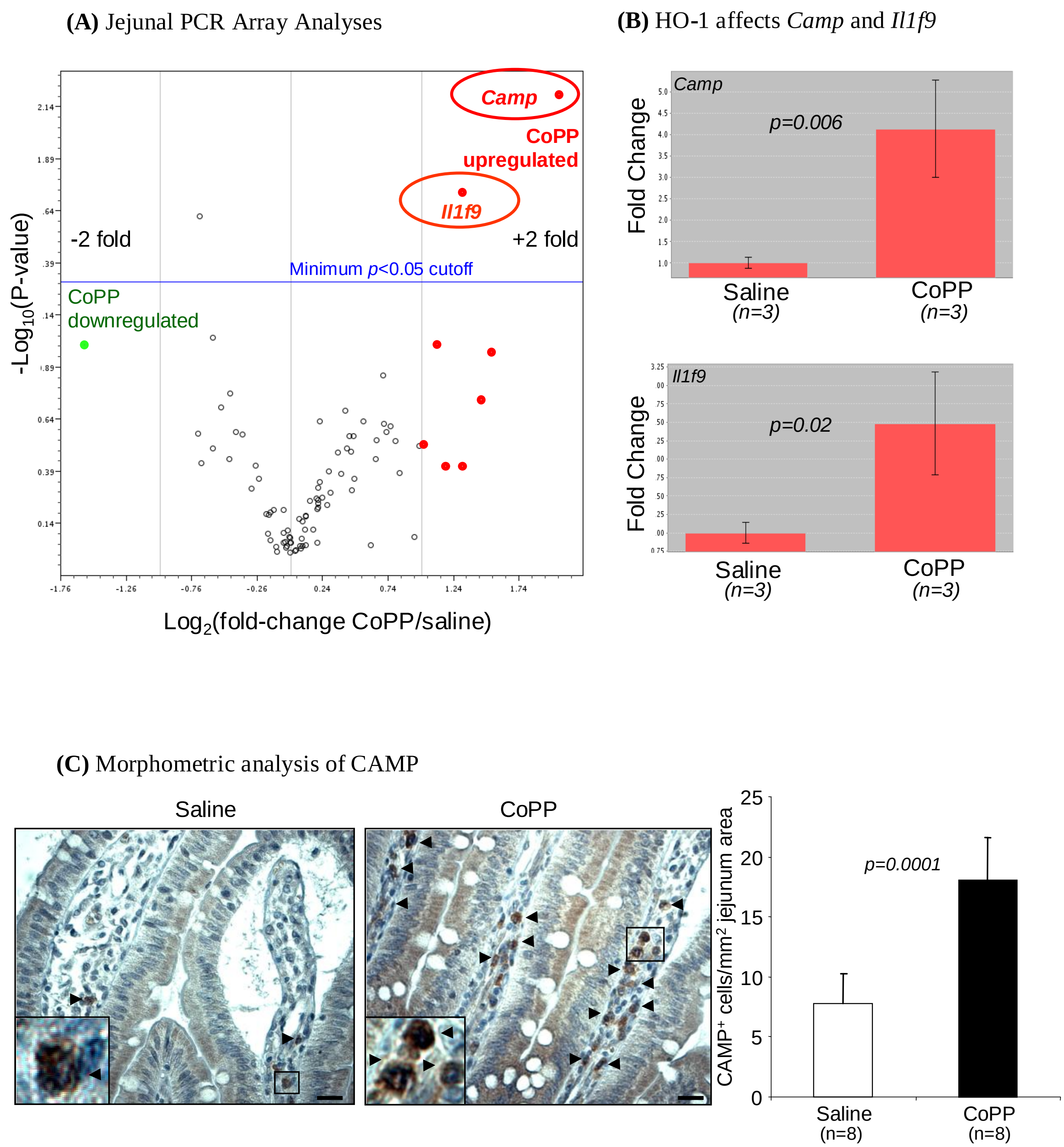
(A) Jejunal PCR Array Analyses
Camp
CoPP
upregulated
Il1f9
-2 fold
+2 fold
Minimum p<0.05 cutoff
CoPP
downregulated
-Log10(P-value)
Log2(fold-change CoPP/saline)
(B) HO-1 affects Camp and Il1f9
Camp
p=0.006
Fold Change
Saline
(n=3)
CoPP
(n=3)
Il1f9
p=0.02
Fold Change
Saline
(n=3)
CoPP
(n=3)
(C) Morphometric analysis of CAMP
Saline
CoPP
CAMP+ cells/mm2 jejunum area
p=0.0001
Saline
(n=8)
CoPP
(n=8)

Figure 14. HO-1 induction upregulates KLF4 in islets and gut. Morphometric analysis revealed an increase in $KLF4^{+}$ cells in the **(A)** pancreas associated with islets as well as in the **(B)** epithelium of 51 d CoPP-treated BBdp rats compared with saline-treated controls. **(C)** Triple immunofluorescence staining revealed a distinct population of triple positive $CD68^{+}HO\text{-}1^{+}KLF4^{+}$ cells (arrows) in between acinar units in the pancreas. Data are expressed as means ± SD. (Bars = 20 μm)

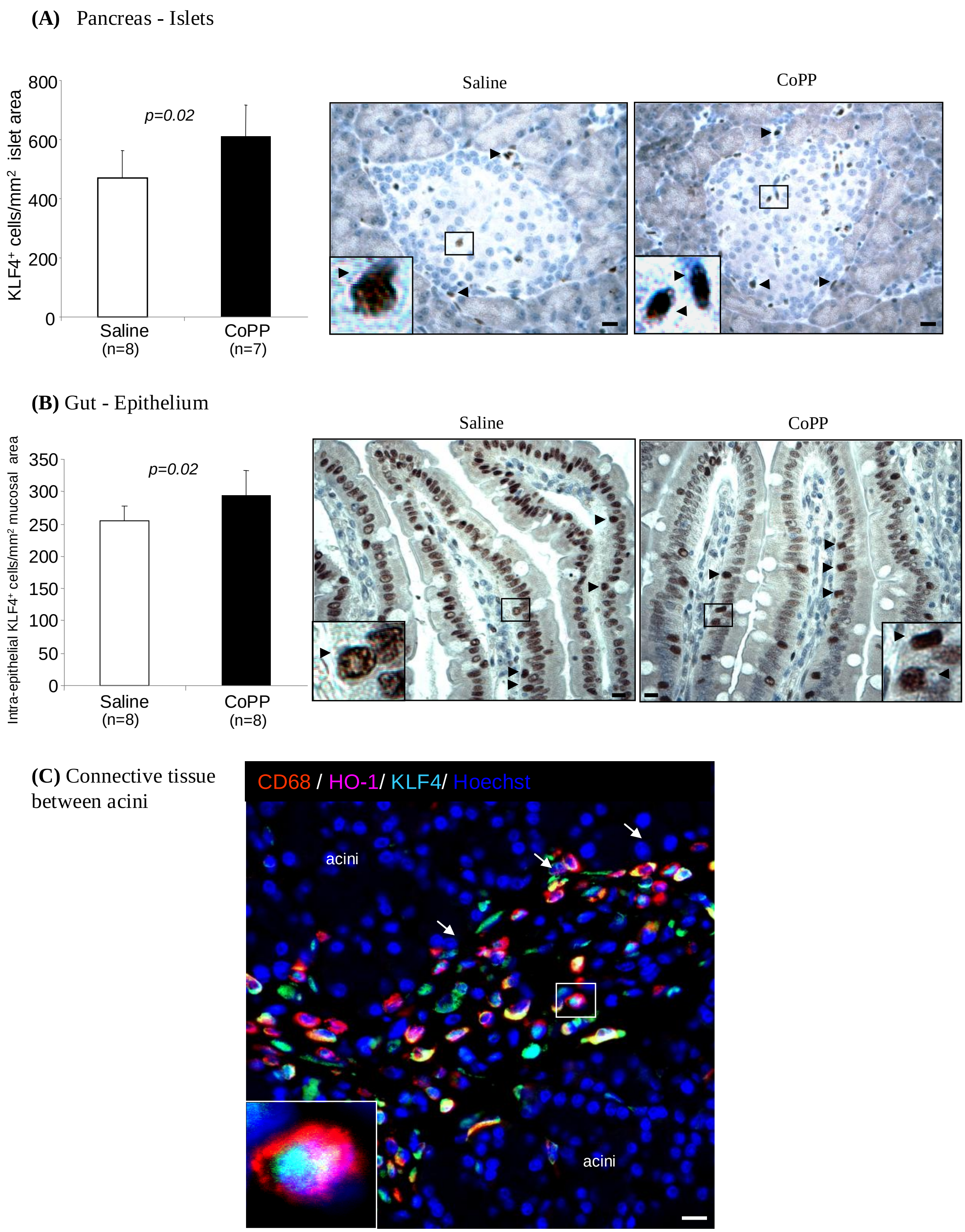
(A) Pancreas - Islets
KLF4+ cells/mm2 islet area
800
600
400
200
0
p=0.02
Saline
(n=8)
CoPP
(n=7)
Saline
CoPP
(B) Gut - Epithelium
Intra-epithelial KLF4+ cells/mm2 mucosal area
350
300
250
200
150
100
50
0
p=0.02
Saline
(n=8)
CoPP
(n=8)
Saline
CoPP
(C) Connective tissue between acini
CD68 / HO-1/ KLF4/ Hoechst
acini
acini

Identification of M2 macrophage subsets

Immunofluorescence labeling allowed for the classification of M2 macrophage subsets in the jejunum of 51 d CoPP-treated BBdp rats. M2a macrophages were identified based on their double staining for CD163 and CD204 while M2c macrophages were $CD163^{+}CD204^{-}$. CAMP was found to co-localize with both subsets of M2 macrophages (Figure 15A,15B).

Impaired HO-1 upregulation in LPMC of BBdp rats

Freshly isolated LPMC were prepared from the gut of BBc and BBdp rats and cultured with LPS, WP or OVA to determine the extent of HO-1 upregulation in the presence of pro-inflammatory stimuli. Flow cytometry analyses revealed an impairment in HO-1 upregulation in BBdp-derived LPMC in response to OVA and WP when compared with LPMC from BBc animals (Figure 16A). Culture supernatants from these BBc and BBdp LPMC stimulated with OVA or WP for 4 d were pooled (n=8/treatment) and analyzed using an antibody array. LPMC from BBdp rats showed an increase in pro-inflammatory cytokines such as IL-1α, IL-1β, IL-6, and IL-17 in response to WP compared with controls (Figure 16B).

Figure 15. Identification of M2 macrophage subclasses. Immunofluorescence labeling of jejunum sections of 51 d and 120 d CoPP-treated BBdp rat with antibodies to CD204 (Alexa 488), CD163 (Cy5) and Camp (Cy3). **(A)** M2a and **(B)** M2c macrophages were identified based on the absence or presence of CD204, respectively in the lamina propria. (Bars = 20 μm)

(A) Gut – M2a and M2c macrophages

(B) Gut – M2c macrophages

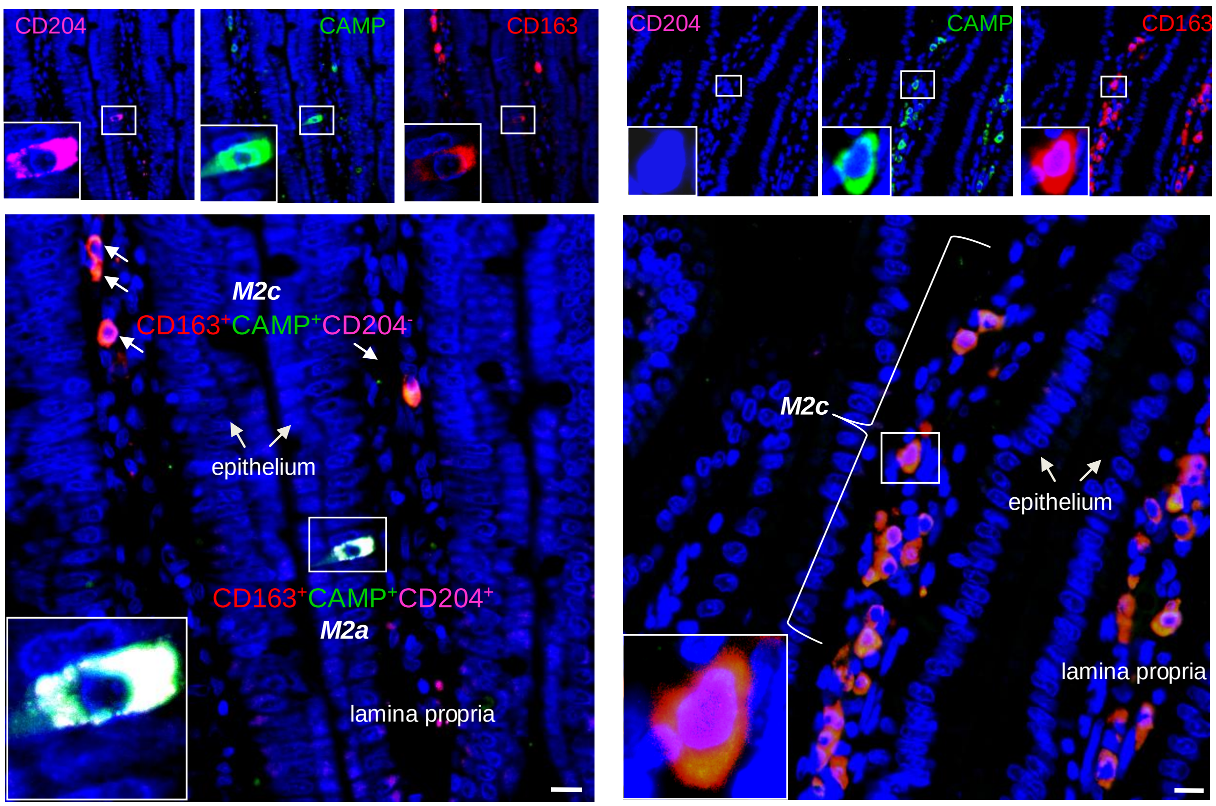

Figure 16. WP-stimulated LPMC from BBdp rats associated with an impairment in HO-1 upregulation and a pro-inflammatory cytokine and chemokine response. (A) Flow analyses representative of n=4 BBdp and BBc rats. Lamina propria mononuclear cells (LPMC) from BBdp (red) rat jejunum displayed impaired HO-1 upregulation in response to lipopolysaccharide (LPS), wheat peptides (WP) or ovalbumin (OVA) compared with control BBc (blue) rats. **(B)** Antibody arrays revealed LPMCs from BBdp rats show increased pro-inflammatory cytokine/chemokine expression in response to WP compared with control BBc rats including IL-1α, IL-1β, IL-6, and IL-17 (each group pooled from n=8, 53 d rats).

(A) Flow cytometry reveals impaired HO-1 upregulation in BBdp rat lamina propria mononuclear cells

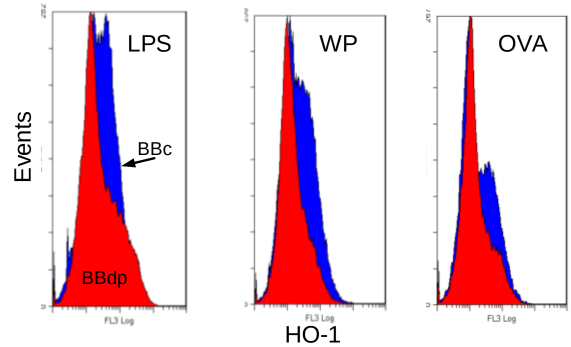

(B) Cytokines and chemokines in supernatants of rat LPMCs – BBdp response to wheat pro-inflammatory

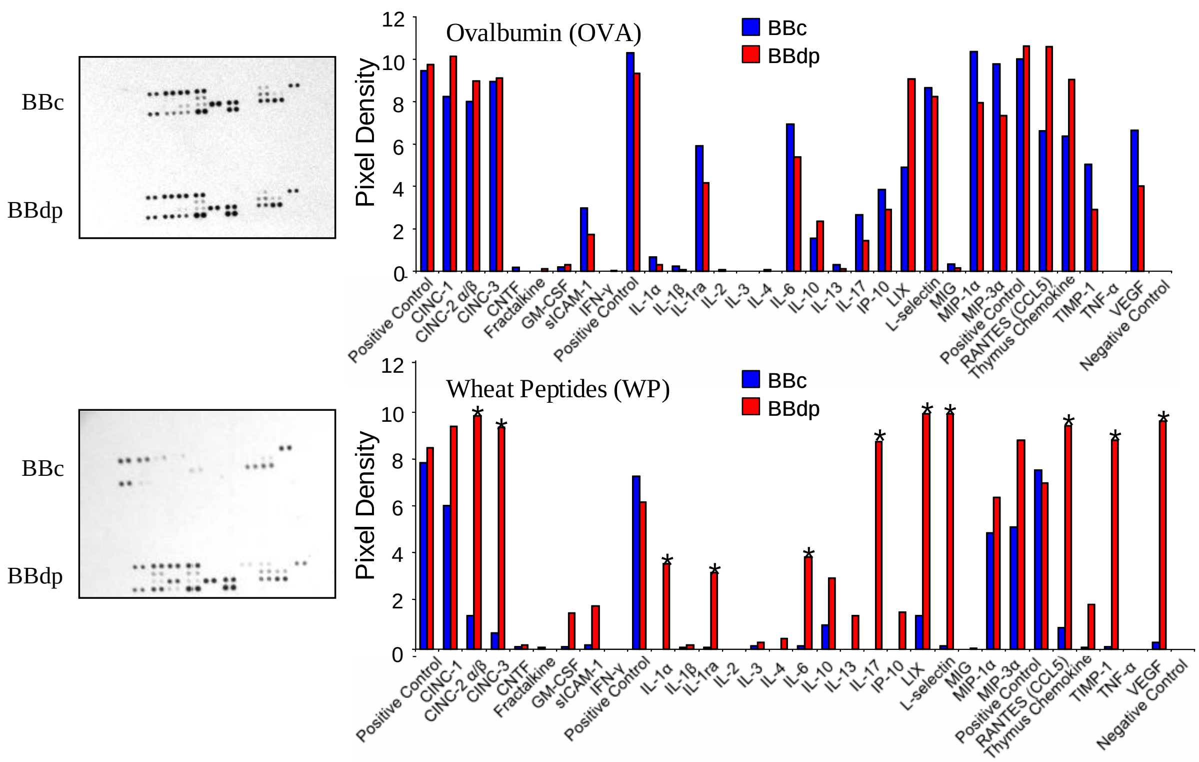

DISCUSSION

The aim of this project was to elucidate a role for the CD163 pathway and its rate-limiting enzyme HO-1 in T1D pathogenesis both *in vitro* and *in vivo*. In unpublished data from our lab, microarray analyses of RNA extracted from BBdp MLN and rat insulinoma β-cells incubated with diabetes-promoting wheat peptides revealed an upregulation of HO-1 gene expression, consistent with wheat peptide-induced oxidative stress in β-cells and in immune cells that drain the gastrointestinal tract. Additional evidence suggested that HO-1 protein was expressed in macrophages that infiltrated BBdp islets. Furthermore, preliminary data indicated that BBdp rats have fewer gut-resident M2 $CD163^+$ macrophages compared with control rats. Since HO-1 is the rate-limiting enzyme involved in the $CD163^+$ macrophage-dependent heme degradation pathway, we hypothesized that impairment in HO-1 upregulation in response to antigen may be associated with T1D. Resident intestinal macrophages represent a key regulatory immune cell population in the gut and are important modulators of oral tolerance (Schenk and Mueller 2007).

In biological systems, toxic heme is oxidized by the enzyme heme oxygenase which exists as three separate isozymes: HO-1, HO-2, and HO-3. HO-1 was the first isozyme to be discovered and has different biochemical and molecular properties than HO-2 and HO-3, despite sharing almost 50% amino acid sequence homology (McCoubrey and Maines 1994; Abraham and Kappas 2008). The *HO-1* and *HO-3* genes produce a single transcript whereas the *HO-2* gene produces two distinct transcripts that differ in terms of polyadenylation signals (Cruse and Maines 1988; McCoubrey and Maines 1994; McCoubrey, Huang et al. 1997). A major distinction between the three isozymes is that both HO-2 and HO-3 are constitutively expressed but HO-1 is induced by a variety of stimuli such as synthetic metalloporphyrins, oxidative stress, hormones and other structurally unrelated pharmacological agents (Maines 1988; Abraham and Kappas 2008). HO-1 and HO-3 are found in most tissues while HO-2 is preferentially expressed in the brain and testis (McCoubrey, Huang et al. 1997; Vijayan, Mueller et al. 2010). HO-1 is undetectable until a stress condition arises whereas HO-2 exists at detectable levels in the absence of stress (Ryter, Otterbein et al. 2002). The heme catalytic domain which is essential for the breakdown of the heme molecule is conserved among HO-1 and HO-2 (72% sequence homology, 100% structural homology) but is not conserved in HO-3 (Maines 1988; McCoubrey, Huang et al. 1997). Many additional well-conserved amino acid sequences and domains between HO-1 and HO-2 are absent in HO-3 and for this reason its role remains unclear due to its poor heme degradative capabilities (McCoubrey, Huang et al. 1997; Ryter, Otterbein et al. 2002). In a cell, HO-1 is predominantly associated with the smooth endoplasmic reticulum although several studies have also found it localized in plasma membrane caveolae, mitochondria, and in the nucleus (Lin, Weis et al. 2007; Ryter and Choi 2009). Indeed, it is thought that HO-1 localizes to the nucleus in the presence of stress where it upregulates cytoprotective genes (Lin, Weis et al. 2007).

There is increasing evidence to suggest a crucial anti-inflammatory and immunoregulatory role for HO-1 and its end products in many different diseases. The degradation of heme by HO-1 generates carbon monoxide (CO), free iron (Fe^{2+}), and the antioxidant molecule biliverdin. Biliverdin is then rapidly converted by the enzyme biliverdin reductase to an additional antioxidant molecule, bilirubin (Abraham and Kappas 2008). While excessive CO gas is detrimental to cells, many studies have identified CO as crucial to many pathways involved in vascular control and tissue viability in small quantities (Pae, Oh et al. 2004; Abraham and Kappas 2008). HO-1-derived CO has been shown to be cytoprotective, anti-apoptotic, vasorelaxant and anti-inflammatory (Nath

2006). While free iron is crucial for many biological processes, high concentrations can be toxic to cells due to its ability to form free radicals (Abraham and Kappas 2008). An inherent protection against HO-1-derived free iron involves the intracellular iron storage protein ferritin, which sequesters the free iron molecules almost immediately (Vijayan, Mueller et al. 2010). The protective effects of bilirubin and biliverdin are also well-documented, ranging from scavenging reactive oxygen species to preventing adhesion molecule expression and neutrophil adhesion (Abraham and Kappas 2008; Vijayan, Mueller et al. 2010). Our data clearly showed that CoPP induced HO-1 expression both at the gene level (~43 fold increase on pancreas microarray gene list) as well as at the protein level. The morphometric analyses of HO-1 showed significant increase in HO-1$^+$ cells associated with islets as well as in the lamina propria of CoPP-treated animals. Therefore, alteration of the HO-1 pathway could affect T1D through changes in immune function and islet homeostasis.

The well-established anti-inflammatory effects of HO-1 have led many to further investigate its role in immunomodulation. Several studies have reported beneficial effects of HO-1 upregulation in allograft protection from chronic rejection (Otterbein and Choi 2000; Lee, Gao et al. 2007; Faleo, Neto et al. 2008). HO-1 may be involved in controlling aspects of both innate and adaptive immune cells. At least three different types of immune cells express HO-1 at significant levels: monocytes/macrophages, dendritic cells, and CD4$^+$ T cells (Simon, Anegon et al. 2011). A study with HO-1 knockout mice revealed that HO-1 activity in antigen presenting cells is crucial for the suppression of effector T cells by CD4$^+$CD25$^+$FoxP3$^+$ regulatory T cells (T_{reg}) (George, Braun et al. 2008). The role of CD4$^+$CD25$^+$FoxP3$^+$ T_{regs} is to suppress the activation and differentiation of naïve T cells into effector CD4$^+$ and CD8$^+$ T cells, but their suppressive functions also extend to natural killer cells, B cells, macrophages and dendritic cells (Sakaguchi, Yamaguchi et al. 2008). T_{regs} express the transcription factor FoxP3 (forkhead box P3) which is a master regulator of T_{reg} development and function. HO-1 expression has been shown to be activated by FoxP3 and therefore participates in FoxP3-mediated immune suppression (Brusko, Wasserfall et al. 2005; Choi, Pae et al. 2005). Inhibition of HO-1 *in vitro* by tin mesoporphyrin (SnMP) induced activation, proliferation, and maturation of naïve human $CD4^+$ and $CD8^+$ T cells, further supporting the immunosuppressive role of HO-1 (Burt, Seu et al. 2010).

As previously mentioned, HO-1 is inducible and its activity may be induced by up to 100-fold by various stimuli including metalloporphyrins (Maines 1988). We increased HO-1 expression in BBdp rats using cobalt protoporphyrin (CoPP), a metalloporphyrin with well-characterized HO-1 induction effects in many tissues (Shan, Lambrecht et al. 2006). CoPP exerts its inductive effects on HO-1 much in the same way as its substrate heme molecule, which also induces HO-1 expression. The induction of HO-1 by metal ions like CoPP is relatively short-lived (72-96 hours) whereas induction by other inducers such as organometal complexes may persist for periods of up to several weeks (Maines 1988). While the term "heme" typically refers to an iron-containing complex, it can also broadly apply to any complex of a metal ion (Fe, Mg, Mn, Co, Cu, etc) chelated in a porphyrin ring, known as protoporphyrin IX (Maines 1988; Shan, Pepe et al. 2000). In this way, a cobalt metal ion complexed to the protoporphyrin IX ring acts as a synthetic analogue of the traditional heme complex yet still exerts the same inductive effect on HO-1 expression without conferring the pro-oxidant qualities associated with heme (Shan, Pepe et al. 2000). Indeed, heme can be associated with the production of cytotoxic reactive oxygen species when it reacts with molecular oxygen however heme is also essential in hemoglobin proteins for the reversible binding of oxygen and transport of electrons (Immenschuh, Baumgart-Vogt et al. 2003). Transcriptional regulation of the HO-1 gene is under the control of two transcription factors, Nrf2 (transcriptional activator) and Bach1 (transcriptional repressor), which are both part of the larger antioxidant response element pathway (Pulkkinen, Yla-Herttuala et al. 2011; Vomhof-Dekrey and Picklo 2012). *In vitro* studies in liver cells have indicated that HO-1 induction by CoPP is primarily mediated by the upregulating Nrf2 protein levels and down-regulating Bach1 protein levels (Shan, Pepe et al. 2000; Gong, Hu et al. 2001; Shan, Lambrecht et al. 2006). It is important to note that CoPP administration may be associated with several unfavorable side effects such as depletion of hepatic cytochrome P450 levels, suppression of thyroid and testicular hormone concentrations in serum and induced weight loss in animals (Schmidt 2007). Several enzymes involved in the heme synthesis pathway can be affected by the same stimuli that alter heme oxygenase activity therefore CoPP may also perturb overall heme biosynthesis (Maines 1988).

Inhibition of T1D development by HO-1 induction

We inhibited development of T1D in BBdp rats through the upregulation of HO-1 using CoPP. As CoPP treatment has been associated with weight loss, we monitored body weight of the animals throughout the study but did not see any detrimental effects. H&E sections were used to assess the morphology of the gut and pancreas. It was noted that CoPP-treated pancreas sections had a more consistent pattern of fibrous connective tissue dispersed throughout and disconnecting acinar lobes than in saline-treated pancreas sections. This could be a sign of pancreatic fibrosis, which is characterized by an acute injury of the mesenchymal, duct and/or acinar cells and increased fibrous tissue brought on by the activation and proliferation of fibroblasts (Kloppel, Detlefsen et al. 2004). As fibrosis can enlarge the pancreas, it might explain the observed significant increase in total pancreas weight in 51 d CoPP-treated rats compared with controls. While a dose response was not carried out in this study, these data suggest that the dosage of CoPP (6.5 mg/kg) might have been too high and its benefits could be afforded at lower doses for future experiments. Insulin staining revealed no difference in β-cell area fraction in pre-diabetic (51 d) or asymptomatic (~120 d) CoPP or saline-treated BBdp rats. It is important to note that true β-cell area can only be accurately determined when analyzing insulin$^+$ area on several neighbouring sections of slides (or 'levels'). As our analysis was performed on only one section per animal we can only report β-cell area as a fraction at that 'level' which is a possible limitation. H&E sections were assessed for islet damage on the basis of the extent of insulitis. Using a previously described scoring system (Hoorfar, Scott et al. 1991) for mononuclear cell infiltration, insulitis was evaluated in pre-diabetic (51 d) and asymptomatic (~120 d) BBdp rats from each treatment group. Interestingly, there was less insulitis in CoPP-treated BBdp rats at both ages which suggests that induction of HO-1 may prevent mononuclear cell infiltration into islets. Furthermore, these key observations suggest that CoPP was not exerting its protective effect through an increase in number of islets and β cells, but rather by a recruitment of key immune cells, possibly protecting islets from invading lymphocytes and mononuclear cells. Two other *in vivo* studies investigating the effect of HO-1 up-regulation by CoPP in the NOD mouse also revealed an inhibition of T1D (Hu, Lin et al. 2007; Li, Peterson et al. 2007) and an *in vitro* study with INS-1 cells and CoPP showed that HO-1 up-regulation results in protection from high glucose-induced apoptosis (Lee, Lee et al. 2011). A transgenic NOD mouse made to express HO-1 locally in pancreatic islets has been generated and has already demonstrated a significant protective role in β cells by preventing T1D (Huang, Chu et al. 2010). This opens a potential therapeutic avenue by which HO-1-overexpressing islets could be used for transplantation purposes (Chuang, Chu et al. 2008; Chou, Huang et al. 2012). It is worth mentioning that although CoPP treatment prevented T1D development in both the BBdp rat and NOD mouse, the mechanism of protection by HO-1 induction may differ in the NOD mouse completely. Differences between the animal models could also be attributed to different concentrations of CoPP used in the respective studies.

Protected animals associated with a predominant M2 macrophage population

One of the main goals of the study was to characterize the innate immune status in the pancreas and gut using markers of M1 and M2 macrophages. A striking finding was the increased expression of $CD68^+$ macrophages associated with islets in CoPP-treated BBdp rats. It is important to note that while there is still a controversy in the literature as to whether CD68 is a pan-macrophage or an M1 macrophage marker, the latter definition was used for the purpose of this work. As CD68 is associated with M1 macrophages, which are pro-inflammatory in nature (Villalta, Nguyen et al. 2009; Tidball and Villalta 2010), it was unexpected to observe their recruitment in a protective setting. While there was no difference in islet-associated and lamina propria M2 $CD163^+$ macrophages in 51 d CoPP-treated animals compared with controls, we did notice a significant increase in $CD163^+$ macrophages in asymptomatic, end of study (~120 d) BBdp rats compared with pre-diabetic (51 d) rats. This finding is especially important in the context of macrophage phenotype switching, a phenomenon whereby macrophages can change their status depending on the microenvironment (Martinez 2011). Our data suggest that M2 macrophages constitute the predominant macrophage population in protected BBdp rats. Indeed, microarray analysis of islets in long-term protected NOD mice revealed preferential expression of M2 macrophage genes, most notably those of the scavenger receptor family including macrophage scavenger receptor 1 (*Msr1*) and class B scavenger receptor (*Scarb1*) (Calderon, Suri et al. 2008). On the other hand, microarray analysis of NOD diabetic islets showed increased gene expression for M1 macrophage genes including *Stat1* and chemokine (C-C motif) ligand 5 (*Ccl5*) (Calderon, Suri et al. 2008). In a recent study macrophages that were polarized *in vitro* toward an M2 phenotype expressing CD163 and other M2 markers were adoptively transferred into pre-diabetic NOD mice preventing T1D development (Parsa, Andresen et al. 2012). Subsequent tagging of these M2 macrophages showed that they predominantly migrated to the pancreas and PLN of the mice and retained their M2 signature once they arrived in the pancreas (Parsa, Andresen et al. 2012). The significant decrease in $CD68^+$ macrophages in the lamina propria of 120 d rats compared with 51 d rats further suggests this shift from an M1 macrophage population toward an M2 macrophage population. HO-1 expression in the pancreas and gut was significantly decreased in the asymptomatic, 120 d BBdp rats compared with 51 d rats, suggesting that HO-1 expression was transient and that a short window of HO-1 upregulation was sufficient to prevent the disease.

Altered macrophage phenotype after HO-1 induction

The staining pattern of CD163 and CD68 correlated with HO-1 staining and for this reason we performed immunofluorescence staining to determine whether HO-1 co-localized with either of these markers. HO-1 was predominantly expressed by $CD68^+$ cells, and to a lesser extent by $CD163^+$ cells. These preliminary results suggest that the macrophages are undergoing phenotype switching. Interestingly, we identified an additional distinct population of triple positive “M2-like” $CD68^+CD163^+HO\text{-}1^+$ cells in the pancreas and gut. CD68 and CD163 have been shown to be upregulated and co-expressed on macrophages in patients with complicated diverticulitis, an inflammatory disease involving perforations in the intestine (von Rahden, Kircher et al. 2011). Novel macrophage and monocyte subsets have also been identified near atherosclerotic lesions ($CD68^{+}CD163^{high}HLA\text{-}DR^{low}$) and after cardiopulmonary bypass surgery ($CD14^{+}CD163^{high}HLA\text{-}DR^{low}$) that were both associated with high expression of HO-1 (Boyle, Harrington et al. 2009; Quimby, Greenidge et al. 2010). The macrophages *in vitro* cleared Hb more quickly and showed less highly reactive oxygen species, oxidant stress and produced IL-10 (Boyle, Harrington et al. 2009). We propose that the triple positive macrophage population found in the pancreas and gut of 51 d CoPP-treated BBdp rats represents transitional macrophages brought on by HO-1 induction providing an immunosuppressive and anti-inflammatory environment. It would be important to characterize these double and triple positive macrophage populations further.

As previously mentioned, there is a controversy in the literature as to whether CD68 is a pan-macrophage marker or an M1 macrophage marker. Should we consider it to be the former in the context of this study, it would still be unexpected to see such a large population of HO-1-expressing macrophages so intimately associated with islets. Indeed, a large macrophage population being recruited in a protective setting only strengthens the often-overlooked role of the innate immune system in a disease that is primarily T-cell driven. It would be helpful to further characterize these macrophages with additional markers of M1 macrophages such as the transcription factors IRF5 and STAT1 to more definitively conclude whether they are true M1 macrophages.

Upregulation of Reg *and* α-Defensin *family of genes in the pancreas after HO-1 induction*

HO-1 upregulation in the NOD mouse was associated with a decrease in $CD11c^{+}$ dendritic cell infiltration into pancreatic tissue which is known to contribute to the destruction of β cells (Li, Peterson et al. 2007). It was proposed that this event along with an increase in anti-apoptotic proteins pAKT and BcL-xL in the pancreas promoted β-cell survival through an unknown mechanism (Li, Peterson et al. 2007). We used microarrays to elucidate potential cellular mechanisms, pathways and factors in the pancreas of BBdp rats after T1D prevention by HO-1 induction. Lists of the differentially-expressed genes from the 51 d BBdp pancreas microarray experiments comparing CoPP-treated and saline-treated gene expression (both up- and down-regulated) in BBdp rats are shown in the Appendix. Of particular interest was the increase in gene expression of the *Reg* and *α-defensin* families of genes in the pancreas which are known to confer antimicrobial and regenerative properties.

One of the most striking findings on the gene list was the marked increase in lipid-related genes. Fatty acid binding protein-1 (*Fabp1,* known also as liver-type fatty acid binding protein, *L-Fabp)* and fatty acid binding protein-6 (*Fabp6*) genes were up-regulated 301 and 246 fold in CoPP-treated versus saline-treated BBdp rats, respectively. FABPs are intracellular lipid chaperones that coordinate lipid responses in cells and are known to target fatty acids and transcription factors such as peroxisome proliferator-activated receptors (PPAR) (Furuhashi and Hotamisligil 2008). In mammals there are three PPAR subtypes, PPAR-α, PPAR-δ and PPAR-γ, which are expressed in many tissues and cell types including immune cells (Chawla 2010). There is mounting evidence to suggest that PPARs, in particular PPAR-γ, are involved in polarizing macrophages towards an M2 phenotype (Bouhlel, Derudas et al. 2007; Odegaard, Ricardo-Gonzalez et al. 2007; Chawla 2010). Interestingly, FABP1/L-FABP is a heme-binding protein (HBP), a cytosolic protein that functions primarily to transport heme intracellularly (Stewart, Slysz et al. 1996; Haase, Bellomo et al. 2010). Apart from intracellular heme trafficking, HBPs may also provide protection from oxidative assaults (Wagener, Volk et al. 2003). Indeed, FABP1/L-FABP has been shown *in vitro* to possess strong antioxidant properties by reducing intracellular reactive oxygen species (Wang, Gong et al. 2005; Yan, Gong et al. 2009). It is possible that the sustained injections of CoPP, a heme analogue, over the three-week period caused an increase in the expression of the heme-binding protein FABP1/L-FABP. The gene expression of *Fabp1*/*L-Fabp* (and many other lipid-related genes) was significantly increased in the colon of mice fed dietary heme compared with controls (Ijssennagger, de Wit et al. 2012) which suggests that a heme analogue could have similar inductive effects on lipid-metabolism related genes.

Reg3γ, *Reg3β*, and *Reg3α* were upregulated (56, 27, and 26 fold, respectively) in CoPP-treated versus saline-treated BBdp rats. Validation by immunohistochemistry revealed no significant difference in intra-islet REG3γ^+ and REG3β^+ cells. It is important to note that microarray analysis was performed on total pancreatic RNA and as such is not necessarily representative of islet-specific changes. REG3β^+ area fraction was, however, significantly higher in the islets of CoPP-treated animals compared with controls. REG3β is also known as pancreatitis associated protein 1 (PAP1) and has been identified as a C-type lectin (Closa, Motoo et al. 2007). It has been shown to be an anti-inflammatory factor *in vitro* and *in vivo,* as well as possessing anti-apoptotic functions (Graf, Schiesser et al. 2006). One study showed that REG3β/PAP1 incubation with intestinal mucosa from active Crohn's disease reduced pro-inflammatory cytokine secretion. This has led many to suggest that REG3β/PAP1 is not restricted to the pancreas and could be a new, generic anti-inflammatory cytokine itself, protecting against inflammatory processes (Closa, Motoo et al. 2007). Indeed, REG3β/PAP1 knockout mice were found to exhibit more extensive inflammation after induction of pancreatitis (Gironella, Folch-Puy et al. 2007) further strengthening its putative anti-apoptotic and anti-inflammatory roles. An additional study in mice showed induced expression of *Reg3β* and *Reg3α* gene expression in exocrine pancreas after activation of glucagon-like peptide receptor, suggesting a potential compensatory mechanism that serves to limit damage to the exocrine pancreas (Koehler, Baggio et al. 2009). Furthermore, *in vitro* over-expression of REG3α (also known as PAP2) in MIN6 insulinoma cells revealed increased expression of cyclin D1 and CDK4, both of which have established roles in β-cell replication (Cui, De Jesus et al. 2009). REG3α/PAP2 has been reported to potentially recruit protective macrophages to the pancreas during acute pancreatitis (Viterbo, Bluth et al. 2008) and has also been attributed to wound healing and repair in skin lesions in psoriasis (Lai, Li et al. 2012).

Gene expression of *α-defensins* 6, 9, and 8 was upregulated (52, 38, and 30 fold, respectively) in CoPP-treated versus saline-treated BBdp rats. α-Defensins are small cationic peptides that function by regulating the bacterial colonization of the gut and in regulating both pro- and anti-inflammatory processes (Yamamoto, Banaiee et al. 2004). They are able to kill bacteria by interacting with membranes and anionic intracellular peptides. α-Defensins are most commonly secreted by paneth cells (in the epithelium of the gut), neutrophils and eosinophils (Yamamoto, Banaiee et al. 2004). A recent study showed that some patients with T1D had a 200-fold upregulation in α-defensin mRNA levels compared with controls (Neuwirth, Dobes et al. 2012). There are several studies that link α-defensins to autoimmune diseases, especially in the context of gut-related inflammation. Most of these studies provide evidence that α-defensins play an important role in preventing invasion of luminal bacteria in the gut mucosa due to their antimicrobial activity (Cunliffe and Mahida 2004; Salzman, Underwood et al. 2007; Kotarsky, Sitnik et al. 2010). A dysfunctional gut barrier and the resulting influx of bacteria and other antigens can break oral tolerance and lead to local inflammation as well as an increased immune response against certain autoantigens. Besides their role in protecting the gut barrier, α-defensins were shown to suppress Th17-cells, a subset of IL-17-producing $CD4^+$ and $CD8^+$ T cells known to amplify inflammatory responses and exacerbate autoimmunity (Janeway, Travers et al. 2008; Lisitsyn, Bukurova et al. 2012). Overall, the presence of three α-defensins in the top 20 "hits" on our list of upregulated genes for pancreatic RNA after HO-1 induction strengthens the importance of the gut immune system in the context of T1D.

KLF4 - evidence for a predominant M2 macrophage phenotype in the pancreas and gut after HO-1 induction

We found evidence for a predominant M2 macrophage phenotype following HO-1 induction after investigating the transcription factor Krüppel-like Factor 4 (KLF4), which is implicated in M2 macrophage activation (Murray and Wynn 2011). Krüppel-like factors are a subfamily of the zinc finger class of DNA-binding transcriptional regulators and have been shown to have important roles in many different cellular processes (Liao, Sharma et al. 2011). KLF4 was initially identified in the epithelial lining of the gut and skin however recent studies have shown KLF4 to promote monocyte differentiation as well as being associated with embryonic stem cells (Feinberg, Wara et al. 2007; Liao, Sharma et al. 2011). Gene expression of *Klf4* was up-regulated ~2 fold in the pancreas of 51 d CoPP-treated BBdp rats compared with saline-treated controls. Morphometric analysis of KLF4 revealed a significant increase in $KLF4^+$ cells in the pancreas and jejunum of 51 d CoPP-treated BBdp rats compared with saline-treated controls. It is important to note that in the jejunum, KLF4 expression was almost exclusively in the nuclei of intraepithelial and epithelial cells. This is to be expected as KLF4 is primarily associated with a terminally differentiated state of epithelial cells (Dang, Pevsner et al. 2000). KLF4 has recently been identified as a novel regulator of macrophage polarization by inhibiting NF-κB activation (needed for M1 polarization) and up-regulating gene expression of *Stat6* to induce an M2 phenotype. Macrophage-specific KLF4 knockout mice were found to have delayed wound healing and were predisposed to developing diet-induced obesity, glucose intolerance, and insulin resistance (Liao, Sharma et al. 2011). Interestingly, these mice also had reduced PPARγ levels in muscle and liver tissue as well as in the KLF4-deleted macrophages themselves which suggests a cooperative interaction of KLF4 and Stat6 with PPARγ to allow for sustained M2 macrophage activation (Liao, Sharma et al. 2011). Triple immunofluorescence staining in 51 d CoPP-treated BBdp rats revealed a population of $CD68^+HO\text{-}1^+KLF4^+$ macrophages in connective tissue interspersed between acinar lobes in the pancreas. We noted distinct cytosolic and nuclear KLF4 expression patterns, with the latter correlating with HO-1 expression. Due to the inherent nuclear localization signal present in the KLF4 protein (Vangapandu 2009), it is primarily localized in the nucleus; however, cytoplasmic localization has also been described in some cell types (Behr, Deller et al. 2007). Analysis of the subcellular localization of KLF4 warrants further investigation in CoPP and saline-treated BBdp rats as it may serve as a marker for different M1 or M2 macrophage activation states.

Increased HO-1 associated with CAMP expression – antimicrobial and novel M2 macrophage marker

PCR array analyses of jejunal RNA revealed *Camp* as the most highly and significantly upregulated gene in 51 d CoPP-treated BBdp rats compared with saline-treated controls. Morphometric analysis of CAMP in the lamina propria showed a significant increase in $CAMP^+$ cells in 51 d CoPP-treated BBdp rats compared with saline controls. *Camp* encodes the protein cathelicidin anti-microbial peptide and much like the defensins, cathelicidin proteins can release an antimicrobial peptide after proteolytic cleavage (Durr, Sudheendra et al. 2006). The peptide that is formed is termed LL-37 due to the two leading leucine residues at the N-terminus and overall peptide length of 37 amino acids (Bals and Wilson 2003; Durr, Sudheendra et al. 2006). In addition to its direct antimicrobial action, many diverse biological roles have been attributed to LL-37 including immunomodulatory properties (Nijnik and Hancock 2009). Indeed, LL-37 has been found to be expressed in neutrophils, T cells, NK cells, and monocytes (Nijnik and Hancock 2009; Nijnik, Pistolic et al. 2009). Many studies have shown CAMP/LL-37 promotes anti-inflammatory activity, angiogenesis, and enhances tissue repair and wound-healing (Morizane 2012). Indeed, CAMP/LL-37 has been shown to selectively decrease mucosal (alveolar) macrophage production of the pro-inflammatory cytokine TNF-α in response to LPS (Brown, Poon et al. 2011). CAMP/LL-37 also inhibited production of TNF-α and nitric oxide (NO) by LPS-stimulated or IFN-γ-polarized pro-inflammatory M1 bone marrow-derived macrophages, while leaving other crucial anti-inflammatory functions unaltered (Brown, Poon et al. 2011). Vitamin D3 has been found to induce CAMP/LL-37 in monocytes and keratinocytes (Segaert 2008). Several studies have shown that administration of vitamin D3 alleviates psoriasis (Morizane 2012), and even completely inhibits T1D in NOD mice (Zella, McCary et al. 2003; Giulietti, Gysemans et al. 2004). Indeed, some epidemiological studies show an inverse correlation between vitamin D status and the incidence of autoimmune diseases such as T1D, multiple sclerosis and rheumatoid arthritis (Baeke, Takiishi et al. 2010; Cooper, Smyth et al. 2011; Jankosky, Deussing et al. 2012). The association of CAMP with HO-1 upregulation is a novel one and has not been reported in the context of T1D.

It is important to mention that gene expression of *Il1f9* was also significantly upregulated ($p=0.02$) along with *Camp* in the jejunum of CoPP-treated BBdp rats compared with controls. IL1F9 is part of larger cytokine family known as IL-36 which comprises the three members IL1F6, IL1F8, and IL1F9 (Carrier, Ma et al. 2011). These cytokines are primarily expressed in epithelial tissues and have been recently implicated in the pathogenesis of psoriasis through their activation by Th17 pro-inflammatory cytokines like IL-17A, IL-22, and TNF-α (Carrier, Ma et al. 2011; Ramadas, Ewart et al. 2011). Interestingly, the three members of the IL-36 family have also been reported to induce the expression of antimicrobial peptides including CAMP in psoriasis skin lesions (Carrier, Ma et al. 2011; Johnston, Xing et al. 2011). As morphometric analysis of IL1F9 was not performed in this study, it would be beneficial to analyze its protein expression especially due to its reported interaction with antimicrobial peptides.

Identification of M2 macrophage subsets in the gut

We also sought to identify distinct M2 macrophage subsets in the lamina propria of CoPP or saline-treated BBdp rats. As previously mentioned, it is plausible that a macrophage phenotype switch is occurring after HO-1 induction as well as in ~120 day old protected animals compared with 51 d animals. While both M2a and M2c macrophages express CD163, only M2a subsets express CD204, also known as macrophage scavenger receptor 1 (MSR1) (Husemann, Loike et al. 2002; Orme and Mohan 2012). We were able to identify distinct M2a and M2c macrophage subset populations in the lamina propria of 51 d and 120 d CoPP-treated BBdp rats. M2a macrophages are known to promote immunoregulatory functions and drive Th2 responses while M2c macrophages are associated with immune suppression, tissue repair and matrix remodeling (Orme and Mohan 2012). A study investigating muscle degeneration in a mouse model of muscular dystrophy found a transient change from M1/M2a macrophages associated with muscle damage to M2c macrophages in later stages of the disease during repair (Villalta, Nguyen et al. 2009). It is tempting to speculate that a similar process is occurring in our study whereby M2a macrophages are the predominant M2 macrophage subset population at 51 d after HO-1 induction and that a phenotype switch occurs in older, protected BBdp rats toward an M2c macrophage population which are suppressing pro-inflammatory immune responses and participating in tissue repair/remodeling in both the pancreas and gut. This would need to be validated with a more detailed and quantitative analyses of the macrophage subsets in CoPP or saline-treated BBdp rats at both ages. Interestingly, CAMP co-localized with both subsets of M2 macrophages in the gut, consistent with its anti-inflammatory and wound-healing properties. Preliminary *in vitro* data from our lab by our senior research technician, Jennifer Crookshank, in which exogenous CAMP protein was added to LPMC of BBdp rats revealed an increase in the number of $CD163^{+}$ M2 macrophages and enhanced production of the anti-inflammatory cytokine, IL-10 compared with LPMC incubated with media alone. The CD163/HO-1/IL-10 axis is an important determinant of the anti-inflammatory/regulatory function of M2-polarized macrophages (Sierra-Filardi, Vega et al. 2010). Taken together, these data provide a promising and novel role for CAMP/LL-37 in M2 macrophage function(s). It would be beneficial to quantify the M2 macrophage subsets along with CAMP/LL-37 in 51 d and 120 d CoPP or saline BBdp rats to further investigate this phenotype switching phenomenon.

Impairment of HO-1 upregulation and a pro-inflammatory profile in the gut in response to wheat peptides

There is increasing evidence to suggest that diet may play a crucial role in promoting T1D in both human and rodents by influencing gut microbiota, gut inflammation, and islet homeostasis. As dietary antigens first make contact with the gut associated lymphoid tissue, where the majority of the immune cells in the body reside, they have been implicated in disease progression. Dietary proteins found in complex, cereal diets based mainly on wheat are the major environmental factor in BB rats. Several studies have found that cereal-fed rats display sporadic celiac-like inflammation of the gut mucosa, increased pro-inflammatory cytokines in the MLN, and the presence of leaky gut in the postnatal period (Graham, Courtois et al. 2004; Chakir, Lefebvre et al. 2005; Courtois, Nsimba et al. 2005; Watts, Berti et al. 2005). When these animals are fed a low antigen, hydrolyzed casein (HC) diet from weaning, T1D onset is delayed and more than half remain diabetes-free (Lefebvre, Powell et al. 2006). Using antibodies from BBdp rats and T1D patients, a wheat protein called Glo-3A was identified as a candidate T1D-related wheat protein (MacFarlane, Burghardt et al. 2003). Indeed, a subset of children at high risk for T1D and a patient with T1D and celiac disease both displayed strong antibody responses to Glo-3A (Mojibian, Chakir et al. 2006; Simpson, Mojibian et al. 2009). Furthermore, a published report from our lab indicated that PBMC from T1D patients showed a pro-inflammatory cytokine response when stimulated with WP including large amounts of IFN-γ, IL-17A, IL-6 and increased TNF, supporting a mechanism by which wheat can promote the development of diabetes (Mojibian, Chakir et al. 2009). LPMC from BBc and BBdp rats had an almost identical cytokine/chemokine response to OVA, an antigen to which they have not been exposed. Interestingly, LPMC from BBdp rats showed a widely pro-inflammatory cytokine/chemokine profile in response to WP compared with BBc rats. This was an especially striking finding since the BB rats used in our study had been on a wheat-based cereal diet since weaning at 23 days of age. It was therefore interesting to see that BBc rats displayed little response to WP, to which they were exposed chronically in the diet and orally tolerized whereas the strong pro-inflammatory response of BBdp rats is consistent with impaired gut immunity and diminished oral tolerance. Indeed, BBdp LPMC upregulated pro-inflammatory cytokine and chemokines in response to WP, much like what was seen in the WP-induced PBMC from human T1D patients. A previous study revealed a lamina propria-specific decrease in CD103 dendritic cells and increase in class II MHC^+ cells, suggesting a pro-inflammatory status in the gut of cereal-fed BBdp rats compared with controls (Graham, Courtois et al. 2004). Our *in vitro* data expand and strengthen the hypothesis that a predominantly pro-inflammatory microenvironment in the lamina propria is associated with exposure to WP.

It is reasonable to expect that the expression of HO-1 would be increased by LPMC when challenged with WP to counteract the pro-inflammatory cytokine/chemokine response including IL-6, IL-1α, IL-17. Interestingly, LPMC from BBdp rats showed impairment in HO-1 upregulation in the presence of WP, OVA, and LPS compared with LPMC from BBc rats. There is increasing evidence to suggest that IL-17-producing T helper cells (Th17 cells) are the main population of pathogenic T cells driving autoimmune diseases such as T1D and that IL-6 is required for the lineage commitment of these pathogenic Th17 cells (McGeachy, Bak-Jensen et al. 2007). A recent study in children with new-onset T1D found that there was an increase in a distinct subset of $FoxP3^+$ T cells that are not suppressive and instead secrete significantly more IL-17 than other $FoxP3^+$ subsets (Marwaha, Crome et al. 2010). Another study reports that T1D develops in the BBdp rats due to an imbalance of Th17 effector ($Th17_{eff}$) and regulatory T cells (T_{reg}), which can be corrected by introducing T_{reg} cells (van den Brandt, Fischer et al. 2010). As HO-1 has been shown to be involved in the suppressive effects of T_{reg} cells, it is likely that the observed impairment in HO-1 upregulation by LPMC from BBdp rats causes them to function improperly. It is then possible that WP expands $Th17_{eff}$ cells much sooner than would normally happen, thereby exacerbating disease progression. Indeed, LPMC from BBdp rats showed a marked increase in both IL-6 and IL-17 in response to WP compared with controls, which is consistent with the idea that IL-6 in tandem with other pro-inflammatory cytokines can promote diabetes development (Mojibian, Chakir et al. 2009; Singh, Nikoopour et al. 2011). These data support a role for HO-1 and the gut innate immune system in T1D, which may drive the adaptive immune system to expand the Th17 population of effector T cells (Mojibian, Chakir et al. 2009; van den Brandt, Fischer et al. 2010).

CONCLUSIONS AND FUTURE DIRECTIONS

We have shown that upregulation of the enzyme HO-1 *in vivo* by CoPP is sufficient to inhibit development of T1D in BBdp rats. Surprisingly, the majority of HO-1 expression was associated with M1 CD68$^+$ cells in the pancreas and PLN. It would be beneficial to quantify the identified population of M2-like CD68$^+$CD163$^+$HO-1$^+$ macrophages in the pancreas and to compare the frequency between treatment groups. Future studies could also investigate whether CoPP treatment could reverse T1D in overt diabetic BBdp rats. In efforts to understand the mechanism of HO-1-mediated protection from T1D, gene expression analysis of pancreatic RNA comparing CoPP-treated BBdp rats with controls revealed many upregulated genes from the *Reg* and *α-defensin* families, which are known to confer anti-microbial and regenerative properties. We also found an increase in *Camp* gene and protein expression in the gut of CoPP-treated BBdp rats compared with controls and that this protein co-localized with M2 macrophages in the gut. As this project has focused largely on aspects of the innate immune system, it would be helpful to characterize the T cell population in the pancreas which could expand on the role of the adaptive immune system in the protective phenotype associated with HO-1 upregulation.

Our *in vitro* work showed that LPMC from BBdp rats have impaired HO-1 upregulation in response to pro-inflammatory stimuli from LPS and WP. Furthermore, LPMC from BBdp rats showed a striking pro-inflammatory cytokine and chemokine profile in response to WP compared with controls. It would be important to validate cytokines and chemokines of interest using ELISA in individual supernatant samples. Taken together, our preliminary *in vivo* and *in vitro* data indicate that HO-1 is indeed an important cytoprotective enzyme in the context of T1D and that HO-1 induction is a key step toward β-cell mass preservation through the recruitment of a distinct population of anti-inflammatory M2 macrophages in the pancreas and gut. The protection is associated with recruitment of macrophages to the pancreas that could be related to upregulation of antimicrobials suggesting important pleotropic roles for these molecules in the context of T1D, possibly linked with the CD163/HO-1 pathway.

STATEMENT OF CONTRIBUTION OF COLLABORATORS

Jennifer A. Crookshank, *M.Sc., Senior Research Technician*, provided assistance with LPMC primary cell isolation and general cell culture maintenance. Jennifer provided instruction for LPMC intracellular staining, ran samples on the flow cytometer and additionally helped with the cytokine/chemokine antibody array.

Dr. Gen-Sheng Wang, *M.D., Ph.D., Research Associate*, designed the CoPP study. Dr. Wang provided instruction and quality control for immunohistochemistry and morphomety techniques as well as detailed instruction on analyzing pancreas sections for insulitis evaluation.

Christopher Patrick, *Ph.D. Candidate*, provided advice and assistance with pancreas RNA isolation for microarray analysis and immunohistochemistry techniques.

Ariana Noel, *M.Sc. Candidate*, provided instruction on generating gene lists from the CoPP microarray experiment and using various bioinformatics resources. Ariana also assisted with the qPCR gene expression experiment.

Annika Hausmann, *Visiting Intern, Friedrich-Wilhelms University, Bonn, Germany***,** performed the qPCR gene expression array experiment using cDNA I had previously generated from saline and CoPP-treated RNA jejunal RNA samples.

Caroline Vergette, *OHRI Stemcore Laboratories***,** evaluated pancreas and jejunal RNA integrity and performed the pancreas microarray analyses.

Garnet Rodger and Pierre Bradley. *Animal technicians at the Animal Care Unit*, maintained the BB rat colonies, performed the CoPP injections at the OHRI Civic Campus, and monitored diabetes in the animals.

REFERENCES

Abraham, N. G. and A. Kappas (2008). "Pharmacological and clinical aspects of heme oxygenase." Pharmacol Rev **60**(1): 79-127.

Baeke, F., T. Takiishi, et al. (2010). "Vitamin D: modulator of the immune system." Curr Opin Pharmacol **10**(4): 482-96.

Bals, R. and J. M. Wilson (2003). "Cathelicidins--a family of multifunctional antimicrobial peptides." Cell Mol Life Sci **60**(4): 711-20.

Behr, R., C. Deller, et al. (2007). "Kruppel-like factor 4 expression in normal and pathological human testes." Mol Hum Reprod **13**(11): 815-20.

Bortell, R. and C. Yang (2012). "The BB rat as a model of human type 1 diabetes." Methods Mol Biol **933**: 31-44.

Bouhlel, M. A., B. Derudas, et al. (2007). "PPARgamma activation primes human monocytes into alternative M2 macrophages with anti-inflammatory properties." Cell Metab **6**(2): 137-43.

Boyle, J. J., H. A. Harrington, et al. (2009). "Coronary intraplaque hemorrhage evokes a novel atheroprotective macrophage phenotype." Am J Pathol **174**(3): 1097-108.

Brown, K. L., G. F. Poon, et al. (2011). "Host defense peptide LL-37 selectively reduces proinflammatory macrophage responses." J Immunol **186**(9): 5497-505.

Brusko, T. M., C. H. Wasserfall, et al. (2005). "An integral role for heme oxygenase-1 and carbon monoxide in maintaining peripheral tolerance by CD4+CD25+ regulatory T cells." J Immunol **174**(9): 5181-6.

Burt, T. D., L. Seu, et al. (2010). "Naive human T cells are activated and proliferate in response to the heme oxygenase-1 inhibitor tin mesoporphyrin." J Immunol **185**(9): 5279-88.

Calderon, B., A. Suri, et al. (2008). "IFN-gamma-dependent regulatory circuits in immune inflammation highlighted in diabetes." J Immunol **181**(10): 6964-74.

Caraher, E. M., M. Parenteau, et al. (2000). "Flow cytometric analysis of intracellular IFN-gamma, IL-4 and IL-10 in CD3(+)4(+) T-cells from rat spleen." J Immunol Methods **244**(1-2): 29-40.

Carrier, Y., H. L. Ma, et al. (2011). "Inter-regulation of Th17 cytokines and the IL-36 cytokines in vitro and in vivo: implications in psoriasis pathogenesis." J Invest Dermatol **131**(12): 2428-37.

Chakir, H., D. E. Lefebvre, et al. (2005). "Wheat protein-induced proinflammatory T helper 1 bias in mesenteric lymph nodes of young diabetes-prone rats." Diabetologia **48**(8): 1576-84.

Chawla, A. (2010). "Control of macrophage activation and function by PPARs." Circ Res **106**(10): 1559-69.

Choi, B. M., H. O. Pae, et al. (2005). "Critical role of heme oxygenase-1 in Foxp3-mediated immune suppression." Biochem Biophys Res Commun **327**(4): 1066-71.

Chou, F. C., S. H. Huang, et al. (2012). "Genetically engineered islets and alternative sources of insulin-producing cells for treating autoimmune diabetes: quo vadis?" Int J Endocrinol **2012**: 296485.

Chuang, Y. P., C. H. Chu, et al. (2008). "Genetic manipulation of islet cells in autoimmune diabetes: from bench to bedside." Front Biosci **13**: 6155-69.

Closa, D., Y. Motoo, et al. (2007). "Pancreatitis-associated protein: from a lectin to an anti-inflammatory cytokine." World J Gastroenterol **13**(2): 170-4.

Cooper, J. D., D. J. Smyth, et al. (2011). "Inherited variation in vitamin D genes is associated with predisposition to autoimmune disease type 1 diabetes." Diabetes **60**(5): 1624-31.
Courtois, P., G. Nsimba, et al. (2005). "Gut permeability and intestinal mucins, invertase, and peroxidase in control and diabetes-prone BB rats fed either a protective or a diabetogenic diet." Dig Dis Sci **50**(2): 266-75.
Cruse, I. and M. D. Maines (1988). "Evidence suggesting that the two forms of heme oxygenase are products of different genes." J Biol Chem **263**(7): 3348-53.
Cui, W., K. De Jesus, et al. (2009). "Overexpression of Reg3alpha increases cell growth and the levels of cyclin D1 and CDK4 in insulinoma cells." Growth Factors **27**(3): 195-202.
Cunliffe, R. N. and Y. R. Mahida (2004). "Expression and regulation of antimicrobial peptides in the gastrointestinal tract." J Leukoc Biol **75**(1): 49-58.
Damci, T., I. Nuhoglu, et al. (2003). "Increased intestinal permeability as a cause of fluctuating postprandial blood glucose levels in Type 1 diabetic patients." Eur J Clin Invest **33**(5): 397-401.
Dang, D. T., J. Pevsner, et al. (2000). "The biology of the mammalian Kruppel-like family of transcription factors." Int J Biochem Cell Biol **32**(11-12): 1103-21.
Davidson, A. and B. Diamond (2001). "Autoimmune diseases." N Engl J Med **345**(5): 340-50.
Denning, T. L., Y. C. Wang, et al. (2007). "Lamina propria macrophages and dendritic cells differentially induce regulatory and interleukin 17-producing T cell responses." Nat Immunol **8**(10): 1086-94.
Durr, U. H., U. S. Sudheendra, et al. (2006). "LL-37, the only human member of the cathelicidin family of antimicrobial peptides." Biochim Biophys Acta **1758**(9): 1408-25.
Fabriek, B. O., C. D. Dijkstra, et al. (2005). "The macrophage scavenger receptor CD163." Immunobiology **210**(2-4): 153-60.
Faleo, G., J. S. Neto, et al. (2008). "Carbon monoxide ameliorates renal cold ischemia-reperfusion injury with an upregulation of vascular endothelial growth factor by activation of hypoxia-inducible factor." Transplantation **85**(12): 1833-40.
Fasano, A. and T. Shea-Donohue (2005). "Mechanisms of disease: the role of intestinal barrier function in the pathogenesis of gastrointestinal autoimmune diseases." Nat Clin Pract Gastroenterol Hepatol **2**(9): 416-22.
Feinberg, M. W., A. K. Wara, et al. (2007). "The Kruppel-like factor KLF4 is a critical regulator of monocyte differentiation." Embo J **26**(18): 4138-48.
Furuhashi, M. and G. S. Hotamisligil (2008). "Fatty acid-binding proteins: role in metabolic diseases and potential as drug targets." Nat Rev Drug Discov **7**(6): 489-503.
George, J. F., A. Braun, et al. (2008). "Suppression by CD4+CD25+ regulatory T cells is dependent on expression of heme oxygenase-1 in antigen-presenting cells." Am J Pathol **173**(1): 154-60.
Gironella, M., E. Folch-Puy, et al. (2007). "Experimental acute pancreatitis in PAP/HIP knock-out mice." Gut **56**(8): 1091-7.
Giulietti, A., C. Gysemans, et al. (2004). "Vitamin D deficiency in early life accelerates Type 1 diabetes in non-obese diabetic mice." Diabetologia **47**(3): 451-62.

Gong, P., B. Hu, et al. (2001). "Cobalt induces heme oxygenase-1 expression by a hypoxia-inducible factor-independent mechanism in Chinese hamster ovary cells: regulation by Nrf2 and MafG transcription factors." J Biol Chem **276**(29): 27018-25.
Goodnow, C. C., J. Sprent, et al. (2005). "Cellular and genetic mechanisms of self tolerance and autoimmunity." Nature **435**(7042): 590-7.
Graf, R., M. Schiesser, et al. (2006). "Exocrine meets endocrine: pancreatic stone protein and regenerating protein--two sides of the same coin." J Surg Res **133**(2): 113-20.
Graham, S., P. Courtois, et al. (2004). "Enteropathy precedes type 1 diabetes in the BB rat." Gut **53**(10): 1437-44.
Haase, M., R. Bellomo, et al. (2010). "Novel biomarkers, oxidative stress, and the role of labile iron toxicity in cardiopulmonary bypass-associated acute kidney injury." J Am Coll Cardiol **55**(19): 2024-33.
Hamelinck, D., H. Zhou, et al. (2005). "Optimized normalization for antibody microarrays and application to serum-protein profiling." Mol Cell Proteomics **4**(6): 773-84.
Hoorfar, J., F. W. Scott, et al. (1991). "Dietary plant materials and development of diabetes in the BB rat." J Nutr **121**(6): 908-16.
Hu, C. M., H. H. Lin, et al. (2007). "Systemic expression of heme oxygenase-1 ameliorates type 1 diabetes in NOD mice." Diabetes **56**(5): 1240-7.
Huang da, W., B. T. Sherman, et al. (2009). "Systematic and integrative analysis of large gene lists using DAVID bioinformatics resources." Nat Protoc **4**(1): 44-57.
Huang, S. H., C. H. Chu, et al. (2010). "Transgenic expression of haem oxygenase-1 in pancreatic beta cells protects non-obese mice used as a model of diabetes from autoimmune destruction and prolongs graft survival following islet transplantation." Diabetologia **53**(11): 2389-400.
Husemann, J., J. D. Loike, et al. (2002). "Scavenger receptors in neurobiology and neuropathology: their role on microglia and other cells of the nervous system." Glia **40**(2): 195-205.
Ijssennagger, N., N. de Wit, et al. (2012). "Dietary heme-mediated PPARalpha activation does not affect the heme-induced epithelial hyperproliferation and hyperplasia in mouse colon." PLoS One **7**(8): e43260.
Immenschuh, S., E. Baumgart-Vogt, et al. (2003). "Differential cellular and subcellular localization of heme-binding protein 23/peroxiredoxin I and heme oxygenase-1 in rat liver." J Histochem Cytochem **51**(12): 1621-31.
Janeway, C., P. Travers, et al. (2008). Immunobiology. New York, Garland Science.
Jankosky, C., E. Deussing, et al. (2012). "Viruses and vitamin D in the etiology of type 1 diabetes mellitus and multiple sclerosis." Virus Res **163**(2): 424-30.
JDRF, F. (2012). General Diabetes Information: Fact Sheet. Juvenile Diabetes Research Foundation.
Jiao, X., B. T. Sherman, et al. (2012). "DAVID-WS: a stateful web service to facilitate gene/protein list analysis." Bioinformatics **28**(13): 1805-6.
Johnston, A., X. Xing, et al. (2011). "IL-1F5, -F6, -F8, and -F9: a novel IL-1 family signaling system that is active in psoriasis and promotes keratinocyte antimicrobial peptide expression." J Immunol **186**(4): 2613-22.
Kloppel, G., S. Detlefsen, et al. (2004). "Fibrosis of the pancreas: the initial tissue damage and the resulting pattern." Virchows Arch **445**(1): 1-8.

Koehler, J. A., L. L. Baggio, et al. (2009). "Glucagon-like peptide-1 receptor activation modulates pancreatitis-associated gene expression but does not modify the susceptibility to experimental pancreatitis in mice." Diabetes **58**(9): 2148-61.

Kotarsky, K., K. M. Sitnik, et al. (2010). "A novel role for constitutively expressed epithelial-derived chemokines as antibacterial peptides in the intestinal mucosa." Mucosal Immunol **3**(1): 40-8.

Lai, Y., D. Li, et al. (2012). "The antimicrobial protein REG3A regulates keratinocyte proliferation and differentiation after skin injury." Immunity **37**(1): 74-84.

Lawrence, T. and G. Natoli (2011). "Transcriptional regulation of macrophage polarization: enabling diversity with identity." Nat Rev Immunol **11**(11): 750-61.

Lee, E. M., Y. E. Lee, et al. (2011). "Protective Effect of Heme Oxygenase-1 on High Glucose-Induced Pancreatic beta-Cell Injury." Diabetes Metab J **35**(5): 469-79.

Lee, S. S., W. Gao, et al. (2007). "Heme oxygenase-1, carbon monoxide, and bilirubin induce tolerance in recipients toward islet allografts by modulating T regulatory cells." Faseb J **21**(13): 3450-7.

Lefebvre, D. E., K. Powell, et al. (2006). "Dietary proteins as environmental modifiers of type 1 diabetes mellitus." Annu Rev Nutr. **26**: 175-202.

Lefrancois, L. and N. Lycke (2001). "Isolation of mouse small intestinal intraepithelial lymphocytes, Peyer's patch, and lamina propria cells." Curr Protoc Immunol **Chapter 3**: Unit 3 19.

Lehuen, A., J. Diana, et al. (2010). "Immune cell crosstalk in type 1 diabetes." Nat Rev Immunol **10**(7): 501-13.

Li, M., S. Peterson, et al. (2007). "Long-lasting expression of HO-1 delays progression of type I diabetes in NOD mice." Cell Cycle **6**(5): 567-71.

Li, M., S. Peterson, et al. (2007). "Interdiction of the diabetic state in NOD mice by sustained induction of heme oxygenase: possible role of carbon monoxide and bilirubin." Antioxid Redox Signal **9**(7): 855-63.

Liao, X., N. Sharma, et al. (2011). "Kruppel-like factor 4 regulates macrophage polarization." J Clin Invest **121**(7): 2736-49.

Lin, Q., S. Weis, et al. (2007). "Heme oxygenase-1 protein localizes to the nucleus and activates transcription factors important in oxidative stress." J Biol Chem **282**(28): 20621-33.

Lisitsyn, N. A., Y. A. Bukurova, et al. (2012). "Enteric alpha defensins in norm and pathology." Ann Clin Microbiol Antimicrob **11**: 1.

Loit, E., C. W. Melnyk, et al. (2009). "Identification of three wheat globulin genes by screening a Triticum aestivum BAC genomic library with cDNA from a diabetes-associated globulin." BMC Plant Biol **9**: 93.

MacFarlane, A. J., K. M. Burghardt, et al. (2003). "A type 1 diabetes-related protein from wheat (Triticum aestivum). cDNA clone of a wheat storage globulin, Glb1, linked to islet damage." J Biol Chem **278**(1): 54-63.

Mackay, I. R. (2000). "Science, medicine, and the future: Tolerance and autoimmunity." Bmj **321**(7253): 93-6.

Maines, M. D. (1988). "Heme oxygenase: function, multiplicity, regulatory mechanisms, and clinical applications." Faseb J **2**(10): 2557-68.

Mantovani, A., A. Sica, et al. (2004). "The chemokine system in diverse forms of macrophage activation and polarization." Trends Immunol **25**(12): 677-86.

Martinez, F. O. (2011). "Regulators of macrophage activation." Eur J Immunol **41**(6): 1531-4.

Marwaha, A. K., S. Q. Crome, et al. (2010). "Cutting edge: Increased IL-17-secreting T cells in children with new-onset type 1 diabetes." J Immunol **185**(7): 3814-8.

McCoubrey, W. K., Jr., T. J. Huang, et al. (1997). "Isolation and characterization of a cDNA from the rat brain that encodes hemoprotein heme oxygenase-3." Eur J Biochem **247**(2): 725-32.

McCoubrey, W. K., Jr. and M. D. Maines (1994). "The structure, organization and differential expression of the gene encoding rat heme oxygenase-2." Gene **139**(2): 155-61.

McGeachy, M. J., K. S. Bak-Jensen, et al. (2007). "TGF-beta and IL-6 drive the production of IL-17 and IL-10 by T cells and restrain T(H)-17 cell-mediated pathology." Nat Immunol **8**(12): 1390-7.

Meddings, J. B., J. Jarand, et al. (1999). "Increased gastrointestinal permeability is an early lesion in the spontaneously diabetic BB rat." Am J Physiol **276**(4 Pt 1): G951-7.

Mojibian, M., H. Chakir, et al. (2009). "Diabetes-specific HLA-DR-restricted proinflammatory T-cell response to wheat polypeptides in tissue transglutaminase antibody-negative patients with type 1 diabetes." Diabetes **58**(8): 1789-96.

Mojibian, M., H. Chakir, et al. (2006). "Immune reactivity to a glb1 homologue in a highly wheat-sensitive patient with type 1 diabetes and celiac disease." Diabetes Care **29**(5): 1108-10.

Mordes, J. P., R. Bortell, et al. (2004). "Rat models of type 1 diabetes: genetics, environment, and autoimmunity." Ilar J **45**(3): 278-91.

Morizane, S., and R.L. Gallo (2012). "Antimicrobial peptides in the pathogenesis of psoriasis." The Journal of Dermatology **39**: 225–230.

Mosser, D. M. and J. P. Edwards (2008). "Exploring the full spectrum of macrophage activation." Nat Rev Immunol **8**(12): 958-69.

Mowat, A. M. (2003). "Anatomical basis of tolerance and immunity to intestinal antigens." Nat Rev Immunol **3**(4): 331-41.

Murray, P. J. and T. A. Wynn (2011). "Protective and pathogenic functions of macrophage subsets." Nat Rev Immunol **11**(11): 723-37.

Nath, K. A. (2006). "Heme oxygenase-1: a provenance for cytoprotective pathways in the kidney and other tissues." Kidney Int **70**(3): 432-43.

Neuwirth, A., J. Dobes, et al. (2012). "Eosinophils from patients with type 1 diabetes mellitus express high level of myeloid alpha-defensins and myeloperoxidase." Cell Immunol **273**(2): 158-63.

Nijnik, A. and R. E. Hancock (2009). "The roles of cathelicidin LL-37 in immune defences and novel clinical applications." Curr Opin Hematol **16**(1): 41-7.

Nijnik, A., J. Pistolic, et al. (2009). "Human cathelicidin peptide LL-37 modulates the effects of IFN-gamma on APCs." J Immunol **183**(9): 5788-98.

Odegaard, J. I., R. R. Ricardo-Gonzalez, et al. (2007). "Macrophage-specific PPARgamma controls alternative activation and improves insulin resistance." Nature **447**(7148): 1116-20.

Orme, J. and C. Mohan (2012). "Macrophage subpopulations in systemic lupus erythematosus." Discov Med **13**(69): 151-8.

Otterbein, L. E. and A. M. Choi (2000). "Heme oxygenase: colors of defense against cellular stress." Am J Physiol Lung Cell Mol Physiol **279**(6): L1029-37.

Pae, H. O., G. S. Oh, et al. (2004). "Carbon monoxide produced by heme oxygenase-1 suppresses T cell proliferation via inhibition of IL-2 production." J Immunol **172**(8): 4744-51.
Parsa, R., P. Andresen, et al. (2012). "Adoptive transfer of immunomodulatory M2 macrophages prevents type 1 diabetes in NOD mice." Diabetes **61**(11): 2881-92.
Polfliet, M. M., B. O. Fabriek, et al. (2006). "The rat macrophage scavenger receptor CD163: expression, regulation and role in inflammatory mediator production." Immunobiology **211**(6-8): 419-25.
Pulkkinen, K. H., S. Yla-Herttuala, et al. (2011). "Heme oxygenase 1 is induced by miR-155 via reduced BACH1 translation in endothelial cells." Free Radic Biol Med **51**(11): 2124-31.
Quimby, K. R., A. Greenidge, et al. (2010). "Phenotypic commitment of monocytes towards a protective hemoglobin scavenging phenotype (CD14(pos)CD163(high)HLA-DR(low))following cardiopulmonary bypass." Cytometry B Clin Cytom **78**(5): 357-60.
Ramadas, R. A., S. L. Ewart, et al. (2011). "Interleukin-1 family member 9 stimulates chemokine production and neutrophil influx in mouse lungs." Am J Respir Cell Mol Biol **44**(2): 134-45.
Ryter, S. W. and A. M. Choi (2009). "Heme oxygenase-1/carbon monoxide: from metabolism to molecular therapy." Am J Respir Cell Mol Biol **41**(3): 251-60.
Ryter, S. W., L. E. Otterbein, et al. (2002). "Heme oxygenase/carbon monoxide signaling pathways: regulation and functional significance." Mol Cell Biochem **234-235**(1-2): 249-63.
Sakaguchi, S., T. Yamaguchi, et al. (2008). "Regulatory T cells and immune tolerance." Cell **133**(5): 775-87.
Salzman, N. H., M. A. Underwood, et al. (2007). "Paneth cells, defensins, and the commensal microbiota: a hypothesis on intimate interplay at the intestinal mucosa." Semin Immunol **19**(2): 70-83.
Schenk, M. and C. Mueller (2007). "Adaptations of intestinal macrophages to an antigen-rich environment." Semin Immunol **19**(2): 84-93.
Schmidt, R. (2007). "Cobalt protoporphyrin as a potential therapeutic agent?" The FASEB Journal **21**(11).
Secondulfo, M., D. Iafusco, et al. (2004). "Ultrastructural mucosal alterations and increased intestinal permeability in non-celiac, type I diabetic patients." Dig Liver Dis **36**(1): 35-45.
Segaert, S. (2008). "Vitamin D regulation of cathelicidin in the skin: toward a renaissance of vitamin D in dermatology?" J Invest Dermatol **128**(4): 773-5.
Shan, Y., R. W. Lambrecht, et al. (2006). "Role of Bach1 and Nrf2 in up-regulation of the heme oxygenase-1 gene by cobalt protoporphyrin." Faseb J **20**(14): 2651-3.
Shan, Y., J. Pepe, et al. (2000). "Induction of the heme oxygenase-1 gene by metalloporphyrins." Arch Biochem Biophys **380**(2): 219-27.
Sierra-Filardi, E., M. A. Vega, et al. (2010). "Heme Oxygenase-1 expression in M-CSF-polarized M2 macrophages contributes to LPS-induced IL-10 release." Immunobiology **215**(9-10): 788-95.
Simon, T., I. Anegon, et al. (2011). "Heme oxygenase and carbon monoxide as an immunotherapeutic approach in transplantation and cancer." Immunotherapy **3**(4 Suppl): 15-8.

Simpson, M., M. Mojibian, et al. (2009). "An exploration of Glo-3A antibody levels in children at increased risk for type 1 diabetes mellitus." Pediatr Diabetes **10**(8): 563-72.
Singh, B., E. Nikoopour, et al. (2011). "Immunomodulation and regeneration of islet Beta cells by cytokines in autoimmune type 1 diabetes." J Interferon Cytokine Res **31**(10): 711-9.
Solly, N. R., M. C. Honeyman, et al. (2001). "The mucosal interface between 'self' and 'non-self' determines the impact of environment on autoimmune diabetes." Curr Dir Autoimmun **4**: 68-90.
Sonier, B., A. Strom, et al. (2011). "Antibodies from a patient with type 1 diabetes and celiac disease bind to macrophages that express the scavenger receptor CD163." Can J Gastroenterol **25**(6): 327-9.
Stewart, J. M., G. W. Slysz, et al. (1996). "Ferriheme and ferroheme are isosteric inhibitors of fatty acid binding to rat liver fatty acid binding protein." Biochem Cell Biol **74**(2): 249-55.
Tidball, J. G. and S. A. Villalta (2010). "Regulatory interactions between muscle and the immune system during muscle regeneration." Am J Physiol Regul Integr Comp Physiol **298**(5): R1173-87.
Tripathi, A., K. M. Lammers, et al. (2009). "Identification of human zonulin, a physiological modulator of tight junctions, as prehaptoglobin-2." Proc Natl Acad Sci U S A **106**(39): 16799-804.
Vaarala, O. (2008). "Leaking gut in type 1 diabetes." Curr Opin Gastroenterol **24**(6): 701-6.
van Belle, T. L., K. T. Coppieters, et al. (2011). "Type 1 diabetes: etiology, immunology, and therapeutic strategies." Physiol Rev **91**(1): 79-118.
van den Brandt, J., H. J. Fischer, et al. (2010). "Type 1 diabetes in BioBreeding rats is critically linked to an imbalance between Th17 and regulatory T cells and an altered TCR repertoire." J Immunol **185**(4): 2285-94.
Van Gorp, H., P. L. Delputte, et al. (2010). "Scavenger receptor CD163, a Jack-of-all-trades and potential target for cell-directed therapy." Mol Immunol **47**(7-8): 1650-60.
Vangapandu, H. a. W. A. (2009). "Kruppel like factor 4 (KLF4): a transcription factor with diverse context-dependent functions." Gene Therapy and Molecular Biology **13**: 194-204.
Vijayan, V., S. Mueller, et al. (2010). "Heme oxygenase-1 as a therapeutic target in inflammatory disorders of the gastrointestinal tract." World J Gastroenterol **16**(25): 3112-9.
Villalta, S. A., H. X. Nguyen, et al. (2009). "Shifts in macrophage phenotypes and macrophage competition for arginine metabolism affect the severity of muscle pathology in muscular dystrophy." Hum Mol Genet **18**(3): 482-96.
Visser, J., J. Rozing, et al. (2009). "Tight junctions, intestinal permeability, and autoimmunity: celiac disease and type 1 diabetes paradigms." Ann N Y Acad Sci **1165**: 195-205.
Viterbo, D., M. H. Bluth, et al. (2008). "Pancreatitis-associated protein 2 modulates inflammatory responses in macrophages." J Immunol **181**(3): 1948-58.
Vomhof-Dekrey, E. E. and M. J. Picklo, Sr. (2012). "The Nrf2-antioxidant response element pathway: a target for regulating energy metabolism." J Nutr Biochem **23**(10): 1201-6.

von Rahden, B. H., S. Kircher, et al. (2011). "Association of steroid use with complicated sigmoid diverticulitis: potential role of activated CD68+/CD163+ macrophages." Langenbecks Arch Surg **396**(6): 759-68.

Wagener, F. A., H. D. Volk, et al. (2003). "Different faces of the heme-heme oxygenase system in inflammation." Pharmacol Rev **55**(3): 551-71.

Wang, G., Y. Gong, et al. (2005). "Antioxidative function of L-FABP in L-FABP stably transfected Chang liver cells." Hepatology **42**(4): 871-9.

Watts, T., I. Berti, et al. (2005). "Role of the intestinal tight junction modulator zonulin in the pathogenesis of type I diabetes in BB diabetic-prone rats." Proc Natl Acad Sci U S A **102**(8): 2916-21.

Yamamoto, C. M., N. Banaiee, et al. (2004). "Alpha-defensin expression during myelopoiesis: identification of cis and trans elements that regulate expression of NP-3 in rat promyelocytes." J Leukoc Biol **75**(2): 332-41.

Yan, J., Y. Gong, et al. (2009). "Molecular mechanism of recombinant liver fatty acid binding protein's antioxidant activity." J Lipid Res **50**(12): 2445-54.

Zella, J. B., L. C. McCary, et al. (2003). "Oral administration of 1,25-dihydroxyvitamin D3 completely protects NOD mice from insulin-dependent diabetes mellitus." Arch Biochem Biophys **417**(1): 77-80.

APPENDIX

Table 5. Partial list of upregulated genes from HO-1 induction by CoPP in pancreas. Abbreviated list of the upregulated genes from the 51 d BBdp pancreas microarray experiments comparing CoPP treated and saline treated gene expression. RNA was isolated at 51 days and pooled (n=8/group) for analysis using Affymetrix Rat Gene 1.0 ST chips. Gene list obtained using AltAnalyze software.

ENSEMBL GENE ID	Gene Symbol	Definition	Probe Value Saline	Probe Value CoPP	Fold Change
ENSRNOG00000024947	j	Fatty acid-binding protein, intestinal (I-FABP) (FABPI). [Source:UniProtKB/Swiss-Prot;Acc:P02693]	2.604873	10.83626	300.53620
ENSRNOG00000003902	Fabp6	Gastrotropin (GT) (Ileal lipid-binding protein) (ILBP) (Intestinal 15 kDa protein) (I-15P) (14 kDa bile acid-binding protein) (I-BABP). [Source:UniProtKB/Swiss-Prot;Acc:P80020]	4.518973	12.46381	246.39628
ENSRNOG00000031067	Si	Sucrase-isomaltase, intestinal [Contains: Sucrase (EC 3.2.1.48); Isomaltase (EC 3.2.1.10)]. [Source:UniProtKB/Swiss-Prot;Acc:P23739]	2.20125	10.03612	228.31312
ENSRNOG00000001794	Muc13	mucin 13, epithelial transmembrane (Muc13), mRNA [Source:RefSeq_dna;Acc:NM_139041]	3.265254	9.922648	100.94280
ENSRNOG00000037374	Ly6a_predict		3.983293	10.54666	94.574106
ENSRNOG00000022411	2010106E10 Rik	hypothetical protein LOC67715 [Source:RefSeq peptide;Acc:NP_080609]	2.352288	8.5635	74.090243
ENSRNOG00000028707	Np4	Neutrophil antibiotic peptide NP-4 precursor (Neutrophil defensin 4) (RatNP-4). [Source:UniProtKB/Swiss-Prot;Acc:Q62714]	2.61007	8.75489	70.757933
ENSRNOG00000029889	Clca6	chloride channel calcium activated 6 [Source:RefSeq_peptide;Acc:NP_958822]	4.236128	10.04882	56.207903
ENSRNOG00000006579	Reg3g	Regenerating islet-derived protein 3 gamma precursor (Reg III-gamma) (Pancreatitis-associated protein 3). [Source:UniProtKB/Swiss-Prot;Acc:P42854]	4.890948	10.68628	55.535254
ENSRNOG00000029522	Defa6	alpha-defensin 6 [Source:RefSeq_peptide;Acc:NP_001028248]	4.04138	9.75203	52.369321
ENSRNOG00000015562	Cdh17	Cadherin-17 precursor (Liver-intestine cadherin) (LI-cadherin). [Source:UniProtKB/Swiss-Prot;Acc:P55281]	3.993672	9.526794	46.305843
ENSRNOG00000026844	LOC686714		4.75037	10.23509	44.778263
ENSRNOG00000014117	Hmox1	Heme oxygenase 1 (EC 1.14.99.3) (HO-1) (HSP32). [Source:UniProtKB/Swiss-Prot;Acc:P06762]	4.838177	10.27698	43.375445
ENSRNOG00000003865	Tmigd_pred		4.081056	9.422592	40.547357
ENSRNOG00000013280	NP_001099522.1	olfactomedin 4 [Source:RefSeq_peptide;Acc:NP_001099522]	3.876808	9.203695	40.137740
ENSRNOG00000021000	Naaladl1	N-acetylated-alpha-linked acidic dipeptidase-like protein (NAALADase L)(EC 3.4.17.21) [Source:UniProtKB/Swiss-Prot;Acc:Q7M758]	4.045978	9.28987	37.893867
ENSRNOG00000006675	Fabp1	Fatty acid-binding protein, liver (L-FABP) (Z-protein) (Squalene- and sterol-carrier protein) (SCP) (p14). [Source:UniProtKB/Swiss-Prot;Acc:P02692]	3.747315	8.988507	37.823015
ENSRNOG00000031464	Defa9	defensin alpha 9 (Defa9), mRNA [Source:RefSeq_dna;Acc:NM_001025763]	4.245945	9.4864	37.803685
ENSRNOG00000011022	Mep1a	Meprin A subunit alpha precursor (EC 3.4.24.18) (Endopeptidase-2) (MEP-1) (Endopeptidase-24.18 subunit alpha) (E-24.18). [Source:UniProtKB/Swiss-Prot;Acc:Q64230]	3.09264	8.25124	35.718510
ENSRNOG00000000251	NP_001099329.1	ST6 (alpha-N-acetyl-neuraminyl-2,3-beta-galactosyl-1, 3)-N-acetylgalactosaminide alpha-2,6-sialyltransferase 1 [Source:RefSeq_peptide;Acc:NP_001099329]	3.31317	8.459837	35.424301

ENSRNOG00000039360			3.07697	8.15902	33.872674
ENSRNOG00000005023	NP_001100195.1	anterior gradient 2 [Source:RefSeq_peptide;Acc:NP_001100195]	4.038426	9.089381	33.150430
ENSRNOG00000013447	NP_001100919.1	chloride channel calcium activated 3 [Source:RefSeq_peptide;Acc:NP_001100919]	4.226781	9.260934	32.766588
ENSRNOG00000039010			4.480485	9.513895	32.749704
ENSRNOG00000038139	Defa8	alpha-defensin 8 [Source:RefSeq_peptide;Acc:NP_001028249]	4.188495	9.106205	30.225828
ENSRNOG00000003740	Gpa33_pred		3.861018	8.762076	29.878959
ENSRNOG00000011598	S15A1_RAT	Oligopeptide transporter, small intestine isoform (Peptide transporter 1) (Intestinal H(+)/peptide cotransporter) (Solute carrier family 15 member 1) (Proton-coupled dipeptide cotransporter). [Source:UniProtKB/Swiss-Prot;Acc:P51574]	4.063453	8.935268	29.279418
ENSRNOG00000008575	Abp1	Amiloride-sensitive amine oxidase [copper-containing] precursor (EC 1.4.3.6) (Diamine oxidase) (DAO) (Amiloride-binding protein) (ABP) (Histaminase). [Source:UniProtKB/Swiss-Prot;Acc:P36633]	3.05512	7.922615	29.191875
ENSRNOG00000020625	Mcpt2	Mast cell protease 2 precursor (EC 3.4.21.-) (Mast cell protease II) (rMCP-II) (rMCP-2) (Group-specific protease). [Source:UniProtKB/Swiss-Prot;Acc:P00770]	3.046398	7.911912	29.151839
ENSRNOG00000008121	Slc13a1	Solute carrier family 13 member 1 (Renal sodium/sulfate cotransporter) (Na(+)/sulfate cotransporter) (NaSi-1). [Source:UniProtKB/Swiss-Prot;Acc:Q07782]	4.121922	8.964802	28.698048
ENSRNOG00000006151	Pap	Regenerating islet-derived protein 3 beta precursor (Reg III-beta) (Pancreatitis-associated protein 1) (Peptide 23) (REG-2). [Source:UniProtKB/Swiss-Prot;Acc:P25031]	7.242337	12.01273	27.291850
ENSRNOG00000017762	Mucdhl	Mucin and cadherin-like protein precursor (Mu-protocadherin) (GP100). [Source:UniProtKB/Swiss-Prot;Acc:Q9JIK1]	4.503744	9.273448	27.278729
ENSRNOG00000006360	Reg3a	Regenerating islet-derived protein 3 alpha precursor (Reg III-alpha) (Pancreatitis-associated protein 2) (Lithostathine 3) (Islet of Langerhans regenerating protein 3) (REG 3) (RegIII). [Source:UniProtKB/Swiss-Prot;Acc:P35231]	7.289943	12.00212	26.212535
ENSRNOG00000020338	Lgals4	Galectin-4 (Lactose-binding lectin 4) (L-36 lactose-binding protein) (L36LBP). [Source:UniProtKB/Swiss-Prot;Acc:P38552]	5.312548	10.01786	26.088010
ENSRNOG00000028008	NP_001102058.1	similar to MGC52019 protein (predicted) (RGD1311652_predicted), mRNA [Source:RefSeq_dna;Acc:NM_001108588]	3.531526	8.199545	25.422253
ENSRNOG00000037073	Clec2h	C-type lectin domain family 2 member H (C-type lectin-related protein F)(Clr-f) [Source:UniProtKB/Swiss-Prot;Acc:Q8C1T8]	4.04621	8.702833	25.222219
ENSRNOG00000028531	Ccl25	chemokine (C-C motif) ligand 25 [Source:RefSeq_peptide;Acc:NP_001032280]	3.78718	8.409895	24.636322
ENSRNOG00000030724	NP_001099516.1	ADAM-like, decysin 1 [Source:RefSeq_peptide;Acc:NP_001099516]	3.13702	7.737415	24.258105
ENSRNOG00000009734	Akr1b8	aldo-keto reductase family 1, member B8 [Source:RefSeq_peptide;Acc:NP_775159]	4.260956	8.749525	22.448836
ENSRNOG00000028288	Tmem12	Clarin-3 (Transmembrane protein 12). [Source:UniProtKB/Swiss-	3.929303	8.390023	22.019655

		Prot;Acc:Q6AYR5]			
ENSRNOG00000026682	Clec2e	C-type lectin domain family 2 member E (C-type lectin-related protein A)(Clr-a) [Source:UniProtKB/Swiss-Prot;Acc:Q80XD9]	4.000115	8.432235	21.587436
ENSRNOG00000008849	Guca2a	Guanylin precursor (Guanylate cyclase activator 2A). [Source:UniProtKB/Swiss-Prot;Acc:P28902]	4.719577	9.115376	21.050753
ENSRNOG00000030524	Defcr4	Defensin 5 precursor (RD-5) (Enteric defensin). [Source:UniProtKB/Swiss-Prot;Acc:P82106]	4.027505	8.420865	21.015181
ENSRNOG00000001466	LOC687842		2.40632	6.774995	20.658663
ENSRNOG00000007758	Hsd17b6	Hydroxysteroid 17-beta dehydrogenase 6 precursor (EC 1.1.1.62) (EC 1.1.1.63) (EC 1.1.1.105) (17-beta-HSD6) (Oxidative 3-alpha hydroxysteroid dehydrogenase) (3-alpha->beta-hydroxysteroid epimerase) (3-alpha->beta-HSE). [Source:UniProtKB/Swiss-Prot;Acc:O54753]	2.74972	7.10225	20.428763
ENSRNOG00000027139	Krt20	Keratin, type I cytoskeletal 20 (Cytokeratin-20)(CK-20)(Keratin-20)(K20) [Source:UniProtKB/Swiss-Prot;Acc:Q9D312]	4.574755	8.80569	18.777524
ENSRNOG00000028889	RGD1565748		4.585218	8.757542	18.029968
ENSRNOG00000001379	Cyp3a9	Cytochrome P450 3A9 (EC 1.14.14.1) (CYPIIIA9) (P450-OLF3) (Olfactive) (3AH15). [Source:UniProtKB/Swiss-Prot;Acc:P51538]	3.38757	7.559585	18.026950
ENSRNOG00000006873	Dnase1	Deoxyribonuclease-1 precursor (EC 3.1.21.1) (Deoxyribonuclease I) (DNase I). [Source:UniProtKB/Swiss-Prot;Acc:P21704]	4.728468	8.862915	17.562747
ENSRNOG00000029007	Ugt2b10_pre		2.873608	6.99562	17.412029
ENSRNOG00000005223	Hnmt	Histamine N-methyltransferase (EC 2.1.1.8) (HMT). [Source:UniProtKB/Swiss-Prot;Acc:Q01984]	2.40884	6.50969	17.158481
ENSRNOG00000018699	NP_0010999 33.1	EPS8-like 3 [Source:RefSeq_peptide;Acc:NP_0010 99933]	3.992306	8.003362	16.123085
ENSRNOG00000007006	Slc3a1	Neutral and basic amino acid transport protein rBAT (B(0,+)-type amino acid transport protein) (NAA-TR) (D2). [Source:UniProtKB/Swiss-Prot;Acc:Q64319]	3.560829	7.556868	15.956142
ENSRNOG00000038957	RGD1305184 _pred		4.22061	8.20907	15.872527
ENSRNOG00000033693	RGD1559914 _pred	Neuronal apoptosis inhibitory protein (Fragment). [Source:UniProtKB/TrEMBL;Acc:Q8R4 U8]	2.89875	6.87487	15.737342
ENSRNOG00000022225	LOC679380	similar to leucine rich repeat containing 19 (LOC680478), mRNA [Source:RefSeq_dna;Acc:NM_0011094 13]	3.24814	7.196483	15.437244
ENSRNOG00000029462	Defa-rs1	alpha-defensin-related sequence 1 [Source:RefSeq_peptide;Acc:NP_0010 28245]	5.221155	9.150195	15.232068
ENSRNOG00000001765	NP_0011005 57.1	similar to RIKEN cDNA D630035O19 (predicted) (RGD1311100_predicted), mRNA [Source:RefSeq_dna;Acc:NM_0011070 87]	5.125156	8.992788	14.597337
ENSRNOG00000014956	Slc11a1	Natural resistance-associated macrophage protein 1 (NRAMP 1). [Source:UniProtKB/Swiss-Prot;Acc:P70553]	5.034481	8.878644	14.361783
ENSRNOG00000024785	Mcpt4	Mast cell protease 4 precursor (EC 3.4.21.-) (Mast cell protease IV) (rMCP-IV) (rMCP-4). [Source:UniProtKB/Swiss-Prot;Acc:P97592]	2.38583	6.13953	13.488892
ENSRNOG00000015460	LOC682510	similar to transmembrane 4 L six family member 20 (LOC691066), mRNA [Source:RefSeq_dna;Acc:NM_0011096 18]	3.968868	7.70262	13.303671

Table 6. Partial list of downregulated genes from HO-1 induction by CoPP in pancreas. Abbreviated list of the downregulated genes from the 51 d BBdp pancreas microarray experiments comparing CoPP treated and saline treated gene expression. RNA was isolated at 51 days and pooled (n=8/group) for analysis using Affymetrix Rat Gene 1.0 ST chips.

ENSEMBL GENE ID	Gene Symbol	Definition	Probe Value Saline	Probe Value CoPP	Fold Change
ENSRNOG00000013552	Scd1	Acyl-CoA desaturase 1 (EC 1.14.19.1) (Stearoyl-CoA desaturase 1) (Fatty acid desaturase 1) (Delta(9)-desaturase 1). [Source:UniProtKB/Swiss-Prot;Acc:P07308]	9.84717	6.4432	-10.5851514
ENSRNOG00000012404	Thrsp	Thyroid hormone-inducible hepatic protein (Spot 14 protein) (SPOT14) (S14 protein). [Source:UniProtKB/Swiss-Prot;Acc:P04143]	9.916965	6.590585	-10.03090592
ENSRNOG00000021555	RGD1310778_predicted		7.08981	4.91749	-4.507476593
ENSRNOG00000039477			6.54259	4.53738	-4.014471302
ENSRNOG00000001821	Adipoq	adiponectin, C1Q and collagen domain containing [Source:RefSeq_peptide;Acc:NP_653345]	9.3453	7.412655	-3.817544568
ENSRNOG00000006025	Lamb3	Laminin chain (Fragment). [Source:UniProtKB/TrEMBL;Acc:P70637]	6.78426	4.86895	-3.771948556
ENSRNOG00000002305	Slc15a2	Oligopeptide transporter, kidney isoform (Peptide transporter 2) (Kidney H(+)/peptide cotransporter) (Solute carrier family 15 member 2). [Source:UniProtKB/Swiss-Prot;Acc:Q63424]	6.71212	4.815275	-3.723979162
ENSRNOG00000034247			6.7947	4.91433	-3.681694705
ENSRNOG00000003510	Fmo2	Dimethylaniline monooxygenase [N-oxide-forming] 2 (EC 1.14.13.8) (Pulmonary flavin-containing monooxygenase 2) (FMO 2) (Dimethylaniline oxidase 2). [Source:UniProtKB/Swiss-Prot;Acc:Q6IRI9]	7.496518	5.72437	-3.415622023
ENSRNOG00000017987	1110017I16Rik	Unique cartilage matrix-associated protein Precursor [Contains Unique cartilage matrix-associated protein C-terminal fragment(Ucma-C)(Gla-rich protein)(GRP)] [Source:UniProtKB/Swiss-Prot;Acc:Q14BU0]	6.98552	5.21806	-3.404540275
ENSRNOG00000006732	NP_001102434.1	sporulation protein, meiosis-specific, SPO11 homolog [Source:RefSeq_peptide;Acc:NP_001102434]	6.3103	4.56522	-3.352134415
ENSRNOG00000011646	Rem2	GTP-binding protein REM 2 (Rad and Gem-like GTP-binding protein 2). [Source:UniProtKB/Swiss-Prot;Acc:Q9WTY2]	6.27907	4.58101	-3.24464356
ENSRNOG00000002085	LOC498350	similar to testicular haploid expressed gene product isoform 2 (LOC498350), mRNA [Source:RefSeq_dna;Acc:NM_001017498]	6.40465	4.71267	-3.230998319
ENSRNOG00000001923	Tprg	transformation related protein 63 regulated [Source:RefSeq_peptide;Acc:NP_001101790]	6.24009	4.57994	-3.160493833

ENSRNOG00000004762	Ak7	Putative adenylate kinase 7 (EC 2.7.4.3) [Source:UniProtKB/Swiss-Prot;Acc:Q9D2H2]	7.399063	5.758986667	-3.116823946
ENSRNOG00000002331	Aldh3a1	Aldehyde dehydrogenase, dimeric NADP-preferring (EC 1.2.1.5) (ALDH class 3) (Tumor-associated aldehyde dehydrogenase) (HTC-ALDH). [Source:UniProtKB/Swiss-Prot;Acc:P11883]	6.44661	4.81871	-3.090627965
ENSRNOG00000002024	Epha5	Ephrin type-A receptor 5 precursor (EC 2.7.10.1) (Tyrosine-protein kinase receptor EHK-1) (EPH homology kinase 1). [Source:UniProtKB/Swiss-Prot;Acc:P54757]	7.57805	5.980595	-3.026090218
ENSRNOG00000033672	Akp5	Embryonic alkaline phosphatase Precursor (EAP)(EC 3.1.3.1) [Source:UniProtKB/Swiss-Prot;Acc:P24823]	6.90354	5.31184	-3.014043001
ENSRNOG00000022268	LOC362972		7.226176	5.639066	-3.004468924
ENSRNOG00000002302	Corin	Atrial natriuretic peptide-converting enzyme (EC 3.4.21.-)(Pro-ANP-converting enzyme)(Corin)(Low density lipoprotein receptor-related protein 4) [Source:UniProtKB/Swiss-Prot;Acc:Q9Z319]	6.22529	4.67329	-2.932233514
ENSRNOG00000011892	Slc36a2	tramdorin 1 [Source:RefSeq_peptide;Acc:NP_647555]	6.963045	5.440766667	-2.872443137
ENSRNOG00000016681	Mc2r	Adrenocorticotropic hormone receptor MC-2 (Fragment). [Source:UniProtKB/TrEMBL;Acc:Q8CIX6]	6.65734	5.13769	-2.867214821
ENSRNOG00000012575	Fath2	Protocadherin Fat 2 precursor (Multiple epidermal growth factor-like domains 1). [Source:UniProtKB/Swiss-Prot;Acc:O88277]	7.20855	5.69471	-2.855691236
ENSRNOG00000014378	Il1r2	Interleukin-1 receptor type II precursor (IL-1R-2) (IL-1R-beta) (CD121b antigen). [Source:UniProtKB/Swiss-Prot;Acc:P43303]	7.14691	5.66452	-2.794112288
ENSRNOG00000010079	Ca3	Carbonic anhydrase 3 (EC 4.2.1.1) (Carbonic anhydrase III) (Carbonate dehydratase III) (CA-III). [Source:UniProtKB/Swiss-Prot;Acc:P14141]	11.34157	9.865725	-2.781465093
ENSRNOG00000031708			8.32067	6.84826	-2.774850412
ENSRNOG00000008996	Dpysl5	Dihydropyrimidinase-related protein 5 (DRP-5) (ULIP6 protein). [Source:UniProtKB/Swiss-Prot;Acc:Q9JHU0]	7.21188	5.75267	-2.749577593
ENSRNOG00000000158	Cdo1	Cysteine dioxygenase type 1 (EC 1.13.11.20) (Cysteine dioxygenase type I) (CDO) (CDO-I). [Source:UniProtKB/Swiss-Prot;Acc:P21816]	9.064935	7.620735	-2.721118906
ENSRNOG00000020244	NP_001101471.1		6.71041	5.27505	-2.704496443
ENSRNOG00000016734	Emilin3_predicted	elastin microfibril interfacer 3	6.887648	5.4686825	-2.67393612

		[Source:RefSeq_peptide; Acc:NP_001103371]			
ENSRNOG00000025403	Klri2	killer cell lectin-like receptor family I member 2 [Source:RefSeq_peptide; Acc:NP_001012666]	6.95381	5.53743	-2.66914929
ENSRNOG00000024923	Nnat	Neuronatin. [Source:UniProtKB/Swiss-Prot;Acc:Q62649]	8.52881	7.1336	-2.630268357
ENSRNOG00000037718	NP_001094438.1	ubiquitin specific protease 43 [Source:RefSeq_peptide; Acc:NP_001094438]	6.58541	5.19562	-2.620405351
ENSRNOG00000013346	Bm259	BM259 (Fragment). [Source:UniProtKB/TrEMBL;Acc:Q923J6]	8.50867	7.1367	-2.588237488
ENSRNOG00000024709	RGD1561223_predicted		6.33488	4.96446	-2.585458235
ENSRNOG00000029429			6.66152	5.29583	-2.576995468
ENSRNOG00000018853	Slc28a3	solute carrier family 28 (sodium-coupled nucleoside transporter), member 3 [Source:RefSeq_peptide; Acc:NP_543184]	6.426155	5.063	-2.572471333
ENSRNOG00000016525	NP_001100811.1	sushi domain containing 3 [Source:RefSeq_peptide; Acc:NP_001100811]	9.25581	7.895135	-2.56805304
ENSRNOG00000024837	NP_001102347.1	transmembrane phosphatase with tensin homology [Source:RefSeq_peptide; Acc:NP_001102347]	6.55798	5.21806	-2.531372815
ENSRNOG00000004404	Tac4	tachykinin 4 [Source:RefSeq_peptide; Acc:NP_758831]	7.23447	5.899025	-2.523533083
ENSRNOG00000000598	NP_001102006.1	tubulin, epsilon 1 [Source:RefSeq_peptide; Acc:NP_001102006]	7.097693	5.773015	-2.504768899
ENSRNOG00000003841	Kcnh1	Potassium voltage-gated channel subfamily H member 1 (Voltage-gated potassium channel subunit Kv10.1)(Ether-a-go-go potassium channel 1)(EAG1)(m-eag) [Source:UniProtKB/Swiss-Prot;Acc:Q60603]	6.679927	5.36184	-2.493352167
ENSRNOG00000039050			6.14655	4.83007	-2.490576974
ENSRNOG00000006874	Opn1sw	Blue-sensitive opsin (BOP) (Blue cone photoreceptor pigment) (Short wavelength-sensitive cone opsin) (S opsin). [Source:UniProtKB/Swiss-Prot;Acc:Q63652]	8.12116	6.80538	-2.489368832
ENSRNOG00000025884	RGD1566300_predicted		6.25807	4.94937	-2.477182226
ENSRNOG00000005367	Slc12a1	Solute carrier family 12 member 1 (Bumetanide-sensitive sodium-(potassium)-chloride cotransporter 2) (Kidney-specific Na-K-Cl symporter). [Source:UniProtKB/Swiss-Prot;Acc:P55016]	7.32842	6.02727	-2.464252347
ENSRNOG00000011193	RGD1565090_predicted		6.22691	4.92983	-2.457310219
ENSRNOG00000030948	EG625464	Putative uncharacterized protein [Source:UniProtKB/TrEMBL;Acc:Q3V040]	8.96836	7.68065	-2.441402223

CURRICULUM VITAE

Mahmoud Husseini

EDUCATION

2010 – Present University of Ottawa
Master of Science (M.Sc.) in Biochemistry
- Thesis: The role of heme oxygenase-1 and the CD163 pathway in type 1 diabetes pathogenesis

2005 – 2009 Carleton University
Bachelor of Science (B.Sc.) Honours in Biochemistry (Magna Cum Laude)
- Thesis: Epitope tagging of a cytoskeletal protein (SBR-BD300) in *Neurospora crassa*

WORK EXPERIENCE

2012 Faculty of Science, University of Ottawa Ottawa, ON
Marker/Exam Proctor (BCH 3120)

2010 – Present Ottawa Hospital Research Institute Ottawa, ON
M.Sc. Candidate
- Project includes investigating subset of immune cells found in the gut immune system and their involvement in autoimmune type 1 diabetes.

2009 – 2010 Star World International LLC Dubai, UAE
Junior Sales Representative/Safety Officer

2008 – 2009 Dubai International Film Festival Dubai, UAE
Events Coordinator

2007 – 2008 Long Bay Camp Ottawa, ON
Administrative Assistant

2005 – 2007 Starbucks Coffee Company Ottawa, ON
Barista

2002 – 2004 American School of Dubai Dubai, UAE
Tutor in Math & Science for High School Students

MANUSCRIPTS IN PREPARATION

Husseini M, Wang G-S, Crookshank JA, Scott FW. Induction of Heme Oxygenase-1 Inhibits Development of Type 1 Diabetes in BBdp Rats.

ABSTRACTS/PRESENTATIONS AT SCIENTIFIC MEETINGS

November 2012 Ottawa Hospital Research Institute Research Day, Immunity and Disease, Ottawa, ON
Oral Presentation: Induction of heme oxygenase-1 inhibits development of type 1 diabetes - potential involvement of antimicrobials and M2 macrophages. **Husseini Mahmoud** J.A. Crookshank, G-S. Wang, and F.W. Scott.

November 2011 Ottawa Hospital Research Institute Research Day, Immunity and Disease, Ottawa, ON
Poster Presentation: The CD163 macrophage pathway and its role in gut-associated lymphoid tissue in the development of type 1 diabetes in the BioBreeding diabetes-prone (BBdp) rat. **Husseini, Mahmoud**, J.A. Crookshank, and F.W. Scott. **Accepted for poster presentation*

October 2011 2nd International Conference on Immune Tolerance, Amsterdam, The Netherlands
Poster Presentation: **Husseini Mahmoud**, J.A. Crookshank, G-S. Wang, and F.W. Scott. Induction of heme oxygenase-1 inhibits development of type 1 diabetes in BBdp Rats. **Accepted for poster presentation*

COMPLETED GRADUATE COURSEWORK

BCH8105 (Winter 2011): Advanced topics in the molecular biology of human diseases II (Grade: A-)
BCH8106 (Fall 2011): Advanced topics in nutrition and metabolism (Grade: A+)

HONOURS AND AWARDS

2012 University of Ottawa
Biochemistry Graduate Student Seminar Day – Second place M.Sc. seminar ($75)

2011 University of Ottawa
Faculty of Graduate and Postdoctoral Studies (FGPS) Travel Grant ($650)

2011 University of Ottawa
Biochemistry, Microbiology, Immunology (BMI) Department Travel Grant ($1000)

2010 University of Ottawa
Faculty of Graduate and Postdoctoral Studies (FGPS) Admission Scholarship ($2500/session)

2009 - 2010 Carleton University
Faculty of Science Dean's Honour List

2005 Carleton University
Gary S. Duck Scholarship in Science ($2000)

2005 Carleton University
Undergraduate Admission Scholarship ($4000/year)